

Electronic Thesis and Dissertation Repository

4-21-2020 2:45 PM

Ultrasonic Techniques for Characterizations of Oils and Their Emulsions and Monitoring Oil Layer Depth of Spill

Kanu Raigan, *The University of Western Ontario*

Supervisor: Anand Prakash, *The University of Western Ontario*

A thesis submitted in partial fulfillment of the requirements for the Master of Engineering Science degree in Chemical and Biochemical Engineering

© Kanu Raigan 2020

Follow this and additional works at: <https://ir.lib.uwo.ca/etd>

 Part of the [Chemical Engineering Commons](#)

Recommended Citation

Raigan, Kanu, "Ultrasonic Techniques for Characterizations of Oils and Their Emulsions and Monitoring Oil Layer Depth of Spill" (2020). *Electronic Thesis and Dissertation Repository*. 6997.
<https://ir.lib.uwo.ca/etd/6997>

This Dissertation/Thesis is brought to you for free and open access by Scholarship@Western. It has been accepted for inclusion in Electronic Thesis and Dissertation Repository by an authorized administrator of Scholarship@Western. For more information, please contact wlsadmin@uwo.ca.

Abstract

Oil-water emulsions encountered during production and refining of crude oil, as well as oil spills present technical challenges. There is need for low-cost technology to understand characteristics such as composition, droplets size distribution and other rheological properties of oils and their emulsions and monitor oil layer depth of spill.

The main purpose of the first part of this work was to develop and test ultrasonic based technology to characterize oils and their emulsions using their acoustic velocities and attenuations. The technique captured an increase in both acoustic velocity and attenuation with asphaltenes concentration in crude oil. Thus, the fast response and low-cost ultrasonic techniques provide a plausible means of monitoring this impurity level in treated and upgraded crude oils. Tests with emulsions of oil samples exhibited that both acoustic velocity and attenuation decreased with time, which indicated water droplets settling. This was confirmed by direct measurements of water separation with time which were consistent with ultrasonic results. These findings have opened a new perspective for the ultrasonic technique to monitor and characterize emulsions online.

The main purpose of the last part of this work was to develop a low-cost ultrasonic-based technique to monitor the oil layer depth of the spills. Layers of water-in-oil emulsion and mineral and crude oil samples were added to the DI water surface at an increment of 1 mm thickness in a jacketed vessel. Acoustic velocity decreased with the thickness of oils and their emulsions layers, while attenuation increased as expected. This is significant progress towards the development of ultrasonic technology to detect and monitor oil spill depth. A suitable device configuration is proposed for further development and field testing.

Keywords: Emulsion characterization, Crude oil, Ultrasonic techniques, acoustic velocity, Film Thickness, Oil Spill.

Summary for Lay Audience

Oil-water emulsions encountered during the extraction and cleaning of crude oil, as well as oil spills present a lot of problems. An emulsion is a mixture of two immiscible liquids which are water and oil in this case. There is a need for a low-cost way of knowing the behavior of oils and their emulsions and knowing the oil layer depth of the spill.

This study first developed and tested ultrasonic based technology (sound waves above human audible limit) to know the behavior such as composition and droplets size distribution of oils and their emulsions. It was observed that both acoustic velocity (speed of sound through a medium) and attenuation (loss of wave signal energy) increased with an increase in the amount of asphaltene (the substance that gives crude oil dark brown color) in crude oil samples. Thus, fast feedback and low-cost ultrasonic techniques provide a reasonable means of monitoring this impurity level in the treated and ready to be transported crude oils. Tests with emulsions of oils showed that both acoustic velocity and attenuation decreased with time, which indicated water settling out. This was confirmed by direct measurements of water separation with time which were consistent with ultrasonic results. These findings have opened a new perspective for the ultrasonic technique to monitor and know the behavior of emulsions online.

The last part of this study developed a low-cost ultrasonic-based technique to monitor the oil layer depth of the spills. Layers of oil samples and their emulsions were added to the deionized water surface at small increments. Acoustic velocity decreased with an increase in the thickness of oils and their emulsions layers, while attenuation increased. This is an important step towards developing ultrasonic technology to identify and measure oil spill depth. A suitable change in the shape of the ultrasonic device and how it works is proposed for further development and field testing.

Acknowledgement

First, I would like to express my sincere gratitude to my supervisor, Dr. A. Prakash for his invaluable support and guidance throughout this research work. It is because of his tireless effort and commitment that this work has been successfully completed.

I would also like to thank staff and colleagues at the department of chemical engineering, Western University, for their support and help.

I am extremely grateful to my family for their love, care, and sacrifices that enabled me to complete this research work.

Finally, I would like to express my appreciation to Imperial Oil Ltd. under its University Research Award program and NSERC under its Collaborative Research and Development program for supporting this work.

Table of Contents

Abstract	ii
Summary for Lay Audience	iii
Acknowledgement.....	iv
Nomenclature.....	xii
Chapter 1. Introduction	1
1.1 Thesis Objectives and Scope.....	5
Chapter 2. Literature Review	6
2.1 Emulsion Formations and Classification.....	6
2.1.1 Emulsion Formation.....	6
2.1.2 Classification of Emulsions	7
2.2 Emulsion Stability	9
2.2.1 Creaming/Sedimentation	10
2.2.2 Flocculation	11
2.2.3 Coalescence	12
2.2.4 Phase Inversion	13
2.2.5 Ostwald Ripening (Disproportionation).....	13
2.3 Emulsifying agent.....	14
2.3.1 Surfactant.....	14
2.3.2 Asphaltenes.....	16
2.3.3 Resins	17
2.3.4 Fine solid particles	18
2.4 Demulsification	20
2.4.1 Chemical demulsification	21
2.4.2 Electrical demulsification	22
2.4.2.1 VIEC - Vessel Internal Electrostatic Coalescer	23
2.4.2.2 LOWACC - Low Water Content Coalescer	24

2.4.3 Thermal Demulsifications	24
2.5 Emulsion characterization techniques.....	25
2.5.1 Microscopy	25
2.5.1.1 Light Microscopy (LM).....	25
2.5.1.2 Cryogenic Scanning Electron Microscopy	26
2.5.1.3 Confocal Laser Scanning Microscopy (CLSM).....	27
2.5.2 Light scattering	28
2.5.3 Nuclear Magnetic Resonance (NMR)	29
2.5.4 Coulter Counter.....	30
2.5.5 The Ultrasonic Spectrometry	31
2.5.5.1 Ultrasonic attenuation spectroscopy.....	33
2.5.5.2 Particle size analysis by Acoustic Spectroscopy.....	33
2.5.6 Ultrasonic Sensor System and Sensor Classification	34
2.5.6.1 Ultrasonic flow sensors	36
2.5.6.2 Ultrasonic state sensors	37
2.5.6.3 Ultrasonic Velocity Sensors.....	38
2.5.6.4 Ultrasonic Attenuation Sensors.....	39
References.....	42
Chapter 3. Characterization of oils and their emulsion by ultrasonic techniques.....	45
Abstract.....	45
3.1 Introduction	45
3.2 Experimental Details.....	48
3.2.1 Materials and Methods	48
3.2.2 Experimental Setup	49
3.2.3 Calculation of Acoustic Parameters	52
3.2.4 Data Analysis.....	53
3.3 Results and Discussions	55

3.3.1 Acoustic properties of oil samples	55
3.3.2. Effects of asphaltenes concentration on acoustic parameters	57
3.3.3 Stability Tests with Mineral Oil Emulsions.....	61
3.3.3.1 DI Water Separation and Attenuation with Mineral Oil Emulsions.....	62
3.3.3.2 DI Water Separation and Measured Acoustic Velocity with Mineral Oil Emulsions	63
3.3.3.3 DI Water Separation and Attenuation with Mineral Oil Emulsions.....	64
3.3.3.4 Acoustic Velocity for the Mineral Oil Emulsions.....	65
3.3.4 Stability Test with Crude oil Emulsions.....	66
<i>Determine Water Fraction from Acoustic Velocity</i>	70
3.3.5 Measurements with blends of crude oil and mineral oil.....	76
3.3.5.1 Effects of adding LMO to HCO on Emulsions Characteristics	79
3.3.5.2 Water Separation Tests with Emulsions of HCO and LMO Blends	79
3.3.5.3 Acoustic parameters in Emulsions of the Blend of HCO and LMO	80
3.4 Conclusions	82
Notations	83
Greek Letters	84
Subscripts	84
References.....	85
Appendix A.....	88
Chapter 4. Ultrasonic based techniques to monitor oil layer depth of spills	92
Abstract.....	92
4.1 Introduction	92
4.2 Experimental Details.....	95
4.2.1 Materials and Methods.....	95
4.2.2 Experimental Setup and Procedures.....	96
Data Analysis	101
4.3 Results and Discussions	103

4.3.1 Measurements with layers of MO on Surface of DI water	104
4.3.2 Measurements with Layers of LMO and its Emulsion on DI Water Surface	107
4.3.3 Measurements of Acoustic Parameters with Layer of HCO and Its Emulsion on	110
Water Surface	110
4.4 Estimation of Oil Layer Thickness Based on Measurement of Acoustic Parameters	115
4.5 Conclusions	119
Notations	120
References	122
Appendix B	124
Chapter 5. Conclusion	126
5.1 Recommendations	127
CURRICULUM VITAE OF KANU RAIGAN	129

List of Tables

Table 3.1. Physical properties of different oil used for emulsion preparation	49
Table 3.2. Comparison of acoustic properties of water and oil samples.....	56
Table 3.3. Contributing terms and their equation for acoustic attenuation	75
Table 3.4. Thermophysical properties of materials from literature	76
Table 3.5. Comparison of measured and calculated values of acoustic velocities in HCO/MO blends	78
Table 4.1. Physical properties of different oils used to prepare emulsions.	96
Table 4.2. Comparison of acoustic velocity using experimental and literature data	104
Table 4.3. Comparison of measured and estimated oil layer thickness	116

List of Figures

Fig. 2.1 Water in oil emulsion (a), Oil in water emulsion (b) (Khan et al., 2011)	8
Fig. 2.2 emulsion destabilization mechanism (El-Sayed, 2012)	10
Fig. 2.3. Diagram of the suggested phase inversion mechanism by Arirachakaran et al. (1989).....	14
Fig. 2.4. a) the structure of surfactant, b) interfacial surfactant molecules, and c) spherical surfactant micelles (Pichot, 2010).	16
Fig 2.5. example of molecular structures in crude oil: Asphaltenes (El-Sayed, 2012).....	17
Fig. 2.6. mechanism of emulsion stabilization by asphaltenes (El-Sayed, 2012)	17
Fig. 2.7. composition of crude oil (El-Sayed, 2012)	18
Fig. 2.8 possible distributions of course and fine solids in an emulsion (Sztukowski & Yarranton, 2005)	20
Fig. 2.9. VIEC Modul ((Silset, 2008).	24
Fig. 2.10. VIEC and LOWACC all installed in the same separator to accomplish total separation ((Silset, 2008).	24
Fig. 2.11 Conventional light microscopy image of a water-in-oil emulsion (Munoz, et al, 1997)	26
Fig. 2.12. Cryo-SEM image of a water-in-oil emulsion showing the interior fracture surface (Munoz, et al, 1997).....	27
Fig. 2.13 Ultrasonic sensor system (Hauptmann, Lucklum, Piittmer, & Henning, 1998).	36
Fig. 2.14 Block diagram showing an ultrasonic device for simultaneous measurement of ultrasonic velocity and attenuation (Hauptmann, Lucklum, Piittmer, & Henning, 1998)	41
Fig. 3.1. Vacuum filter assembly for the asphaltenes concentration measurement	49
Fig. 3.2. Schematic diagram of the experimental setup for emulsion characterization	51
Fig. 3.3 Changes in ultrasonic signal for LMO & LMO Emulsion at 1200 rpm.	52
Fig 3.4 Scatter plot of TOF data obtained with LMO emulsion	54
Fig 3.5 Frequency distribution of TOF data obtained with LMO emulsion	54
Fig. 3.6 Acoustic velocity values calculated from TOF by Eq. 3.2.....	55
Fig. 3.7. Calculated attenuation values from recorded amplitude	57
Fig. 3.8. Example of molecular structures in crude oil: Asphaltenes (El-Sayed, 2012).....	57
Fig. 3.9 Mechanism of emulsion stabilization by asphaltenes (El-Sayed, 2012).....	58
Fig. 3.10 Variation of acoustic velocity with asphaltenes concentration in crude oil	59
Fig. 3.11 Asphaltenes concentration vs acoustic impedance	60
Fig. 3.12 Effects of asphaltenes concentration on acoustic attenuation	61
Fig. 3.13. Water separation and attenuation in LMO emulsions.....	63
Fig. 3.14. DI Water separation and acoustic velocity in MO emulsions	64
Fig. 3.15. Water separation and attenuation in MO emulsions	65

Fig. 3.16. Water separation and acoustic velocity in MO emulsions	66
Fig. 3.17. Pictures of light mineral oil and crude oil emulsions.....	67
Fig. 3.18. Variations in amplitude values recorded with time with light crude oil emulsions.....	68
Fig. 3.19 Variations of attenuation obtained with emulsions of LCO	68
Fig. 3.20. Variations of acoustic velocity with time in LCO emulsions.....	69
Fig. 3.21. Calibration curve to determine water fraction in emulsions of LCO.....	71
Fig. 3.22. Measured attenuation in HCO emulsions.....	72
Fig. 3.23. Variation of acoustic velocity in HCO Emulsions.....	72
Fig. 3.24. The Acoustic velocity for HCO/LMO and their blend in varying composition	77
Fig. 3.25. The Attenuations for HCO, LMO and their blend in varying composition	79
Fig. 3.26. Variations of acoustic velocity with time in emulsions of HCO/LMO blends.....	81
Fig. 3.30. Change of attenuation with time in the emulsions of blends.....	82
Fig. A3.28 Water separation % for LMO emulsions.....	88
Fig. A3.29. Acoustic Velocity for LMO emulsions	89
Fig. A3.30. Attenuation for LMO emulsions.....	89
Fig. A3.31. Effect of adding LMO in HCO on its acoustic velocity	90
Fig. A3.32. Variations of acoustic velocity with time in emulsions of HCO/LMO blends.....	91
Fig. 4.1. Schematic diagram of the experimental setup	97
Fig. 4.2. Details of the ultrasonic probe.....	97
Fig. 4.3. Comparison of ultrasonic signal in DI water vs. layer of MO and its emulsion in DI water	100
Fig 4.4. Frequency distribution plot for 1 mm film of LMO	102
Fig 4.5. Scatter plot for data collected with 1 mm oil film of LMO	102
Fig. 4.6. The acoustic velocities for fluids used in this work.....	103
Fig. 4.7. Amplitude and the Calculated Attenuation values for fluids	104
Fig.4.8. Variation of acoustic velocity with increasing thickness of MO layer	105
Fig. 4.9. Changes in attenuation recorded with increasing thickness of MO layer	106
Fig. 4.10. Pictograph showing mineral Oil sticking on the surface of the Probe	107
Fig. 4.11. Ultrasonic velocity for the Film of MO + Emulsion.....	108
Fig. 4.12. Attenuation of the Film of LMO + Emulsion.....	109
Fig. 4.13. Comparison of stability of LMO and LCO emulsions.....	110
Fig. 4.14. Photographs showing layers of crude oil on water surface in the test vessel	111
Fig. 4.15. Changes in ultrasonic signal for DI Water Layer + 5 mm HCO Layer.....	112
Fig. 4.16. Acoustic Velocity of DI water + HCO layers and DI water + HCO Emulsions + HCO using the new procedure.	113

Fig. 4.17. Attenuation of DI water + HCO layers and DI water + HCO Emulsions + HCO using the new procedure.....	114
Fig. 4.18. Proposed procedure to detect oil and emulsion layers a) probe at the surface of oil layer; b) probe at the surface of emulsion layer; c) probe at the surface of water column	118
Fig. 4.19. Expected trajectory of the measured acoustic velocity as the probe moves from oil layer to water phase.....	118
Fig. B4.20. Comparison of acoustic velocity for film of LMO and CO and their emulsions layers.....	124
Fig. B4.21. Attenuation of mineral oil – Water content (10 & 20%)	125

Nomenclature

LMO	Light Mineral Oil
LCO	Light Crude Oil
HCO	Heavy Crude Oil
DI	Deionized
Tween 20	Polyoxyethylene-20-sorbitan Monolaurate
TOF	Time of Flight (μs)
W/O	Water-in-oil emulsion
O/W	Oil-in-water emulsion
Rpm	Revolutions per minute
HLB	Hydrophile-Lipophile Balance
A_0	Reference/initial amplitude (amplitude of water)
A	Final amplitude (amplitude of the sample)
FFT	Fast Fourier Transform
CO	Crude oil
MO	Mineral Oil
LURSOT	The Laser Ultrasonic Sensing of Oil thickness
UV/IR	Ultraviolet/infrared
USEPA	U.S. Environmental Protection Agency
C_p	Specific Heat Capacity
NMR	Nuclear Magnetic Resonance
c	acoustic velocity ($\text{m}\cdot\text{s}^{-1}$)
d	distance between transducer and receiver (m)
d_w	Water layer (mm)
d_{em}	Emulsion layer (mm)
d_o	Oil layer thickness (mm)
ToF_{owe} water (μs)	Time of flight recorded with layers of oil, emulsion and water (μs)

ToF _o	Time of flight of oil (μs)
ToF _w	Time of flight of water (μs)
ToF _{em}	Time of flight of emulsion (μs)
V _o	Acoustic velocity of oil ($\text{m}\cdot\text{s}^{-1}$)
V _w	Acoustic velocity of water ($\text{m}\cdot\text{s}^{-1}$)
V _{em}	Acoustic velocity of emulsion ($\text{m}\cdot\text{s}^{-1}$)
V _{owe}	Acoustic velocity of oil, water and emulsion ($\text{m}\cdot\text{s}^{-1}$)
Z	acoustic impedance of the medium ($\text{kg}\cdot\text{m}^{-2}\cdot\text{s}^{-1}$)

Greek Letters

α	attenuation coefficient (m^{-1})
β	bulk modulus of the medium (Pa)
λ	pulse wavelength (μm)
ρ	density of medium ($\text{kg}\cdot\text{m}^{-3}$)
ω	angular frequency ($\text{rad}\cdot\text{s}^{-1}$)
κ	isentropic compressibility (Pa^{-1})
φ	fraction of dispersed phase (-)
f	ultrasonic frequency (MHz)

Chapter 1. Introduction

During the process of production of crude oil, water and crude oil are co-produced in the form of an emulsion that is highly undesirable due to compromised product quality. Emulsion which is a colloid of two or more immiscible liquids where one liquid is dispersed into the other liquid appearing as droplets are formed because of the intimate contact between these immiscible liquids. An emulsion system comprises two phases; the dispersed droplets are the internal phase while the external phase (continuous phase) is the liquid surrounding the dispersed droplets. An emulsion can either be stable (tight) or unstable (loose). Impurities such as asphaltene and fine solid particles, which are found in crude oil, stabilize emulsions (El-Sayed, 2012). Tight emulsions are difficult to separate into their phases, therefore increasing the cost of refining crude oil (Abdurahman H, 2006).

The water-in-oil emulsion is the most common type of emulsion in the petroleum industry. It is a fine dispersion of water-in-oil or oil diameter may range from $0.1\mu\text{m}$ - $20\mu\text{m}$ (Lissant, 1988). Although emulsions are generally undesirable, it is helpful when producing and transporting heavy crude oil. Heavy crude oil can be highly viscous and therefore water is usually added to reduce its viscosity for easy transportation (Zadymova et al., 2017). During extraction of oil sand, steam is injected into the underground reservoir to pressurize crude oil to the surface in the form of water-in-crude oil emulsions (Dalglish et al, 2007). These emulsions are sent to the central processing facility to reduce the water content to approximately 0.5 to 2.0 %, which is the acceptable level for pipeline transportation because water contains dissolved salt that may cause corrosion (Silset et al, 2008). These impurities of salts and fine particles in crude oil are removed in a desalter unit during refinery. Process water is mixed with incoming crude oil to dissolve out the salts, and the

emulsified mixture then enters separation vessels where the cleaned oil leaves from top and water containing dissolved salts leave from the bottom.

The emulsion destabilization process involves several steps which include flocculation, sedimentation, coalescence, and finally phase separation due to the density difference between oil and water. Flocculation of water globules involves the aggregation of droplets to form clusters that sediment under the influence of gravity. During the coalescence step, flocculated droplets fuse to form larger ones leading to phase separation (Graham et al., 2008). The coalescence step can be slowed down by the presence of stabilizing agents such as clay particles and crude oil components such as asphaltenes, resins, and acids (Moradi et al., 2011; Graham et al., 2008). Emulsion stability can be determined by several methods such as bottle tests and electrical methods (Wang and Alvarado, 2009). Bottle tests that rely on water resolution are more common due to low cost and ease of tracking. It can be combined with other methods such as electrical and acoustic techniques.

The high demand for petroleum products makes it necessary to transport these products using underwater pipelines or maritime ships internationally. Oil transportation leads to involuntary oil spill due to pipeline rupture, and ship accidents in addition to intentional petroleum waste spill in seawater. The European Space Agency puts the annual worldwide oil spill estimate at 4.5 million tons. Oil spills in seawater have a lasting effect on the maritime environment. These spills affect the ecosystem starting with marine life and extending to human life as well as environmental disasters. An oil spill can be spread across large water bodies by wind and water current with a few hours, therefore, making it more dangerous (Hammoud et al., 2019).

The oil spill is a major local and global environmental concern (Onwurah et al., 2007). The toxic effect of the oil spill can last over a decade because the bulk of oil remains in the less-weathered subsurface. U.S. Environmental Protection Agency (USEPA) found 35% leaks in randomly

sampled oil storage tanks (United Press International, 1986). One of the biggest challenges facing researchers in the study of oil spills are the ability to measure oil layer thickness. More specifically, there are no laboratory methods or reliable field techniques to measure oil on water thickness. The desire to measure oil thickness is driven by the need for significant advances in the primary understanding of how oil thickness spread and the effective response like spill cleanup. Another motivation for determining the oil thickness is to determine the amount of oil spilled. Remote sensing is a widely used technology to monitor the oil spill. Remote sensing is the use of a sensor, that does not include the human eye to detect a specific target from a distance. Aerial remote sensing (employing aircraft) is the widely used remote sensing in oil spills. Satellite remote sensing has not been successful as it requires locating features at sites with an already known oil spill. The existing method of using airborne surveillance of oil thickness with the sensors usually overestimates oil quantity (Brown et al., 1998).

Emulsions formed at sea due to wave current have been observed to be different and have varying film thicknesses. Their thickness range between 2 μm to 20mm. Currently, there is no existing technology to measure thick emulsions. Optimare, a three-channel microwave instrument is the only instrument currently available for measuring oil spill thickness. Despite microwave radiometry being a proven technique to remotely measure the thickness of fresh oil spill on the water surface, it has many limitations including water uptake is expected to degrade the signal, or otherwise may remove it completely, applicable to range between 0.5 to 1.2 mm oil layer thickness above which the signal is ambiguous – not suitable for thicker layers freshly spilled oil (Fingas, 2018). Microwave radiometer sensors are expensive and complicated to install for operation. It requires numerous oil properties and environmental characteristics for accurate detection of the oil

spill. For these reasons, a microwave is not used for slick imaging presently (Hammoud et al., 2019).

There are two main focusses of the present work:

The first being the development and testing of ultrasonic based technology to characterize oils and their emulsions as well as monitor changes in emulsion characteristics over time. These characteristics include composition, droplets size distribution and other rheological properties of oils. The emulsion characteristics are expected to be a function of the type of oil, level of impurities and mixing intensities, temperature, etc. The ultrasonic parameters recorded are changes in acoustic velocity, signal attenuation, and its frequency spectrum. The ultrasonic techniques were selected for their several advantageous features including; lower power consumption, in-line measurement, long-term stability, non-invasiveness, high resolution and accuracy, and rapid response. The technique provided good information regarding emulsion stability, changes in droplet size distribution, and concentration. Emulsions were prepared with mineral oil and crude oil samples and the effects of various factors including surfactant, and asphaltene content were investigated. Emulsion droplet structure is observed, and stability is examined by tracking the changes in ultrasonic parameters with time.

The second focus of the current work is the development of low-cost ultrasonic-based technique to detect oil spills as well as to estimate the thickness of oil and emulsion layers. The approach is based on simultaneous measurements of two main acoustic parameters, namely acoustic velocity (or time of flight) and attenuation (or amplitude). These parameters depend on the physical and thermodynamic properties of the propagating medium. It is envisaged that a low-cost device with acceptable accuracy can be developed based on ingenious ideas while taking advantage of the new developments in the field.

1.1 Thesis Objectives and Scope

The following are the main objectives of this work:

- Develop and test the potential of ultrasonic based technology to detect sample oils characteristics such composition, droplets size distribution and other rheological properties of oils. Use these oil characteristics as the basis to detect and monitor emulsions characteristics such as ultrasonic parameters, acoustic velocity and attenuation. Investigate the effects of asphaltenes and deionized water content on emulsion stability and characteristics.
- Development of an ultrasonic-based technique to quickly measure asphaltenes concentration online. First use the time-consuming solvent treatment and filtration off-line method to estimate the asphaltenes content in the crude oil emulsions. Then test the potential of ultrasonic technique to detect changes in asphaltenes concentration by recording the acoustic velocity and attenuation of the same crude oil samples.
- Development of low-cost ultrasonic-based technique(s) to detect the presence of oil spill as well as to estimate the thickness of oil and emulsion layers on the deionized water surface. The approach is based on simultaneous measurements of two main acoustic parameters, namely acoustic velocity, and attenuation. Layers of both mineral and crude oil and their emulsions are created in a jacketed vessel to simulate the experiments.

Chapter 2. Literature Review

Emulsions are very significant in various applications (petroleum/detergent industries and food processing) and industrial products (pharmaceuticals or cosmetic products and food products). It contains a minimum of one immiscible liquid thoroughly distributed in other liquid appearing as droplets, whose diameter may range from 0.1 μ m-20 μ m. Where its stabilization is contributed by emulsifying agent, asphaltenes, resins, and finely dispersed solids. It is a fine dispersion of water-in-oil or oil-in-water with these micron-sized droplets.

An emulsion system comprises two phases; the dispersed droplets are the internal phase while the external phase (continuous phase) is the liquid surrounding the dispersed droplets. The emulsifying agent is responsible for the separation of these dispersed droplets from the external phase (Lissant, 1988). During the previous century, research on the emulsions under deformation has been done resulting in significant and sequential theoretical and experimental studies. Many engineers and scientists participated in such investigations with a persistent interest in the understanding of nature and variance of the rheological properties of emulsions. These studies have been remained of prominent empirical attention due to its wide existence in daily routine.

2.1 Emulsion Formations and Classification

2.1.1 Emulsion Formation

Schubert and Armbruster 1992 proposed three major criteria, which are required for the formation of crude oil emulsions;

- Involvement of two immiscible liquids.
- The presence of Surface-active compounds as an emulsifying agent.
- Appropriate agitation to facilitate dispersion of one liquid into another as droplets.

When water and oil come into contact in the presence of the emulsifying agent and sufficient mixing, the crude oil emulsions are formed. For emulsion formation, the efficiency of agitation and the presence of emulsifier is very crucial. In oil production processes, there are multiple methods used for agitation, sometimes known as the shear amount.

In general, more agitation results in small-sized droplets very distributed in oil, consequently tightening the emulsion formed. The enormous studies on emulsion provided the fact that the size of these water droplets may differ from less than one micrometer extending up to more than a thousand micrometers. The presence of emulsifiers is another element required for emulsion formation. The existence, quantity, and nature of emulsifier more considerably determine the emulsion type and its "tightness." In crude oils, natural emulsifiers exist in heavy fractions.

Because of the variation of heavier fractions in crude oils, the tendency of emulsification widely differs. Less stable emulsions are produced with crudes having a lower quantity of emulsifier, resulting in emulsions that separate quickly. Many stable emulsions are formed in crudes which may have the proper type and adequate amount of emulsifier.

2.1.2 Classification of Emulsions

In a system containing oil and water, there are different classes of emulsions:

- Water in oil emulsion consists of aqueous globules dispersed throughout the crude oil.
- Oil in water emulsion is composed of oil globules dispersed into the water
- Oil-in-oil (O/O), this class can be illustrated as the emulsion having polar oil as an internal phase dispersed in non-polar oil (continuous phase) or conversely, a non-polar oil as internal phase scattered in a polar oil (continuous phase).

In addition to principal styles, an unusual type of emulsion that is referred to as multiple emulsion can exist. Multiple emulsion is a complex system, in which two classes of emulsions

(oil in water emulsion and water in oil emulsion) are dispersed throughout another immiscible phase; which includes oil in water in oil emulsion and water in- oil-in-water emulsion (Schramm, 1992; Pal, 1994).

Emulsions can also be categorized based on the droplet size present in the continuous phase. The term Macro-emulsion is used when these droplets are greater than 0.1 micrometers in size.

Thermodynamically, such emulsions are not stable (concerning time, these two phases split up due to the proneness of the emulsion to minimize its interfacial energy due to coalescence and separation). Although, a stabilization mechanism can minimize or even diminish the droplet coalescence. Most oilfield emulsions are of such types.

On the contrary, another class is known as Micro-emulsions. In the presence of two immiscible phases, such emulsions are generated spontaneously due to their exceptionally minimal interfacial energy. Such type of emulsions has a relatively tiny size of droplets i.e. less than nanometer and are very stable thermodynamically. This class of emulsion differs very much from macro-emulsions in the account of their stability and formation. Fig. 2.1 illustrates the types of emulsions.

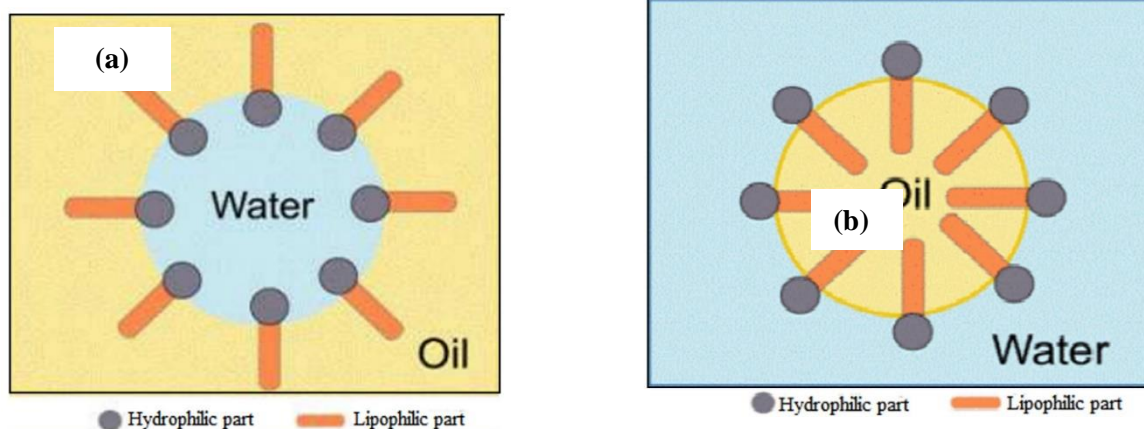


Fig. 2.1 Water in oil emulsion (a), Oil in water emulsion (b) (Khan et al., 2011)

2.2 Emulsion Stability

Emulsion stability is a significant feature of water-in-oil emulsions and refers to the firmness and tenacity of an emulsion in the respective surrounding. Few types of emulsions, on removal from the sea surface, rapidly deteriorate into discrete phases (oil and water) but some are quite stable and can persist for days to years. Stable dispersions result due to the small size of drops with the existence of an interfacial film surrounding drops. For this reason, the suspended droplets do not float rapidly and do not coalesce quickly (Luma, 2002).

Emulsion stability is considered against three different procedures, which are:

1. Creaming (sedimentation)
2. Aggregation
3. Coalescence

The separation velocity relies on certain factors which include the viscosity of dispersed phase (droplet size) and the continuous phase as well as the difference in density of the two fluids.

Variety of methods can be used to reduce separation i.e.

- Minimization of the density difference between phases.
- Reduction of the droplet size: Tiny droplets are formed due to the increase in energy input of the system, which lessens interfacial tension between oil and water and therefore it prevents coalescence.
- Increase in viscosity of continuous phase: Elevating the viscosity of the surrounding liquid leads to the decreased velocity at which the droplets will move up.
- Increase in the number of droplets: Due to substantially elevated concentration, droplets are compressed and become tightly packed, preventing their flow. Although, it may remain inflexible to raise the concentration of droplets due to physicochemical restrictions of the system.

Due to their thermodynamic nature, most emulsions tend to separate into two phases over time. Consequently, characteristics of emulsion such as droplet size distribution and flow behavior are altered. An emulsion can reach the stability level after the examined different mechanisms that could take place during the demulsification stage (emulsion breakdown), these mechanisms are summarized in Fig. 2.2.

In most cases, the emulsion droplets and continuous phases have different densities. The force of gravity causes droplets in the emulsion to move up or down through the continuous phase. Low-density droplets tend to move up high to produce a layer at the surface of emulsion that is referred to as the creaming process. Conversely, high-density droplets, tend to move down to produce bottom layer known as the sedimentation process. Since the density of water is higher than the density of oil, the droplets for water in oil emulsion tend to sediment. On the other hand, droplets for oil in water emulsions will tend to cream.

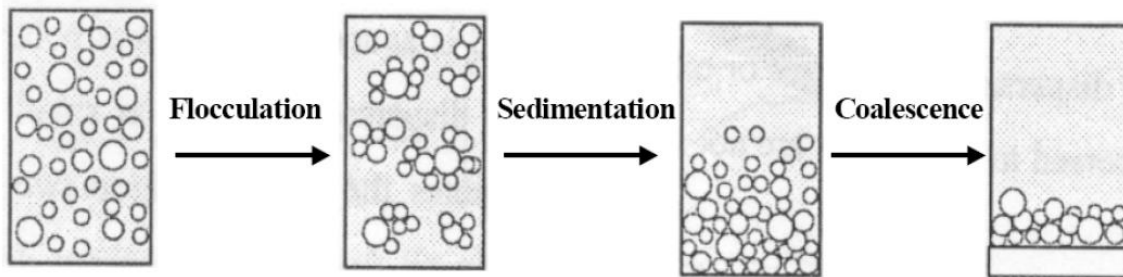


Fig. 2.2 emulsion destabilization mechanism (El-Sayed, 2012)

2.2.1 Creaming/Sedimentation

Certain exterior forces are responsible for Creaming and Sedimentation. These can be gravitational force or centrifugal phenomena. In some instances, the concentration gradient is generated if the external forces overreach Brownian motion of droplets. This results in either creaming of large droplets, shifting rapidly up at the surface (density of droplets < density of medium) or to the sedimentation phenomena in which droplets rests at the bottom of the

container (density of droplets > density of medium). In restrictive situations, droplets can assemble in a close-packed display either at the top or bottom of the container while the rest of the volume of the container filled by the continuous liquid phase.

Creaming is the opposite of sedimentation, resulting from the density difference between the two liquid phases. The term Sedimentation is used if the particles show movement in the direction in which gravity acts ($\Delta\rho > 0$). Alternatively, in the case of the flow against gravity ($\Delta\rho < 0$), the process refers to Creaming. The sedimentation process applies to most water-in-oil emulsions and solid dispersions, whereas the creaming process applies to most oil-in-water emulsions and bubbles dispersed in liquids.

2.2.2 Flocculation

Flocculation is the accumulation of droplets of emulsions (with their size remaining the same) to form bigger sizes. This is due to the existence of Vander Waals forces, usually prevailing in all dispersive systems. Flocculation occurs when the repulsive forces to retain the droplets at a distance is not enough due to weak Vander Waals forces. The flocculation intensity depends on the force of attractive energy in the system.

In the account of controlling the texture and structure of emulsions, the understanding of the flocculation process is very significant. Mathematical models have been progressed to clarify the process occurring during the formation of droplet flocs (frequency and efficiency of collisions) to foresee the effects of flocculation on the stability of emulsions, but these will not be described here. Relying on the need and choice of final products, different methods can be applied to control flocculation. The method can be chosen as directed by the components and nature of emulsion to be developed (it includes texture, structure, appearance, etc.).

2.2.3 Coalescence

Coalescence is the disintegrative phenomenon of the liquid film between small droplets, resulting in merging. The combination of these little droplets produces bigger ones. The drawback of coalescence is the total separation of the emulsion into their liquid phases. For coalescence, film or surface variation is the main driving force that brings droplets close. Here, the strong van der Waals forces hinder separation.

The combination of droplets occurs when the tinny thickness of the continuous phase separating two droplets breaks, and they fuse quickly to form a single large drop. Therefore, the rate of coalescence is a key factor in which the stability of an emulsion system depends. It should be noted that the characteristics of the thin film will determine whether emulsions are stable or unstable.

The merger of these droplets to form a massive drop is followed by the emergence of an oil layer at the surface of the emulsion. It only happens because of the breakup of the thin film between the two droplets. When droplets are in the close neighborhood, their shape may get distorted, and the surface of droplets in contact may get flattened. This deformation increases the surface area between droplets in contact, and consequently, droplets show more proneness for coalescence.

The estimation of coalescence can be significantly predicted by the rate of rupture of the thin film.

Droplets are always in continuous motion with very brief collision time with each other. On the other hand, periods longer than how long are needed to form the film for emulsion stabilization, prevention of droplet coalescence is a big issue. For prevention and control of coalescence, few methods have been established. Since the coalescence greatly relies on colloidal and hydrodynamic interactions among droplets, as well as the physicochemical behavior of the

mechanism applied in the emulsion, minimization or restriction in the interaction of droplets as well as the breakup of thin film constitute key factors where much research and efforts are required. Adsorption of emulsifiers at the oil-water interface is the reason behind the coalescence of the droplet. The ability of surfactants in restricting coalescence relies on their physicochemical features such as, the electrostatic repulsion between the droplets, which tends to prevent droplet contact.

2.2.4 Phase Inversion

This inversion phenomenon is very much evident, although the concept is not clear yet. There are two modes of dispersion that are observed based on phase fraction and initial circumstances. Phase inversion is usually observed at the time mixture go through some variations in the phase dispersal. It is a phase inversion point when inversion occurs at critical phase fraction. The dispersion undergoes continuous coalescence i.e. breakup of the thin film between dispersed droplets. This dynamic process may reach equilibrium at low dispersed phase fractions. When dispersed phase fraction elevates, the phenomena may get unstable, resulting in much dominant coalescence due to the closeness of dispersed droplets. Ultimately, when these two phases are swapped their continuity results in phase inversion (Angeli, 1996; Nädlerand Mewes, 1995).

2.2.5 Ostwald Ripening (Disproportionation)

Ostwald Ripening or disproportionation appears due to the limited solubility of liquid phases. Immiscible liquids have mutual solubility which cannot be negated. For poly-dispersive emulsions, tiny droplets will have a comparatively higher solubility than huge droplets because of the curvature effects. These tiny droplets may vanish with a certain time interval, where they merge into the system to get left on the bigger droplets resulting in a distribution of droplets sizes to larger units.

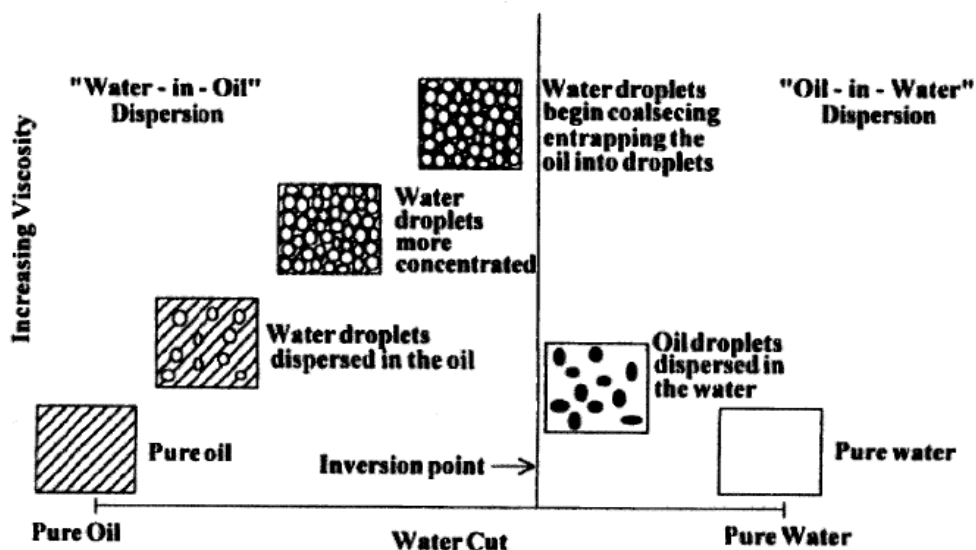


Fig. 2.3. Diagram of the suggested phase inversion mechanism by Arirachakaran et al. (1989).

2.3 Emulsifying agent

Emulsifying agent refers to the substances which aim to maintain the stability of the emulsion thus preventing the disperse phase from coalescing, flocculation, etc. The mechanism of each emulsifying agent is different. For instance, surfactant, as one broad kind of emulsifying agent, aims to lower the interfacial tension at the interface. The other agent, such as solid particles, create mechanical barriers at the interface.

2.3.1 Surfactant

Surfactants are a prevalent emulsifying agent, having adsorbing characteristics on interfaces and it can significantly change their interfacial free energy. In general, surfactants contain polar hydrophilic “heads” and non-polar hydrophobic “tails.” The polar “heads” would be the major classification of the surfactant. The most common species are non-ionic surfactants of polyoxyethylene moieties, which include alkylphenol ethoxylate. Further nonionic surfactants are lauric acids, ethoxylated sorbitan esters of oleic (M. Sztukowski, 2005). The nature of “head” and “tail” of surfactants differs, directing too many variations in properties of surfactant.

Surfactant solubility in the aqueous medium is also established by the affinity of the hydrophilic part of the surfactant with water. There are two limits to the surfactant concentration during emulsion preparation. Any concentration of emulsifier below the order of thousands of ppm (0.1%), implies the emulsifier is not enough to fully create a stable emulsion. While concentration above 5%, will not change the stability of the emulsion. The ideal surfactant concentration is in the range of 0.2-3%. Using a mixture of many surfactants as emulsifier minimizes cost and increase efficiency (Henríquez, 2009). Surfactants are classified based on the type of hydrophilic group present:

- *Anionic*: the presence of negative charge as the head moiety
- *Cationic*: the presence of positive charge as the head moiety
- *Non-ionic*: no apparent charge observed in a head moiety
- *Zwitterionic*: both negative and positive charge observed in the head moiety

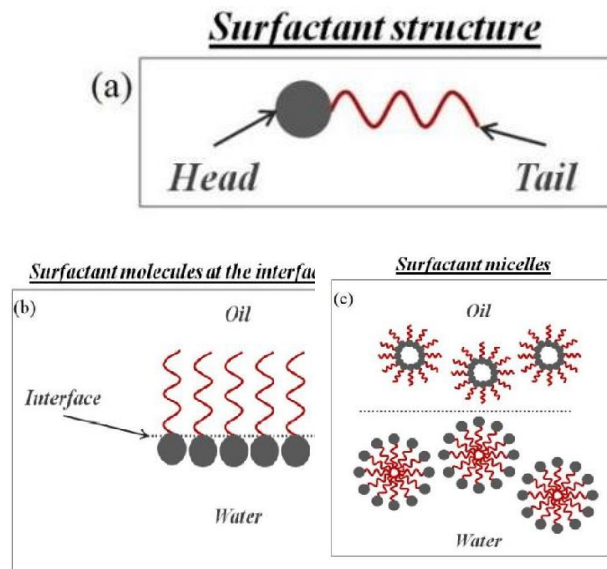


Fig. 2.4. a) the structure of surfactant, b) interfacial surfactant molecules, and c) spherical surfactant micelles (Pichot, 2010).

After surfactants dissolved in liquid, micelles would be formed by either adsorb at the interface or self-assembled. A micelle is an aggregate of surfactant molecules dispersed in a liquid colloid. The adsorbed surfactants at the interface offer an expanding force that weakens the natural tension between the continuous phase and the dispersed phase. This reduces interfacial free energy and increases the chance of emulsion not separating into their phases. Also, surfactants have the potential to increase the interfacial viscosity. This causes mechanical resistance to coalescence. Finally, the surfactant can form an electrostatic repulsion force among each micelle and reduce the chances of flocculation. The combination of these effects would thus essentially result in emulsion stabilization.

2.3.2 Asphaltenes

Asphaltenes are the largest molecular weight fraction in crude oil, have a density ranging from 1132 to 1193 kg/m³ (Akbarzadeh et al., 2004).

Asphaltenes have surface-active characteristics that prove them suitable emulsifiers. The collection of asphaltene molecules at the boundary leads to the creation of a rigid thickness, which restricts coalescence. For coalescence in between two droplets, the thin film needs to break up and drained off. However, this drainage of the film is prevented due to the natural presence of asphaltene. The principle feature for such restraint is steric repulsion exhibited by high molecular weight components of asphaltene present in the thin film. Asphaltenes are distinguished from the rest of the oil components because of their likelihood to self-aggregate (El-Sayed, 2012).

The physical state of asphaltenes existing in crude oil provides remarkable outcomes on the properties of its emulsion stability. Asphaltenes in the colloidal state stabilize the emulsions, but

it is strongly evident that its stabilizing properties are notably intense when it occurs in the solid state as precipitated from crude.

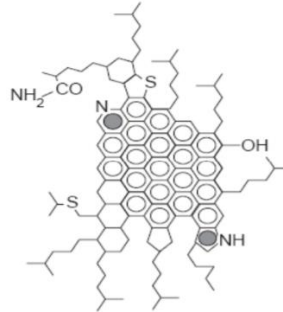


Fig 2.5. example of molecular structures in crude oil: Asphaltenes (El-Sayed, 2012)

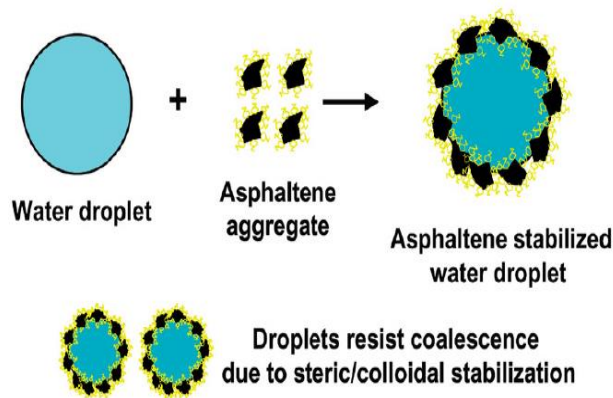


Fig. 2.6. mechanism of emulsion stabilization by asphaltenes (El-Sayed, 2012)

2.3.3 Resins

Like asphaltenes, resins are also large molecules which are complex compounds with high molecular weight and are insoluble in ethyl acetate but are soluble in n-heptane. It has a great tendency to couple with asphaltenes, resulting in the formation of the asphaltene-resin micelle. It plays a vital part in stabilizing emulsions. The asphaltene: resin ratio in the crude oil reveals the

type of film formed (solid or mobile), and emulsion stability directly depends on it. Fig. 2.7 represents the composition of crude oil. Figure 2.7 shows the composition of crude oil.

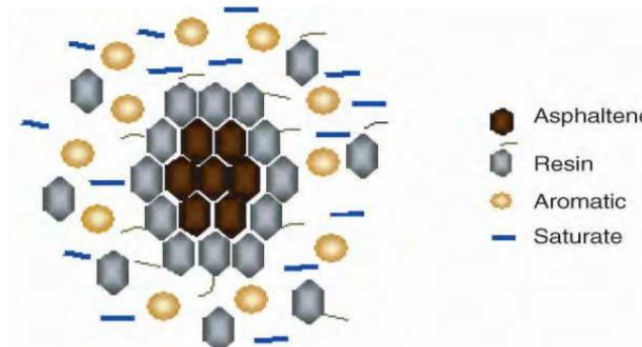


Fig. 2.7. composition of crude oil (El-Sayed, 2012)

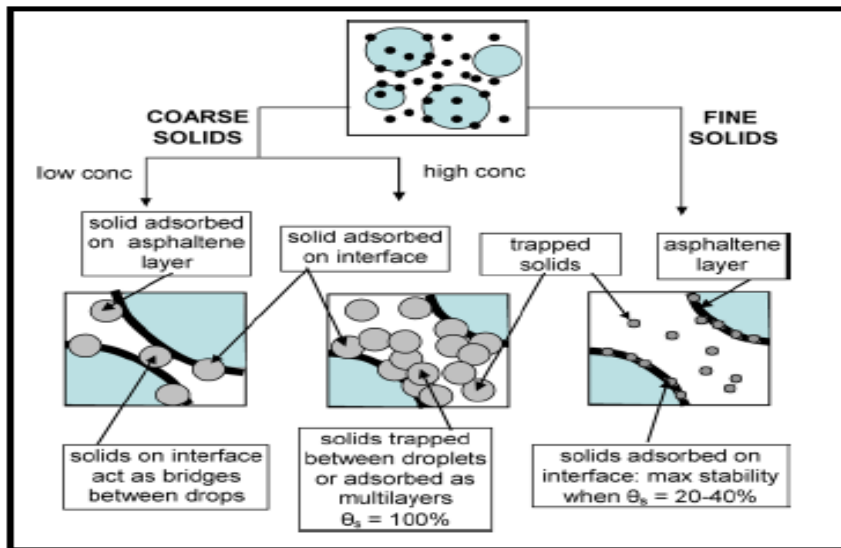
2.3.4 Fine solid particles

The fine solid particles are fine silicate, clays or ash in crude oil which are non-asphaltenic solids (Kotlyar et al., 1993). Numerous features determine the role and efficiency of these solids in stabilizing emulsions. These include density, concentration, and size distribution. When asphaltenes interact with these fine solids through adsorption or desorption, the result is the stabilization of emulsions.

These fine solids particles can stabilize an emulsion by getting adsorbed directly on the interface of water and oil as well as adsorption on the film of the surfactant. Regardless of how fine solids are adsorbed, they can generate steric hindrance between neighboring water droplets, and resisting droplet collisions (Tambe and Sharma, 1993;). In the case where strong particle-particle interaction exists, these particles can majorly cause the mechanical rigidity of the thickness forming a compact system (Tambe and Sharma, 1993). When these fine solids partially cover the surface, it can be enough to stabilize emulsions (Vignati *et al.*, 2003). When these fine solid particles are confined between the droplets, they may have the ability to decrease the process of

the aggregating emulsion as well as minimizes the probability of coalescence of droplets (Yan *et al.*, 2001). This may increase the overall emulsion viscosity which will minimize the potential of discrete separation of oil and water (Aveyard *et al.*, Houache and Yaghi, 2003. Solids-stabilized emulsions and intensity at where fine solids elevate stability of the emulsion are based on factors such as size, shape, the morphology of particle, and density, concentration, surface interaction, and wettability of system. It can be established that the stability of an emulsion maximizes in the case of a minimum size of particle and density and elevating particle concentrations. Potentially suitable arrangement of fine solids at the interface is where water in oil emulsions are stabilized by oil-wet solids, while oil in water emulsions are stabilized by water-wet solids (Fig. 2.8).

Solids cause a mechanical barrier at the interface.



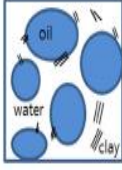
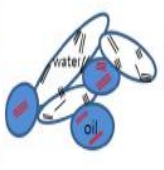
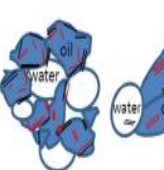
Combination of clay	Hydrophilic clay	← Mixture of clays →	Hydrophobic clay
Location of clay	Water phase/interface	Interface/phases	Oil phase
Effect of clay	Increase of interfacial area	Formation of complex interface	Increase of oil viscosity
Microstructure of Emulsion			

Fig. 2.8 possible distributions of coarse and fine solids in an emulsion (*Sztukowski & Yarranton, 2005*)

2.4 Demulsification

The application of certain procedures accomplishes the demulsification of water-in-crude oil emulsion. It can be a mechanical process, chemical procedures, thermal process, or electrical application. Several other techniques may also be applied to attain demulsification, like pH adjustment, membrane separation technique, filtration process, and heat treatment applications (Gafonova, 2000). For fast and quick separation, a vast understanding of salient features of the emulsion is needed with knowledge of mechanisms that are intricately during coalescence of water droplets (Ese et al., 1999). Demulsification is a breakdown phenomenon of the emulsion into distinct phases, majorly water and oil. The initial process needed compulsorily in oil refining is the segregation of water from crude oil. It is a common requirement for either a petrochemical industry or an oil refinery. Presently, certain emulsion breakers are widely used as chemical additives to break the water-in-oil emulsions.

The demulsification methods like thermal, mechanical, electrical or chemicals depend preferably on the physicochemical structure of oil from which they are formed, emulsification conditions,

and Aging. It concludes that the approach of demulsification for treating the water in oil emulsion may differ in respective industries.

Demulsification is splitting of an oil emulsion into two phases i.e. oil and water. For an oil refinery, the processes are carried out to ensure the following aspects,

- (a) Rate of separation
- (b) The residual amount of water after demulsification

The aspects that escalate the emulsion breaking phenomena include:

- Removal of solid particles
- Reduced agitation
- High temperature
- Increased retention time
- Control of emulsifying agents

The most common methods for emulsion treatment are:

2.4.1 Chemical demulsification

The addition of chemicals, named as demulsifiers is a very familiar procedure of treating emulsions. Such additives intend to counteract emulsifiers which tend to stabilize emulsions.

Demulsifiers being surface-active compounds, act on the oil-water interface to destabilize and breaks hard film to speed up coalescence of water droplets. Following steps are needed for optimal demulsification:

- Proper selection of demulsifier Appropriate amount of demulsifier
- Enough agitation
- Enough retention time within treaters to settle water droplets
- Facilitating the system with the thermal application, electric grids, coalescers, etc. as per requirement

Demulsifiers consists of various solvents such as benzene, toluene, xylene, short-chain alcohols, and heavy aromatic naphtha, as well as surfactants, wetting agents and flocculants. Its functions are accomplished by partially or completely dismissing the stabilization polar interface thickness surrounding emulsion droplets. Removing the film can cause numerous changes in properties like viscosity or elasticity at the interface of the protecting film, which leads to destabilization. Some demulsifiers modify the wettability of fine solids that stabilizes emulsions and therefore resulting in the rupture of film.

Dosage: Insufficient amount of demulsifier leaves the emulsion unresolved, and a high dosage can have disastrous consequences in the procedure because like emulsifiers, they are surface-active, and it may produce stable emulsions if dosed excessively. It substitutes the natural emulsifiers at the interface.

Since various components exist in crude, the efficiency of the demulsifier is majorly contributed by crude oil nature. Adsorption and displacement process rely on pH, salt content & temperature. The demulsifiers which quickly displaces the preformed rigid films and leave a mobile film (which shows minimal resistance to coalesce) as a substitute are the most efficient ones.

2.4.2 Electrical demulsification

Demulsification can also be done through the application of high voltage electricity. It is commonly accepted that water droplets are charged, and in an electric field, the droplets move quickly, the collisions between them lead to coalescence. Interface film is equally disrupted by an electric field through the relocation of the polar molecules. This reduces its rigidity and promotes coalescence. High voltage current is therefore supplied by the electrical system consisting of a transformer that is equipped with electrodes. Because the electrical field is

perpendicular to the direction of flow, the alignment of these electrodes is a very important factor.

Some designs allow for adjustable distance between the electrodes. It helps to variate the voltage to meet the need for emulsion being treated.

This type of demulsification is rarely used alone. It is used in synchronicity with the addition of chemical and application of heat. However, always the usage of electrostatic dehydration techniques is useful in terms of reducing the need for thermal application. Minimal temperature requirements result in reduced consumption of fuel, fewer troubles caused due to scale formation and corrosion and a decrease in losses of lighter fractions. Additionally, it may reduce the use of emulsion breaking chemicals.

2.4.2.1 VIEC - Vessel Internal Electrostatic Coalescer

VIEC is one of the three main separators (electrostatic coalescer) currently available. This equipment comprises high voltage modules that are isolated and fitted to the separator wall, specifically for the oil-water emulsion phase (Fig. 2.9). The main purpose of the high voltage electrostatic field is to induce coalescence of the droplets in oil, therefore, enabling easy separation. VIEC is highly flexible because it allows for the mixing of water, oil, and gas, hence it can be mounted in the first stage separator without monitoring. It promotes less heating, less chemical consumption, and cleaner oil, therefore improving performance. VIEC can reduce the water content in the emulsion from 13 to less than 5% while enhancing the capacity of water treatment as well as regulation of separator (Silset, 2008).

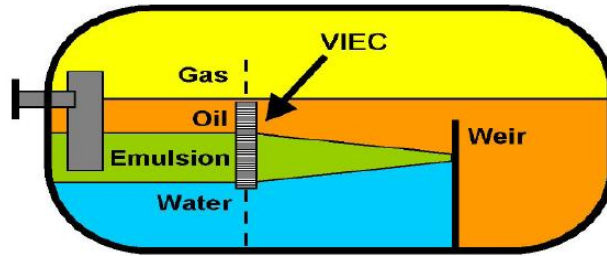


Fig. 2.9. VIEC Modul ((Silset, 2008).

2.4.2.2 LOWACC - Low Water Content Coalescer

After VIEC, LOWACC is mounted to promote the quality of oil leaving the system (Fig. 2.10).

The main component of LOWACC includes two corrugated electrode plates through which oil flow as it let smaller droplets to coalesce more. Using both VIEC and LOWACC promotes heavy oil and one step separation by subjecting water in an oil emulsion to the created electrostatic field. Short-circuiting may be avoided by insulating the electrodes. LOWACC is primarily designed for use in both high- and low-pressure separators, as well as for separators with problematic separation (Silset, 2008).

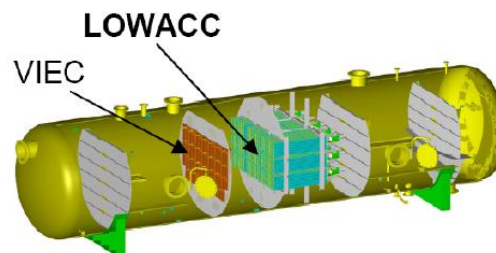


Fig. 2.10. VIEC and LOWACC all installed in the same separator to accomplish total separation ((Silset, 2008).

2.4.3 Thermal Demulsifications

The heating process enhances the breakage and separation of Emulsions. It decreases the oil viscosity and elevates the rate of settling for water. Low interfacial viscosity caused by elevated temperatures may also result in destabilizing rigid films. Additionally, the higher thermal energy of droplets promotes the coalescence frequency among water droplets i.e. heat promotes

demulsification. Despite the above facts, thermal demulsification rarely fixes the emulsion issue alone. High temperatures may have some damaging impacts as well.

Primarily, heating the stream costs much. Secondly, it may lead to loss of lighter fractions of crude oil minimizing its volume and API gravity. Lastly, due to increased temperatures, treating vessels are more prone to corrosion and scale deposition. So, the decision to use heat for demulsification should be made after investigating the overall economic analysis of the treatment facility.

2.5 Emulsion characterization techniques

Various analytical techniques have been established to characterize the droplets in emulsions, e.g. electron microscopy, light microscopy, dynamic and static light scattering, neutron scattering and electrical conductivity, and Nuclear Magnetic Resonance (NMR). However, most of these techniques have limitations, or they are appropriate only for dilute applications, while most emulsions of practical status are concentrated and optically opaque.

2.5.1 Microscopy

The microscopic technique is used as a first step to characterize the emulsion system to determine the best option between physical and chemical separation techniques. There are different microscopic methods to characterize the two main types of emulsions (oil in water and water in oil emulsion). The three main microscopic techniques used in the crude oil industry for the separation of emulsions into their phases are as follow:

2.5.1.1 Light Microscopy (LM)

Light microscopy is primarily employed at Fuel Processing Laboratory (FPL) to investigate various samples. It is very important to remember that a very thin sample for transmitted light observation leads to misrepresentation of the original sample. In addition to this, it can also

reverse water in oil emulsion into oil in water emulsion upon pressing it between two glass slides. Fluorescence is a property of many organic materials and this includes aromatic groups bonded to aliphatic polyenes, polar aromatics, and asphaltenes. Few inorganic particles have fluorescence properties like those of organic components concerning fluorescing color and intensity. Therefore, it is possible to identify the mineral and oil phases in each sample by LM. For instance, quartz and clay and most of the inorganic particles do not exhibit fluorescence whereas most of the oil components do.

The small depth of field that makes an accurate determination of droplet sizes difficult, is the main drawback of optical microscopy. The water-in-oil emulsion has only a few droplets in focus as shown in Fig. 2.11. The ones above the plane of focus are larger than they are with fuzzy halos. Those below the plane of focus appear as points of reflected light. An image such as this is not amenable to automated image analysis.

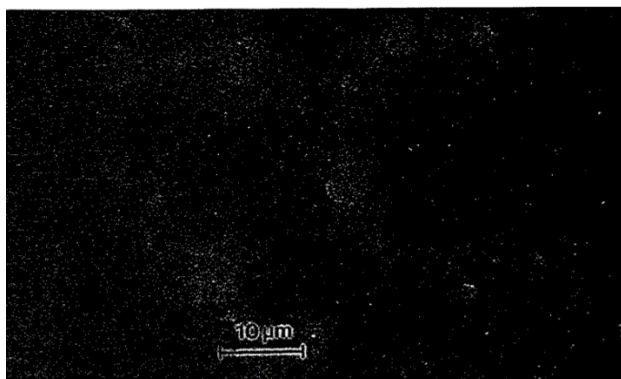


Fig. 2.11 Conventional light microscopy image of a water-in-oil emulsion (Munoz, et al, 1997)

2.5.1.2 Cryogenic Scanning Electron Microscopy

The principle of scanning electron microscopy comprises scanning the surface of a sample that is initially metal coated with a beam of electrons. However, for this technique to be significant, the samples must be solid. Therefore, Samples are frozen for the study purpose in the vacuum of a

scanning electron microscope (SEM). Rapid freezing in liquid nitrogen (78 K) or in a nitrogen slush (68 K), is typically accompanied by the fracturing of the sample to reveal the interior. It is important to rapid freeze samples to avoid changing morphology or the interaction between different parts. The frozen sample on a cold stage in the electron microscope allows imaging an emulsion as well as getting compositional information from the x-rays released as the electron beam penetrates the sample. When samples have high water content, water can be sublimed under controlled conditions, to reveal the associations between the various components.

As shown in Fig. 2.12, a large depth of field in the SEM, make it relatively easy to determine the size distribution of the dispersed phase and with the electron probe exciting x-ray emission, we can get chemical compositional information about the sample as well. Until recently, this was the method of choice for characterizing emulsion systems. With the development of inexpensive computing power, an improvement in optical microscopy called confocal laser scanning microscopy is rapidly supplanting cryo-SEM (Munoz, et al, 1997).

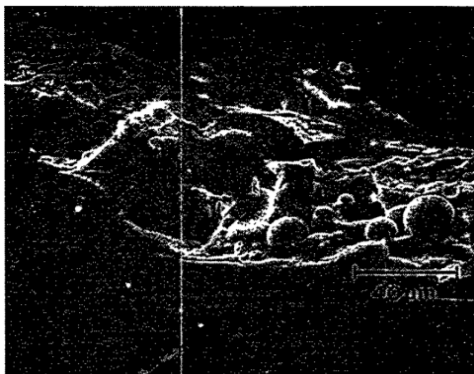


Fig. 2.12. Cryo-SEM image of a water-in-oil emulsion showing the interior fracture surface (Munoz, et al, 1997)

2.5.1.3 Confocal Laser Scanning Microscopy (CLSM)

This technique compensates for the depth of field limitations arising from light microscopy characterization. It combines some aspects of light microscopy and scanning electron

microscopy (SEM). Using a finely focused laser beam, CLSM scans the sample features point-by-point. The most important aspect of CLSM is its ability to remove information that is out of focus from the image through a spatial filter that comprises of modifiable iris set. With digitized images and computer manipulation, a series of images collected as a function of depth can be combined and reconstructed with a depth of field like that in scanning electron microscope images. Through this, independent imaging of structures that are different in height differences on the order of the wavelength of the light source, therefore allowing construction of profiles, three-dimensional representations, and measurable dimensions of elevation. (Munoz, et al, 1997).

2.5.2 Light scattering

Static light scattering techniques, also known as laser diffraction techniques for particle size characterization rely on the principle that the scattering pattern emitted as a result of the laser beam being focused on unstable emulsion correlates with the particle size dispersal of the emulsion. Equipment utilizing this technique is usually incorporated with software that comprises mathematical models which are often based on “Mie theory.” The models predict the scattering pattern from the particle characteristics: absorption coefficient, diameter, and refractive index ratio. Thereafter, the software that uses the measured scattering pattern and the predicted one establishes the best-fit and then generates reports as a data table or plots (particle concentration versus particle size. It should be noted that the concentration can either be in volume or number, while the size in either diameter or radius. Light scattering instruments that are commercially available are well suited for particle size ranging from ca. 0.1 to 1000 μm . Typically, the instrument requires sample preparation to a relatively low concentration (≤ 0.1 wt. %) to ensure the translational passage of a light beam while avoiding multiple scattering effects.

Therefore, emulsion samples need to be carefully and sufficiently diluted without compromising its microstructural properties.

Dynamic light scattering (DLS) techniques exploit the temporal fluctuations in intensity, when a light is scattered by particles whose spatial locations change frequently owing to Brownian motion, for particle size characterization. The frequency of the fluctuations depends on the speed of the particle which is influenced by the particle size. Smaller particles move faster than bigger counterparts, thus would result in more relatively fast concentration variations. Emulsion's particle size distribution is obtained from the alteration in the concentration of dispersed waves in each time at a scattering angle through applicable mathematical models. Commercially available DLS instruments are suitable for particles whose diameters range from 0.003 to 5 μm . However, the concentration requirement varies with the method used for determining the intensity fluctuations. Some instruments measure transmitted light through an emission, thus limiting their suitability to sufficiently dilute emissions ($< 0.1 \text{ wt } \%$); while others measure back-scattered light instead, thereby making them suitable for both concentrated and dilute emissions (0.001 – 10 wt %). Moreover, diffusing wave spectroscopy (DWS) is an advanced DLS technique that extends the analytical capacity of light scattering to opaque samples (Dalglish, 2006). Generally, DWS works like DLS except for the detected photons which follow diffusive paths because of the highest multiple scattering in the opaque media, as opposed to sole scattering. The best application of the DWS technique is analyzing the mean size of particles or aggregates.

2.5.3 Nuclear Magnetic Resonance (NMR)

NMR-based particle sizing employs the interactions that exist between the proton nuclei and radio waves to provide insight on the microstructure of emulsions. It operates by subjecting an

emulsion to a static magnetic field gradient, which excited some of the nuclei to higher energy levels. The excitation, in turn, leads to a detectable signal whose amplitude relies on the motion produced by the nuclei in the sample. This amplitude has an inverse relationship with the motion of the nucleus. Hence, the rate of reduction in the signal amplitude is used for studying the molecular motion. Unlike in a bulk liquid, the motion of a liquid within an emulsion droplet undergoes restricted diffusion owing to the presence of interfacial boundaries. However, this phenomenon is not apparent within a short-time domain given the distance covered. The attenuation in NMR signals at different instances is used to determine when the diffusion is restricted, which is in turn utilized to estimate the droplet size distribution via suitable mathematical models. Commercially available NMR-based instruments are appropriate for particles ranging from 0.2 to 100 μm in size, whose concentrations in an emulsion may range from 1 to 80 wt %; thus, in most cases, dilution is not necessary. This technique determines the actual size of individual droplets in flocculated emulsion (not floc size) because the restricted diffusion is not affected by the flocculation process. Furthermore, using NMR techniques for a continuous phase of emulsions (flocs) provides insights into the structural organization of droplets within flocs. NMR techniques for particle size distribution are non-destructive and suitable for concentrated and optically opaque emulsions

2.5.4 Coulter Counter

Coulter counter techniques, also known as electrical pulse counting techniques relied on the difference in electrical conductivities when a dilute emulsion passed through a small orifice to count and size particles. In simple form, the emulsion under investigation is contained in the beaker containing two dipping electrodes, one of which is housed in a glass tube with a tiny hole for the suction of the emulsion. Upon the passage of each particle through the orifice, a transient

drop in electrical current is observed, owing to the relatively lower electrical conductivity of oil. The instrument records the transient drop as an electrical pulse, which in turn is converted to another useful parameter such as droplet concentration and particle size distribution (PSD). The concentration of droplets is estimated as the number of pulses through the hole in each volume of emulsion, while the PSD is analogous to the distribution of specific pulse height because an electrical pulse height depends on the volume of the particle. Commercially available colter counter determines the PSD for particle size ranging from 0.4 to 1200 μm . Typically, such a large range of particle size is usually covered by using a series of glass tubes with varying sizes of holes. For sample preparation, the instrument requires a relatively low concentration (≤ 0.1 wt. %) to ensure the passage of a single particle through the hole at a time. Hence prior to analysis, emulsion samples need to be well-diluted without compromising its microstructural properties.

2.5.5 The Ultrasonic Spectrometry

It is based on the variation of ultrasonic attenuation relative to frequency, as well as the shape of its spectra is a function of particle concentration and size distribution. An emulsion is positioned in a controlled chamber (temperature monitored) with provision for ultrasonic spectrum measurement, typically 0.1 – 150 MHz. Ultrasonic spectrometry instruments are usually incorporated into software (e.g. ECAHtheory) that allows the prediction of ultrasonic spectra of emulsions from the particle characteristics and the physical properties of dispersed and continuous phases. Particle characteristics include concentration, size and size distribution. Using the software, the best-fit particle size distribution is determined by comparing measured ultrasonic spectra and hypothetically projected ones and then generate suitable data which are presented as tables or plots of particle size against the concentration of particle. Most large-scale ultrasonic spectrometers have a measurement range of 0.01 to 1000 μm for particle diameter,

which in principle works for emulsions within the range of 1 – 50 wt % (particle concentration). However, at higher droplet concentrations or flocculated emulsion, the governing principle becomes non-applicable, and as such any data obtained outside the earlier specified range become inaccurate. (Chanamai, Alba & McClements, 2000a). It is important to note that ultrasonic spectrometry measurements are non-destructive hence may be performed *in situ* for optically opaque emulsions.

The following are the advantages of ultrasound techniques:

1. The sample does not need to be diluted in ultrasound spectroscopy, because it may change particle structure, causing aggregates to disperse and therefore contaminate the sample.
2. Particle sizing is based on a thorough and essential theory, where the only requirement is requisite physical constants are known, and calibration is not required. Implying a high level of accuracy.
3. Compared to light scattering intensity which varies with the sixth power of particle diameter, ultrasound scattering in aqueous systems is controlled by thermal and viscous-inertial scattering for the smallest particles that vary as the inverse square power of particle diameter. Therefore, combining light scattering and ultrasound scattering will prove very efficient to characterize systems that contain both nanoparticles and larger particles.
4. It has high measurement versatility and confidence in the determined the particle size distribution because it can measure both phase and signal amplitude simultaneously.
5. Extant multiple scattering theories are capable of generalization to systems of several types of particles, allowing particle sizing in heterogeneous industrial systems.

6. Ultrasound spectroscopy can be engineered to provide particle size information, non-intrusively and in-process, making it suitable for industrial use.
7. It allows for a reduced impact of particle shape by selecting a suitable frequency range. Even in the case of rods, the volume fraction, diameter and length can often be determined.

2.5.5.1 Ultrasonic attenuation spectroscopy

All the various approaches to ultrasound attenuation spectroscopy have some common problems. For instance, accurate measurement of the speed of sound requires correction for diffraction and interference effects. These considerations create the need for fast signal processing, electrical matching circuitry and frequency generators which when combined comprise a significant investment in electronics and software.

There are few instruments that measure the absolute speed of sound and attenuation. The most accurate being laser interferometry that directly measures the wavelength of an acoustic standing wave, produced at a known frequency (Vance and Brown, 2010).

Very good data for water are used and then instruments are calibrated using water; even though it introduces several errors, it is a widely used technique. The greater the difference between the speeds of sound in the measuring system than the water, the bigger the errors are. Water temperature at 20 °C, gives the coefficient of the speed of sound as 3 m/ (s K). Temperature fluctuations as small as 0.1 °C will create velocity fluctuations of 0.3 m/ (s K), therefore, temperature control is an important parameter for accurate velocity spectrometry. On the other hand, temperature control is generally less critical where attenuation spectrometry is concerned.

2.5.5.2 Particle size analysis by Acoustic Spectroscopy

The analysis of the particle size by Acoustic Spectroscopy include:

- Measuring the attenuation and velocity spectra in the dispersion and normally the pure suspending phase
- Predicting the spectra for a general particle size distribution and concentration by scattering theory
- Inverting the measured spectrum to obtain the particle size distribution and the concentration by finding the predicted spectrum that best fits the measured spectrum.

2.5.6 Ultrasonic Sensor System and Sensor Classification

The effective use of ultrasonic sensors requires their combination with sensitive transmitter/receiver electronics and suitable data-acquisition electronics. As opposed to the past, current ultrasonic systems are feasible as compact devices at low cost due to modern microelectronics.

Fig. 2.13 presents an ultrasonic sensor system and possible sensor configurations. There are two distinct methods: The first being the active transmission of acoustic waves and receiving of these waves later by ultrasonic sensors. Usually, piezoelectric transducers are used to transform an electrical signal into an ultrasonic wave and converse is true. The ability to use the same transducer for both transmitting and receiving functions in many applications makes important. Following the requirement for the acoustic path, characteristic parameters of the ultrasonic wave are modified. Therefore, the ultrasound signal carries information about the properties between transmitter and receiver, where an intelligent sensor system must extract this information. A time resolution of fewer than 1 ns down to a few picoseconds can be attained for the propagation time determination. This is equivalent to accuracy for the ultrasonic velocity better than 0.1% and the flow velocity of a liquid medium better than 1%. The amplitude accuracy is normally measured in the range of 1%. The higher resolution of both parameters can be reached by special electronic

circuits (e.g., 12- to 14-bit ADCs and very fast circuits), averaging and specific signal evaluation. The reliability of these measures depends on parameters such as pressure, temperature and so on, determined at the same time as ultrasonic parameters with extreme accuracy. Understanding these relations is necessary in order to develop new applications for ultrasonic sensors, for instance, in process control, for special distance measurements and others. The second way of using ultrasonic sensor system principles is shown in Figure 18, represented by 3 and 4, where one sensor is directly coupled with the medium under investigation and influenced by it. In example 3 the acoustic impedance or the reflection or transmission coefficient is measured by detection of the amplitude changes. The sensor acts as both transmitter and receiver. In example 4 the resonance frequency of an ultrasonic sensor is changed by deposition of a material onto the sensor surface or by the interaction of a sensitive layer on the sensor with surrounding species in a gas or a liquid. The latter is the basis for the so-called mass-sensitive sensors. They can play an increasing role in the sensor scenery in the future. Based on the type of change ultrasonic signal following its path from transmitting to receiving transducer undergoes, ultrasonic sensors can be divided into four groups:

- Flow sensors
- Distance sensors
- State sensors
- Micro-sensors

The advantages of ultrasonic sensors include:

- Being non-invasive
- They have high resolution and accuracy
- Ability to do an in-line measurement

- They have excellent long-term stability
- Rapid response, usually a fraction of a second
- They have a low power consumption

The disadvantages of ultrasonic sensors are:

- Increase in electronics for high accuracy and information)
- Integration along the entire sound path
- There is an increase of the attenuation of sound with a frequency

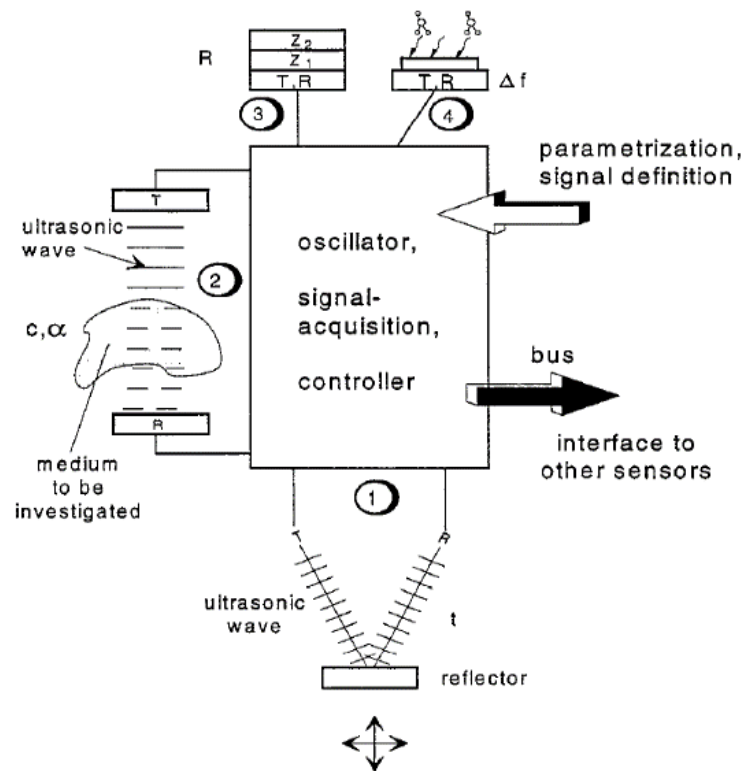


Fig. 2.13 Ultrasonic sensor system (Hauptmann, Lucklum, Piittmer, & Henning, 1998).

2.5.6.1 Ultrasonic flow sensors

Many applications require measurement of the volume-flow velocity and mass-flow velocity. For this reason, flow sensors have been applied extensively in industrial processes compared to temperature and pressure sensors. For all these applications there is a trend towards a strong,

accurate measuring device without moving parts and with a minimum distortion of the flow.

Besides ultrasonic flow meters, only thermal methods and vortex meters comply with this trend.

Various methods available for ultrasonic flow meters are based on three acoustic effects. These include: (i) the drift effect (ii) the Doppler Effect and (iii) the attenuation or diffraction effect.

2.5.6.2 Ultrasonic state sensors

Many branches of industry such as chemistry, oil, biotechnology, food, and agriculture have turned their attention to ultrasonic techniques for process monitoring and control. Ultrasonic state sensors are ultrasonic sensors for the detection of typical process parameters. There were many limitations for ultrasound in-process monitoring in the past due to the lack of a technical base (Bergmann, 1954). In the present time, microelectronics can handle data with high speed and resolution, where it can be stored and compared. Using special software, new information can be extracted from experimental data. Therefore, giving new opportunities for ultrasonic techniques. An important advantage of ultrasonic techniques is the fact that they can be used non-invasively. The containment materials, particularly metals, are usually 'transparent' to ultrasound. Other advantages of ultrasonic techniques are that:

- No moving parts are involved, making response time fast
- The energy levels are low and non-hazardous equipment can be constructed
- Provide a range of mutually compatible techniques.

Another important feature of ultrasonic techniques, which makes them better than optical techniques, is that the velocity of ultrasound is relatively low compared with that of light. Hence, the wavelength of an acoustic wave, e.g., in the order of megahertz frequencies, is in the millimeter range. The following are the disadvantages of ultrasonic techniques:

- Integral information is always received (ultrasonic techniques are not suitable for trace analysis)
- Very often special knowledge of the substance properties is necessary
- Development and handling of sophisticated electronics

The principal ultrasonic parameters which can be measured are velocity, attenuation, and impedance. From these parameters, one can derive the particle sizes or particle distributions of dispersed phases. Most ultrasonic state sensors use compressional ultrasound. The frequency is typically in the range of 0.5 - 10 MHz except for attenuation particle-size sensors. The ultrasound is normally generated by piezoelectric transducers of the small and convenient size which are readily available commercially. Some form of 'coupling' is used to transmit the ultrasound from the transducer into and back from the system under investigation. Electronic systems are developed and available which enable transducers to generate either continuous waves or pulses, or which detect and amplify the received signals, determine the time between a transmitted pulse and the received echoes and carry out data processing. Very high resolution and accuracy must be achieved, otherwise ultrasonic state sensors are not interesting for the applications mentioned (Hauptmann, Lucklum, Piittmer, & Henning, 1998).

2.5.6.3 Ultrasonic Velocity Sensors

Ultrasonic measurement principles for sound velocity are well known. An example is with a fixed distance of transmitter and receiver, which is the most commonly used arrangement in technical applications. The velocity is determined using the time of flight over a known distance. For very accurate measurements special tricks for the triggering of the echoes with different amplitudes are used and the thermal-expansion coefficient of the content material must be considered. This velocity can also be determined by other techniques such as interferometric or

resonance principles, but they do not play a role in applications in industrial equipment.

Currently, the most significant ultrasonic parameter for use in-process monitoring and control is the velocity of sound. Once the velocity of ultrasound in the medium is determined, the data can be used in several ways. These include identification of liquids, concentrations of solutions, the behavior of mixtures of liquids and two-phase liquid systems. One of the most remarkable examples of this application is the continuous on-line measurement of the original gravity of beer (Sterbinger, 1985). Beer is a three-component mixture consisting of alcohol, extract, and water (Hauptmann, Lucklum, Piittmer, & Henning, 1998).

2.5.6.4 Ultrasonic Attenuation Sensors

It is very difficult to measure the attenuation of ultrasound more especially under plant conditions. The primary reason is the fact that ultrasonic signal strength decreases not entirely due to attenuation in the medium under investigation, but also because of other factors such as reflections at the interfaces, beam divergence and changes in transmitter and receiver performance because these factors are difficult to keep constant. The electronics challenge is to obtain the same or a similar accuracy and resolution for the attenuation determination in a wide range of received ultrasound signal amplitudes which can differ by a few orders of magnitude due to substance properties. In most cases, attenuation and velocity are measured simultaneously. Thus, the electronic requirements are stricter. When dealing with commercial systems for detecting the ultrasonic velocity, high accuracy is only achieved for a special category of liquids, e.g., two- or three-component solutions, special mixtures, etc. The question of whether the measurement of attenuation supplies new or more information about the investigated liquid systems, is answered as follows:

- Attenuation is only determined when dealing with a complicated multi-component system where the measurement of ultrasonic velocity is not very accurate or is very costly. Fig. 2.14 illustrates the block diagram of an ultrasonic device for simultaneous measurement of velocity and attenuation (Puttmer et al., 1995). It works at a frequency of 1.5 MHz. The accuracy of the ultrasonic velocity is about 0.1%. The measurement of attenuation has an approximate error of 1%.
- It is important to determine attenuation when ultrasound is used for particle-size determination. The relationships between acoustic parameters and the influences of several material data are relatively complicated. It is important to consider the ultrasonic attenuation in emulsions, suspensions or similar systems is caused by different effects, that include thermal, viscous, scattering and relaxation effects. They are determined strongly by specific material parameters (thermal conductivity, viscosity, particle diameter, etc.) and the applied frequency. A particle analyzer based on acoustic attenuation spectroscopy uses a frequency range from 1 - 100 MHz and particle diameters and distributions from 0.01 to 10 micrometers can be detected (Bedford Hills, 1995). The most interesting property of this analyzer is that it can measure volume fractions from 0 to 50% (Hauptmann, Lucklum, Piittmer, & Henning, 1998)

References

- Dalgleish, T., Williams, J. M. G., Golden, A.-M. J., Perkins, N., Barrett, L. F., Barnard, P. J., Watkins, E. (2007). *Journal of Experimental Psychology: General*, 136(1), 23–42.
- El-Sayed, M. (2012). Factors Affecting the Stability of Crude Oil Emulsions. *Crude Oil Emulsions- Composition Stability and Characterization*.
- Hauptmann, P., Lucklum, R., Piittmer, A., & Henning, B. (1998). Ultrasonic sensors for process monitoring and chemical analysis: state-of-the-art and trends, *67(97)*, 32–48.
- Henríquez, C. (2009). *W/O Emulsions: Formulation, Characterization and Destabilization*. Thesis. Retrieved from
- Kilpatrick, P. K. (2012). Water-in-crude oil emulsion stabilization: Review and unanswered questions. *Energy and Fuels*, 26(7), 4017–4026.
- Munoz, V. A., & Mikula, R. J. (1997). Characterization of petroleum industry emulsions and suspensions using microscopy. *Journal of Canadian Petroleum Technology*, 36(10), 36–40
- Silset, A. (2008). *Anne Silset Emulsions (w/o and o/w) of Heavy Crude Oils. Destabilization and Produced Water Quality*.
- Munoz, et al. “Characterization of Petroleum Industry Emulsions and Suspensions Using Microscopy.” *Application of Super High-Density Drilling Fluid Under Ultra-High Temperature on Well Shengke-1 - One Petro*, Society of Petroleum Engineers, 1 Oct. 1997.
- Reza Zolfaghari (2016), ‘Demulsification Techniques of Water-in-Oil and Oil-in-Water Emulsions in Petroleum Industry,’ *Separation and Purification Technology*, 170, 377–407.
- Souleyman A Issaka, Abdurahman H Nour, and Rosli Mohd Yunus (2015). ‘Review on the Fundamental Aspects of Petroleum Oil Emulsions and Techniques of Demulsification,’ 6.2
- Dominique Langevin and Jean-françois Argillier (2015)., ‘Interfacial Behavior of Asphaltenes’, *Advances in Colloid and Interface Science*, 233 x, 83–93.
- (Yan & Masliyah, 1993)
- Peter K Kilpatrick (2015). ‘Water-in-Crude Oil Emulsion Stabilization: Review and Unanswered Questions,’ x.
- Mes Abdel-Raouf (2015)., ‘Factors Affecting the Stability of Crude Oil Emulsions,’ *Crude Oil Emulsions – Composition Stability and Characterization*, x, 183–204.
- Ahmed M. Al-Sabagh, Notaila M. Nasser and Tahany M. Abd El-Hamid (2015)., ‘Investigation of Kinetic and Rheological Properties for the Demulsification Process,’ *Egyptian Journal of Petroleum*, 22.1 x, 117–27.

M. Al-Yaari and others, 'Effect of Water Salinity on Surfactant-Stabilized Water-Oil Emulsions Flow Characteristics,' *Experimental Thermal and Fluid Science*, 64.July 2016 (2015), 54–61.

S. N. Ashrafizadeh and M. Kamran, 'Emulsification of Heavy Crude Oil in Water for Pipeline Transportation,' *Journal of Petroleum Science and Engineering*, 71.3–4 (2010), 205–11.

Bernard P. Binks and Andrew T. Tyowua, 'Particle-Stabilized Powdered Water-in-Oil Emulsions', *Langmuir*, 32.13 (2016), 3110–15.

Joseph D Mclean and Peter K Kilpatrick, 'Effects of Asphaltene Aggregation in Model Heptane – Toluene Mixtures on Stability of Water-in-Oil Emulsions,' 34.196 (1997), 23–34.

Manar El-sayed Abdel-raouf, 'Factors Affecting the Stability of Crude Oil Emulsions Factors Affecting the Stability of Crude Oil Emulsions,' 2016.

David Julian McClements (2007), 'Critical Review of Techniques and Methodologies for Characterization,' 649, 611–49.

F. Alba and others, 'Acoustic Spectroscopy as a Technique for the Particle Sizing of High Concentration Colloids , Emulsions, and Suspensions,' 1999, 495–502.

David Julian McClements, 'Ultrasonic Measurements in Particle Size Analysis', 2016.

John N Coupland and D Julian McClements (2001), 'Droplet Size Determination in Food Emulsions : Comparison of Ultrasonic and Light Scattering Methods', 50, 117–20.

Nils Van Der Tuuk Opedal, Geir Sørland and Johan Sjöblom (2009), 'Methods for Droplet Size Distribution Determination of Water-in-Oil Emulsions Using Low-Field NMR,' *Diffusion-Fundamentals.org*, 9.7, 1–29.

Liyana Nadirah, H N Abdurahman and D Rizauddi (2014), 'Rheological Study of Petroleum Fluid and Oil-in-Water Emulsion,' *NadirahInternational Journal of Engineering Sciences & Research Technology*, 3.1, 129–34.

Encarnación Jurado et al (2007) 'Estimation of the Distribution of Droplet Size, Interfacial Area and Volume in Emulsions,' *Colloids and Surfaces A: Physicochemical and Engineering Aspects*, 295.1–3, 91–98.

I.N.a. Anisa and H.a. Nour (2010), 'Effect of Viscosity and Droplet Diameter on Water-in-Oil Emulsions: An Experimental Study,' *Engineering and Technology*, 38.2, 213–16.

Peter Hauptmann et al (1998), 'Ultrasonic Sensors for Process Monitoring and Chemical Analysis : State-of-the-Art and Trends', 67.97, 32–48.

D. J. McClements (1996), 'Principles of Ultrasonic Droplet Size Determination in Emulsions', *Langmuir*, 12.14, 3454–61. Clint P Aichele and others, 'Characterization of Water-in-Crude-Oil Emulsions in a Complex Shear Field,' *Experimental Thermal and Fluid Science*, 53 (2014), 190–96.

Ronaldo Gonçalves dos Santos, Antonio Carlos Bannwart and Watson Loh (2014), 'Phase Segregation, Shear Thinning and Rheological Behavior of Crude Oil-in-Water Emulsions,' *Chemical Engineering Research and Design*, 92.9, 1629–36.

Jerzy Bałdyga, Magdalena Jasi and Adam J Kowalski (2015), 'Chemical Engineering Research and Design Effect of Rheology of Dense Emulsions on the Flow,' 8 3–12.

Chapter 3. Characterization of oils and their emulsion by ultrasonic techniques

Abstract

An ultrasonic based method to characterize oils and their emulsions have been developed through a series of tests in different systems. The two measured acoustic parameters of the low intensity propagating wave are the time of flight and amplitude from which acoustic velocity and attenuation are estimated. The variations in asphaltene content of crude oil samples are linked to the stability of its emulsions. It is demonstrated that the changes in the composition of crude oil emulsions that cannot be seen visually, can be analyzed using acoustic parameters. The analyzed results show that the ultrasonic technique has high potential to be used for monitoring emulsion stability and track changes in emulsions characteristics such as droplet size and water content.

3.1 Introduction

Formation of emulsions specially water-in-oil emulsion presents challenging problems in many industrial operations more notably in crude oil production and its refining and petrochemical processes. The emulsions are created as a result of intimate contact between the hydrocarbon and aqueous phases involved. This is the case during crude oil production steps where comingled water generates water-in-oil emulsions (Kokal, 2005; Yan et al., 2001). The crude oil collected from the ground also contains high levels of salts which can give rise to several problems such as heat exchanger fouling and catalyst poisoning in the downstream refining processes. The impurities of salts and sand in crude oil are removed in a desalter unit in an oil refinery. Here process water is mixed with incoming crude oil to dissolve out the salts, and the emulsified mixture then enters separation vessels where the cleaned oil leaves from top and water containing dissolved salts leave from the bottom. However, the separation rate of the emulsion into the individual phases is affected by many factors such as crude oil composition, asphaltene content, droplet size distribution, presence of fine particles, etc. The emulsion destabilization

process involves several steps which include flocculation, sedimentation, coalescence and finally phase separation due to the density difference between oil and water. Flocculation of water globules involves the aggregation of droplets to form clusters that sediment under the influence of gravity. During the coalescence step, flocculated droplets fuse to form larger ones leading to phase separation (Graham et al., 2008). The coalescence step can be slowed down by the presence of stabilizing agents such as clay particles and crude oil components such as asphaltenes, resins, and acids (Moradi et al., 2011; Graham et al., 2008). Emulsion stability can be determined by several methods such as bottle tests and electrical methods (Wang and Alvarado, 2009). Bottle tests that rely on water resolution are more common due to low cost and ease of tracking. It can be combined with other methods such as electrical and acoustic techniques.

The emulsion properties such as appearance, stability, and rheological behavior rely on their natures and droplet interactions as well (Derkach, 2009 and McClements, 1996). Various analytical techniques have been established to characterize the droplets in emulsions, e.g. electron microscopy, light microscopy, dynamic and static light scattering, neutron scattering and electrical conductivity, and Nuclear Magnetic Resonance (NMR) (Derkach, 2009; Coupland and McClements, 2001; McClements, 1996). However, most of these techniques have limitations or they are appropriate only for dilute applications, while most emulsions of practical status are concentrated and optically opaque (Coupland and McClements, 2001). For example, the NMR approach was utilized effectively to measure droplet size distribution and volume fraction of the dispersed phase. However, NMR spectrometers are quite expensive to purchase and are not easily adapted for on-line measurements. Moreover, they are not suitable for smaller droplets characterization, as well as require highly skilled operators. Ultrasonic attenuation spectroscopy

(UAS) is emerging as an attractive technique among other technologies to measure droplet size distributions in emulsions because of its ability to analyze concentrated and optically opaque emulsions. It depends on the conversion of the ultrasound measurements including the acoustic velocity and attenuation coefficient into droplet size information (Su et al, 2008 and McClements, 1996). Ultrasonic waves have frequencies ranging from 20 kHz to 10000 GHz (Ensminger and Bond, 2012). However, ultrasonic frequencies below 20MHz are the most commonly used in industrial applications. The attenuation coefficient of the propagating wave is affected by fluid viscosity and frequency (Atkinson and Kytomaa, 1992). The systematic monitoring of acoustic properties of an emulsion including sound velocity and sound absorption (attenuation) may offer insightful information regarding the droplet size distribution and emulsion stability (Shukla et al., 2010 and Atkinson and Kytomaa, 1992).

The focus of the present work is the development and testing of ultrasonic based technology to characterize oils and their emulsions as well as monitor changes in emulsion characteristics over time. The emulsion characteristics are expected to be a function of the type of oil, level of impurities and mixing intensities, etc. The ultrasonic parameters recorded are changes in acoustic velocity, signal attenuation, and its frequency spectrum. The ultrasonic techniques were selected for their several advantageous features including; lower power consumption, in-line measurement, long-term stability, non-invasiveness, high resolution and accuracy, and rapid response. The technique provided good information regarding emulsion stability, changes in droplet size distribution and concentration. Emulsions were prepared with mineral oil and crude oil samples and the effects of various factors including mixing speed, surfactant, and asphaltene content were investigated. Emulsion droplet structure is observed, and stability is examined by tracking the changes in ultrasonic parameters with time.

3.2 Experimental Details

3.2.1 Materials and Methods

The light mineral oil (LMO) used in the experiments was purchased from VWR International and the samples of different types of crude oils were provided by Imperial Oil Ltd. The properties of these oil samples are listed in Table 3.1. Density measurements were conducted using SG-Ultra Max Ex Petrol Density Meter, by Eagle Eye Power Solutions. Brookfield digital Rheometer was employed to determine the rheology of the emulsion at different temperatures controlled by a water bath thermostat. The commercial non-ionic hydrophilic surfactant Tween 20 (Polyoxyethylene-20-sorbitan Monolaurate) with chemical formula $C_{58}H_{114}O_{26}$, was used as an emulsifying agent during the preparation of light mineral oil emulsions. It has a density of 1110 kg/m^3 , viscosity of 450 cP at 25°C . Deionized (DI) water with a density of 997.7 kg/m^3 was used as a dispersed phase of the emulsions.

Asphaltene content in crude oil samples was determined based on the modified ASTM D2007-80 procedure. To achieve this, n-heptane was added to 100 mL of crude oil sample in a 1000 ml conical flask using a solvent-to-crude oil ratio of 5:1. The mixture was agitated for 45 minutes using a magnetic stirrer. The flask was covered with aluminum foil, to stop the evaporation of the solvent. After mixing, the content was left in the fume-hood for 48 hours. It was then vacuum filtered using a $0.22 \mu\text{m}$ filter paper funnel assembly (Fig. 3.1). The filter paper with asphaltenes content was left in the fume to dry for approximately 5 days to achieve constant weight. The dry asphaltenes were then transferred into the glass vial. Equation 3.1 is used to calculate the weight of asphaltenes:

$$\text{asphaltene Concentration} = \frac{\text{Weight of dried asphaltene(g)}}{\text{Weight of 100 mL crude oil sample}} \quad (3.1)$$

For the blend of crude oil, the concentration is estimated numerically using the equation like

the one applied for the density of the mixture.



Fig. 3.1. Vacuum filter assembly for the asphaltenes concentration measurement

Table 3.1. Physical properties of different oil used for emulsion preparation

3.2.2 Experimental Setup

Physical property	LMO	LCO	HCO	DI Water
Sp. gravity @ 60 F ⁰	0.861	0.872	0.909	1.0
Density (kg/cm ³)	858.7	860.6	907.4	997.7
API ⁰	32.08	31.17	24.23	10
Kinematic viscosity (cP) @ 20.2 ⁰ C	91.20	11	107	1.02
Asphaltene (wt %)	0	1.45	13.17	-

A schematic of the experimental set up used for emulsion preparation and testing is shown in

Fig. 3.2. The transducers for generating and receiving the acoustic pulse were mounted on a

probe at a fixed distance of 51.2 mm. The probe was connected to an ultrasonic pulse-receiver (UTEX Inc.) capable of exciting ultrasonic transducers with center frequencies from 1MHz to 150MHz. However, the probe used in this study had a frequency of 3.5MHz. It was controlled by a software interface which allowed remote control and configuration of the instrument.

Transducer excitation was achieved with an ultra-fast square wave pulse featuring adjustable pulse width and adjustable pulse voltage. The amplifiers in the instrument were directly gain controllable eliminating the need for attenuators that contribute to receiver noise. Data were collected at a sampling interval of 0.05 over 60 second to get 1200 data points of time-of-flight and amplitude per run. The arithmetic average of each set of values was calculated and subsequently used to calculate acoustic velocity and attenuation, respectively. The standard deviation of each set was also calculated to ensure the data was uniform and free of outliers.

Emulsions were prepared in a jacketed vessel with the help of an agitator (from IKA) at a constant agitation speed of 1200 rpm. To prepare water-in-mineral oil emulsions, a measured volume of the oil sample representing 90 or 80 vol.% oil content was placed in the jacketed vessel, then 1 wt.% of Tween 20 surfactant was added to the oil phase to prepare stable emulsions. The mixture was stirred for about 5 minutes to ensure a homogenous solution. This was followed by the gradual addition of 10 or 20 vol.% de-ionized content while maintaining constant stirring speed for about 30 minutes. For water-in-crude oil emulsions, no surfactant was needed to prepare a stable emulsion due to the presence of natural surfactants such as resins and asphaltenes in the crude oil. The prepared emulsion was then transferred into a graduated cylinder and an ultrasonic probe was inserted for data collection. At the initial stage of the experiment, readings were taken every one hour for the first 6 hours, then after 24 hours. There was an insignificant change in the data taken after 4 hours. Therefore, readings up to 4 hours

were only considered. In the first 1 hour, readings were taken every 15 minutes, then every 30 minutes for the last 3 hours.

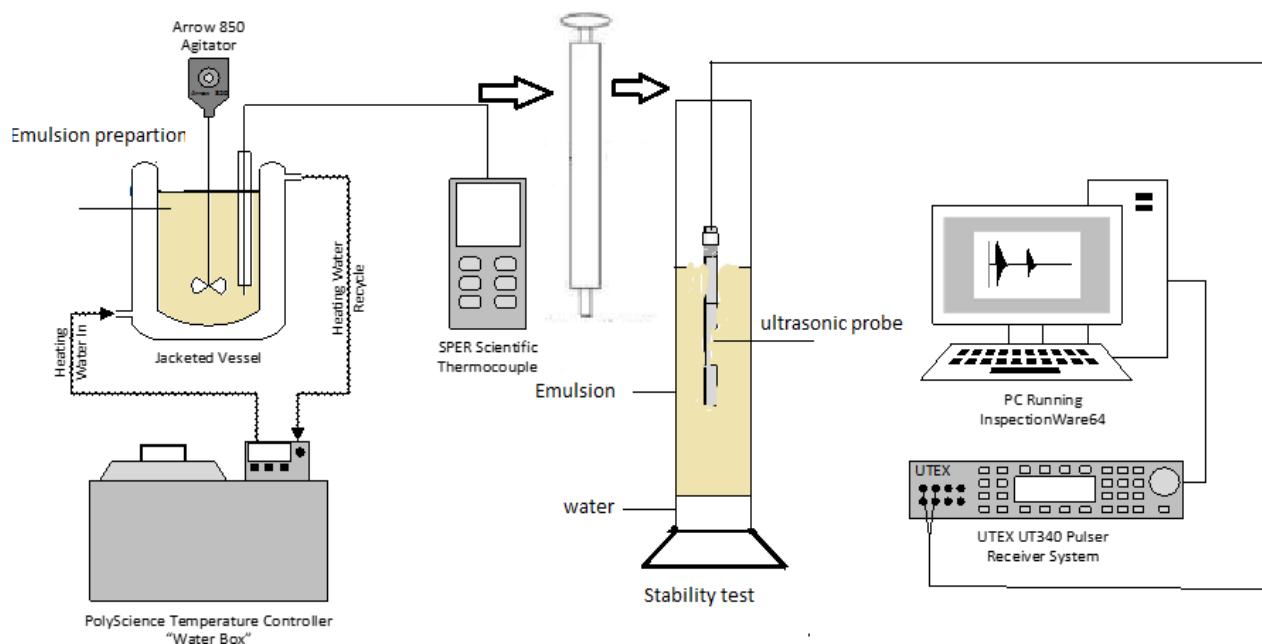


Fig. 3.2. Schematic diagram of the experimental setup for emulsion characterization

Fig. 3.3 is a waveform for LMO and LMO emulsion captured by the receiver. Where amplitude (voltage) is on the y-axis while TOF on the x-axis. As it is expected, the probe captured a bigger signal for the sample of LMO, compared to the emulsion of this sample where the signal is smaller. This is due to the change in the composition of MO when water and emulsifier are added.

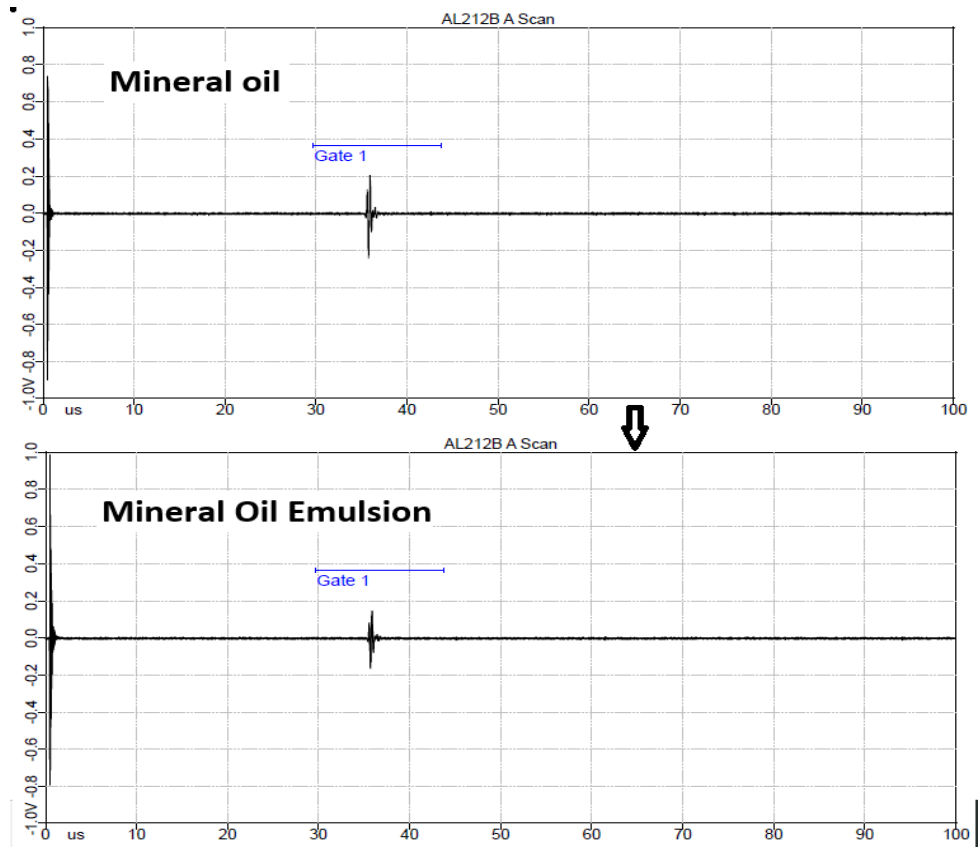


Fig. 3.3 Changes in ultrasonic signal for LMO & LMO Emulsion at 1200 rpm.

3.2.3 Calculation of Acoustic Parameters

Acoustic Velocity

Acoustic velocity and attenuation of the propagating wave are the two ultrasonic parameters used to characterize the emulsions prepared in the experimental part of this work. The ultrasonic probe which operates in transmission mode is used to measure amplitude and TOF. The distance between the transmitter and the receiver of the probe is d . TOF is the time it takes the wave to travel from the transmitter to the receiver. d and TOF were used to calculate the speed of sound in each medium; in this case emulsions and oil samples (equation 3.2).

$$v = \frac{d}{TOF} \quad (3.2)$$

Acoustic velocity (v) equation 3.3 is governed by the thermodynamic properties of the medium through which it is traversing. Based on the concept that sound is propagated as a harmonic longitudinal compression wave, the Newton-Laplace equation presents acoustic velocity through a given medium as a function of its bulk modulus (β) and density (ρ) (Ament, 1953; Urlick, 1947).

$$v = \sqrt{\frac{\beta}{\rho}} = \frac{1}{\sqrt{\rho\kappa}} \quad (3.3)$$

If bulk modulus and density data are available, values for acoustic velocity can be predicted for different media using above equation.

Attenuation

The measured decline in the amplitude of an ultrasonic wave, traveling a known distance through the sample, was used to approximate the attenuation coefficient (α) as presented in equation 3.4.

$$\alpha = -\frac{1}{d} \ln\left(\frac{A}{A_0}\right) \quad (3.4)$$

Where A_0 , is the reference amplitude and A is the final amplitude of the transmitted signal. The reference amplitude in this work is the amplitude of the transmitted signal in the DI water sample. Whereas A is the amplitude of other samples or emulsions. To help understand the samples used in this experimental work, their physical properties are presented in table 3.1.

3.2.4 Data Analysis

The raw data collected for each run was analyzed for consistency and outliers and appropriate data filtration was applied before its usage. Fig. 3.4 presents a scatter plot for the time of flight data points collected in the emulsion of light mineral oil. The purpose of the scatter plot is to identify outliers and categorize potential sources such as suspended impurities and bubbles etc. Data filtration was applied based on the theoretical consideration that for the emulsion of DI

water in LMO, the data points should fall within the range of DI water and oil samples. For this reason, data points that fall outside this range are considered an effect of bubbles, hence filtered out. The frequency distribution plot as shown in Fig. 3.4 provides a clearer picture of the data points and helps identify the peak and the effects of filtration on peak value. The average of remaining data points for TOF is then used to calculate acoustic velocity and standard deviation. The procedure ensured that the standard deviation was less than 2%.

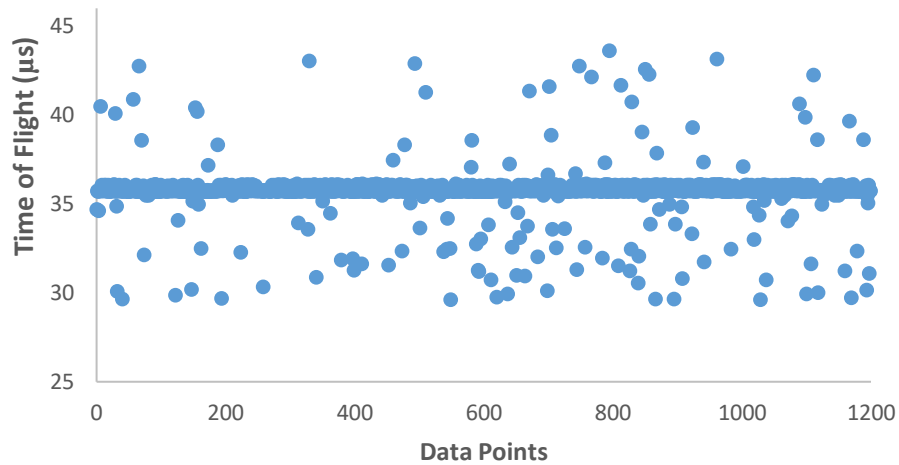


Fig 3.4 Scatter plot of TOF data obtained with LMO emulsion

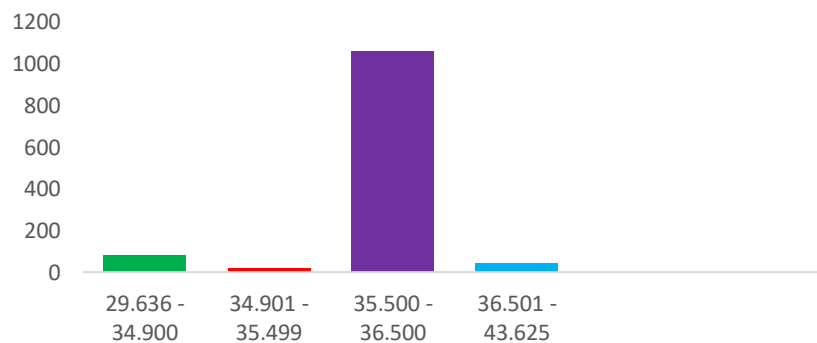


Fig 3.5 Frequency distribution of TOF data obtained with LMO emulsion

3.3 Results and Discussions

3.3.1 Acoustic properties of oil samples

The acoustic and physical properties of the mineral and crude oils used for the tests were first measured due to a clear and direct link with emulsion properties. Fig. 3.6 compares the measured acoustic velocities values of oil samples with that of DI water. DI water has the highest acoustic velocity followed by mineral oil, heavy and light crude oils respectively. Deionized water and mineral oils are used as reference fluids for crude oil emulsion characterization.

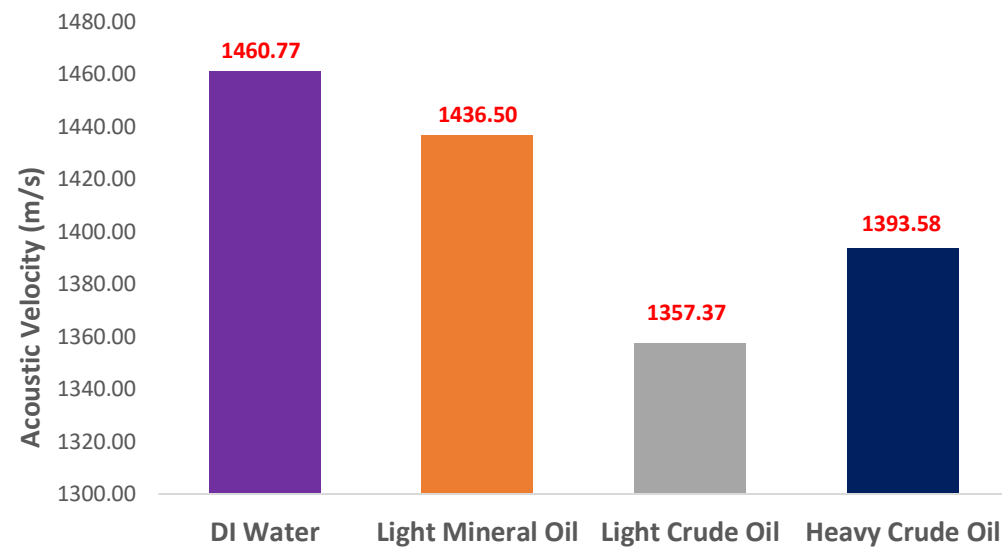


Fig. 3.6 Acoustic velocity values calculated from TOF by Eq. 3.2

Acoustic impedance (z) and bulk modulus (β) are two useful material-specific acoustic parameters which can be estimated knowing the acoustic velocity and density of a fluid.

$$Z = \rho.v \quad (3.5)$$

$$\beta = \rho.v^2 \quad (3.6)$$

Acoustic impedance determines the behavior at interfaces between different materials. The higher the difference between the acoustic impedances of materials, the greater is the intensity of the reflected wave. Table 3.2 lists the values of acoustic impedances and bulk modulus of water and different oils calculated based on measured densities and acoustic velocities. The table also

lists the values of bulk modulus reported in the literature and shows the percent difference for different media. The small percentage errors indicate that estimations based on ultrasonic techniques are reliable. The error observed can be mainly attributed to the density difference between oil samples and the literature studies.

Table 3.2. Comparison of acoustic properties of water and oil samples

Sr. No.	Fluid	Density (Kg/m³)	Acoustic velocity (m/s) [Exptl.]	Bulk Modulus (pa) (calc.)	Bulk Modulus (pa) [18]	% Relative Absolute Error
1	DI Water	997.7	1460.77	2.14E+09	2.15E+09	0.47
2	Light Mineral Oil	857.46	1436.50	1.686E+09	1.66E+09	1.54
3	Light Crude Oil	860.6	1357.37	1.51E+09	1.50E+09	0.66
4	Heavy Crude Oil	907.4	1393.58	1.68E+09	NA	

Fig. 3.7 Compares the calculated attenuation by equation 3.4 of different liquids used in this work. Attenuation normalizes the raw amplitude values with respect to a reference value (A_0). Amplitude is a raw signal whose value can vary from one run to another for the same fluid depending on instrument settings such as gain applied voltage. DI water has the lowest attenuation compared to oil samples. Low attenuation implies a lower loss of energy as the wave propagates through the medium. In this study, amplitude recorded in DI water is used as the reference for calculation of attenuation in oil samples.

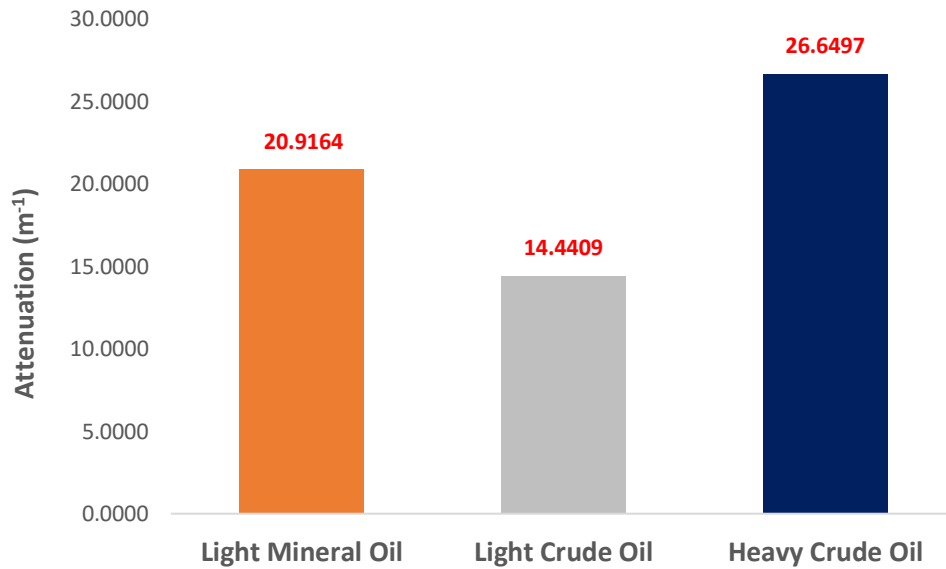


Fig. 3.7. Calculated attenuation values from recorded amplitude

3.3.2. Effects of asphaltenes concentration on acoustic parameters

As pointed out in chapter 2, asphaltenes and resin molecules found in crude oils have a remarkable effect on its emulsion properties. Asphaltenes in the colloidal state stabilize the emulsions, but it is strongly evident that its stabilizing properties are notably intense when it occurs in the solid state as precipitated from crude oil.

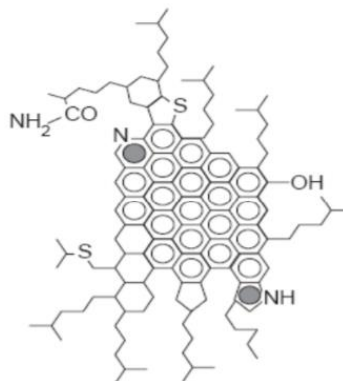


Fig. 3.8. Example of molecular structures in crude oil: Asphaltenes (El-Sayed, 2012)

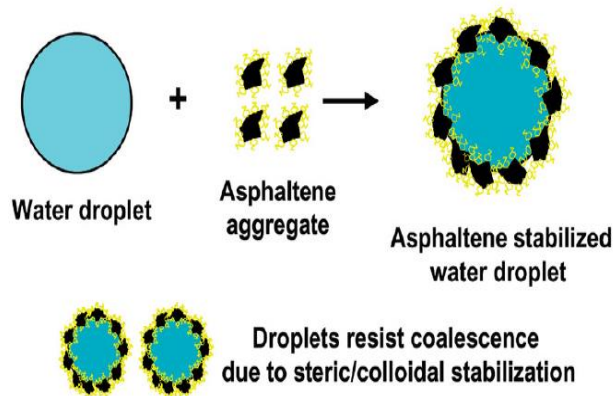


Fig. 3.9 Mechanism of emulsion stabilization by asphaltenes (El-Sayed, 2012)

Like asphaltenes, resins are also large molecules which are complex compounds with high molecular weight and are insoluble in ethyl acetate but are soluble in n-heptane. It has a great tendency to couple with asphaltenes, resulting in the formation of the asphaltene-resin micelle. It plays a vital part in stabilizing emulsions. The asphaltene: resin ratio in the crude oil reveals the type of film formed (solid or mobile), and emulsion stability directly depends on it.

Asphaltenes concentration in crude oils is usually determined using a time-consuming offline method based on solvent treatment and filtration. Therefore, using the ultrasonic method will significantly save time because it takes only 60 seconds to take over 1200 data points of a single reading and the average of this provides an accurate value. Higher asphaltenes content contributes to higher viscosity, density, and results in highly stable emulsions. Two samples of crude oil light and heavy, along with two blends of these samples were used for the asphaltenes concentration measurements. Fig. 3.10 represents the effect of asphaltenes concentration on the acoustic velocity. It can be observed that higher asphaltenes concentration led to an increase in acoustic velocity. Hence, the acoustic velocity for the heavy crude oil was highest in all the crude oil samples

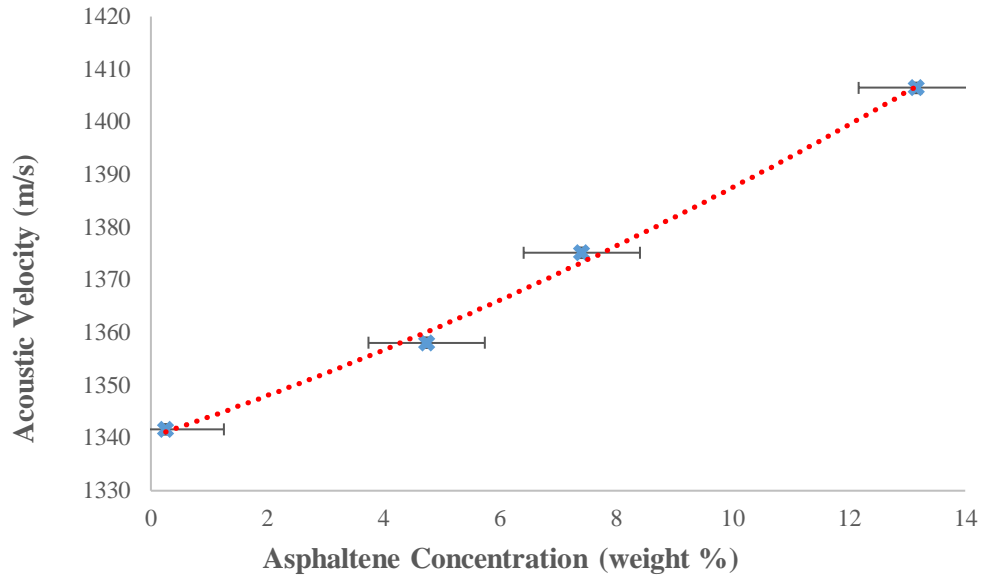


Fig. 3.10 Variation of acoustic velocity with asphaltenes concentration in crude oil

The effect of asphaltenes on the acoustic velocity was also observed by calculating acoustic impedance using equation 3.5. The plot of acoustic impedance vs asphaltenes concentration is presented in Fig. 3.11. Where density and acoustic velocity were reported in kg/m^3 and m/s respectively giving the acoustic impedance in $\text{kg/m}^2\text{s}$. An increase in acoustic impedance with asphaltene concentration indicates a higher degree of reflection from the interface and therefore higher attenuation of the transmitted wave. This can be observed below from attenuation calculated from measurements of the amplitude of transmitted waves.

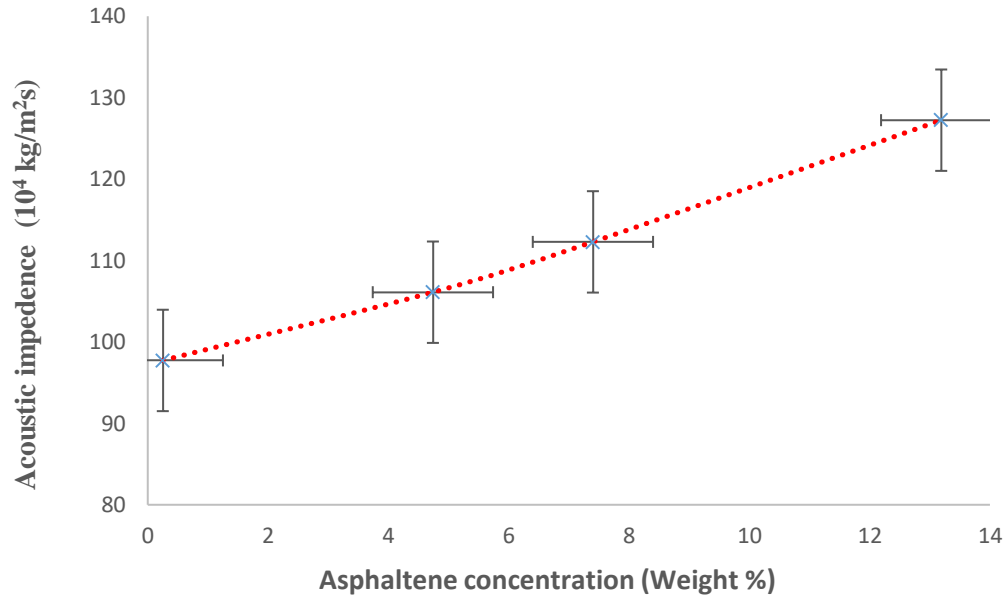


Fig. 3.11 Asphaltenes concentration vs acoustic impedance

It can be seen from Fig. 3.12 Asphaltene concentration was found to increase with increasing attenuation. For the light crude oil, the asphaltenes concentration was the lowest giving the lowest attenuation. An increase in attenuation indicates a loss of energy as the wave propagates through the medium. This can be attributed to the absorption of energy by the larger asphaltene molecules in heavier crude oil samples. The propagating wave will experience intrinsic absorption as it interacts with the large dissolved asphaltenic molecules. As discussed above, the heterogeneous composition of heavy crude oils due to the presence of heavy asphaltenic molecules is contributing to this behavior.

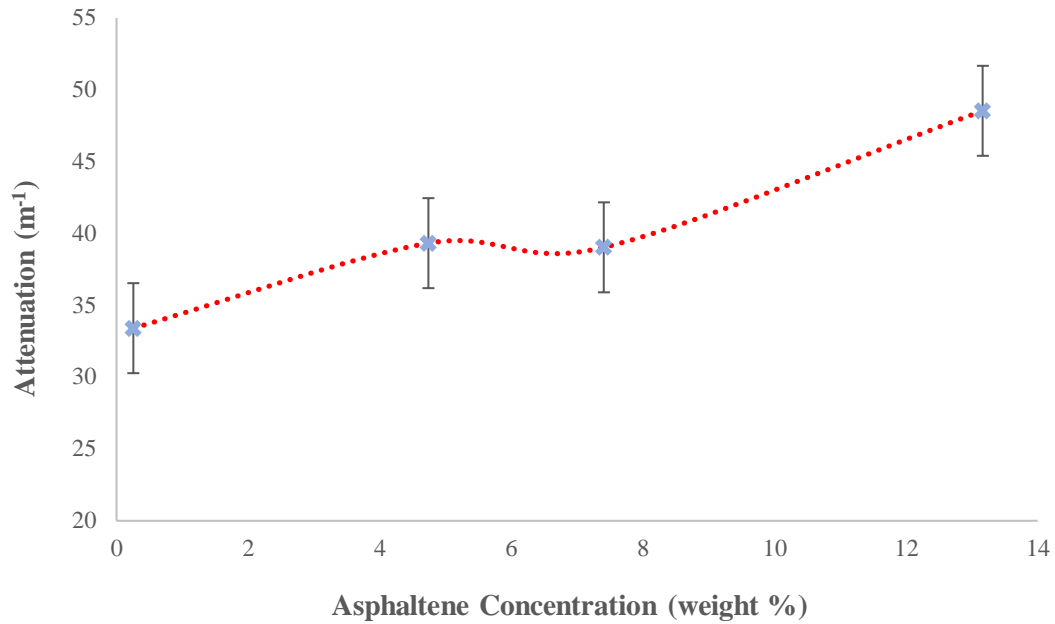


Fig. 3.12 Effects of asphaltenes concentration on acoustic attenuation

It is also observed from Fig. 3.12 that changes in attenuation going from 4.7 to 7.4% asphaltene level is not significant which represents a change of about 2.7% while for the remaining points, the change is nearly 4%. This indicates that attenuation does not capture very small changes in asphaltenes. This is possibly because the ultrasonic probe frequency is not sensitive enough. This indicates the need to improve the sensitivity of attenuation measurements possibly by increasing wave frequency.

3.3.3 Stability Tests with Mineral Oil Emulsions

As pointed out earlier, the first set of stability tests were conducted with mineral oil emulsions which allowed visual observations of dispersion of water droplets and their separation compared to nearly opaque emulsions of crude oil. The thermodynamic instability of most emulsions causes them to separate into their phases when leftover time. The process of destabilization follows several steps that also include flocculation, sedimentation, and coalescence and finally phase

separation. Consequently, the characteristics of the emulsion such as composition, droplets size distribution and other rheological properties also change with time. Unstable emulsions are expected to separate into their phases faster than the stable emulsions.

3.3.3.1 DI Water Separation and Attenuation with Mineral Oil Emulsions

Fig. 3.13 shows the relationship between separation % of DI water and recorded variations of attenuation of propagating waves in the light mineral oil emulsions. A comparison of the two curves shows a reverse trend between water separation and attenuation. The increase in the separation curve is followed by a decrease in attenuation. This confirms that attenuation has captured changes in the characteristic of LMO emulsions since settling of DI water changes the composition of water in mineral oil emulsions. 90% LMO content and 10% DI water emulsion showed gradual separation. Near-complete separation for the emulsion of 10% DI water in light mineral oil is achieved in the first 1 hour. Thus, fast water separation leads to a corresponding fast drop in attenuation indicating a strong contribution of dispersed water droplets to acoustic attenuation. Higher residual attenuation with 10% DI water emulsions indicates the role of smaller droplets of more stable emulsions to acoustic attenuation. Equation 3.7 is used to calculate water separation percentages:

$$\text{Water separation \%} = (\text{Settled water in emulsion} / \text{Initial water content in emulsion}) * 100 \quad (3.7)$$

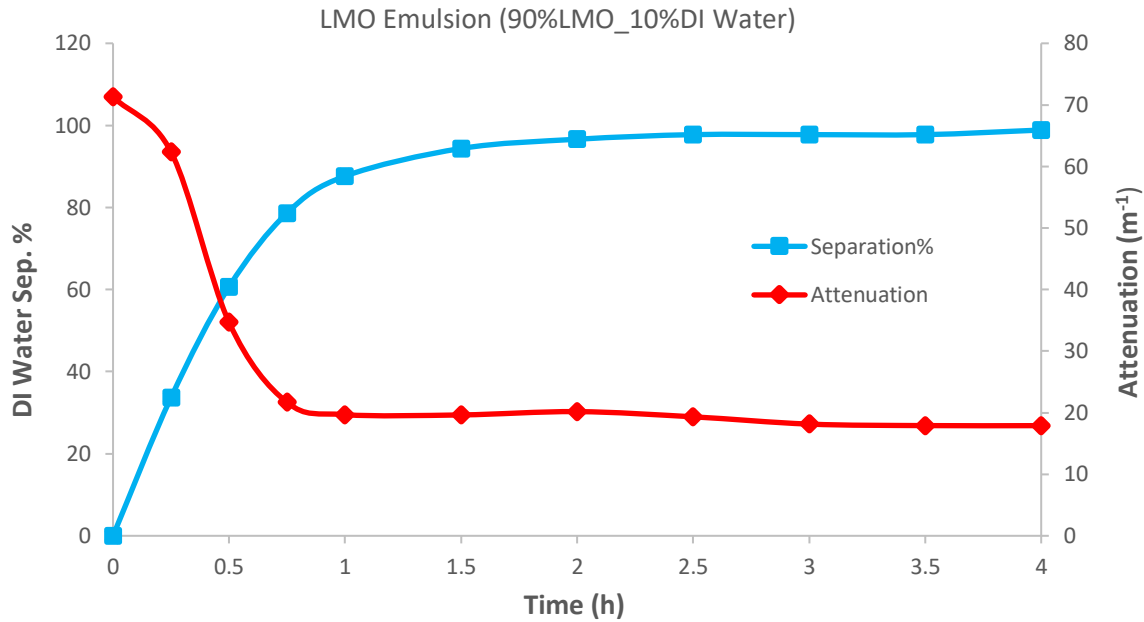


Fig. 3.13. Water separation and attenuation in LMO emulsions

As discussed in the later section, several loss mechanisms such as scattering losses, viscous and thermal dissipations can contribute to attenuation of the wave. Their relative contribution needs to be ascertained for the system under investigation.

3.3.3.2 DI Water Separation and Measured Acoustic Velocity with Mineral Oil Emulsions

Fig. 3.14 shows the relationship between separation % of DI water and recorded acoustic velocity in the mineral oil emulsions of the corresponding Fig. 3.13. Acoustic velocity calculated from TOF is another important ultrasonic parameter for testing and characterizing emulsions.

Fig. 3.14 illustrates a gradual decrease in acoustic velocity for the emulsions of 90% LMO content and 10% DI water content. As noted earlier (Fig. 3.7), acoustic velocity in DI water is higher than in mineral oil. Thus, a decrease in acoustic velocity with time corresponds to a decrease in the water content of the emulsion. This is consistent with the plot of the DI water separation percentage (Fig. 3.14). The highest drop in acoustic velocity is observed at about 1 hour where there is near complete separation of the water phase. This indicates the ability of the

ultrasonic probe to detect changes in the characteristics of LMO emulsions using acoustic velocity.

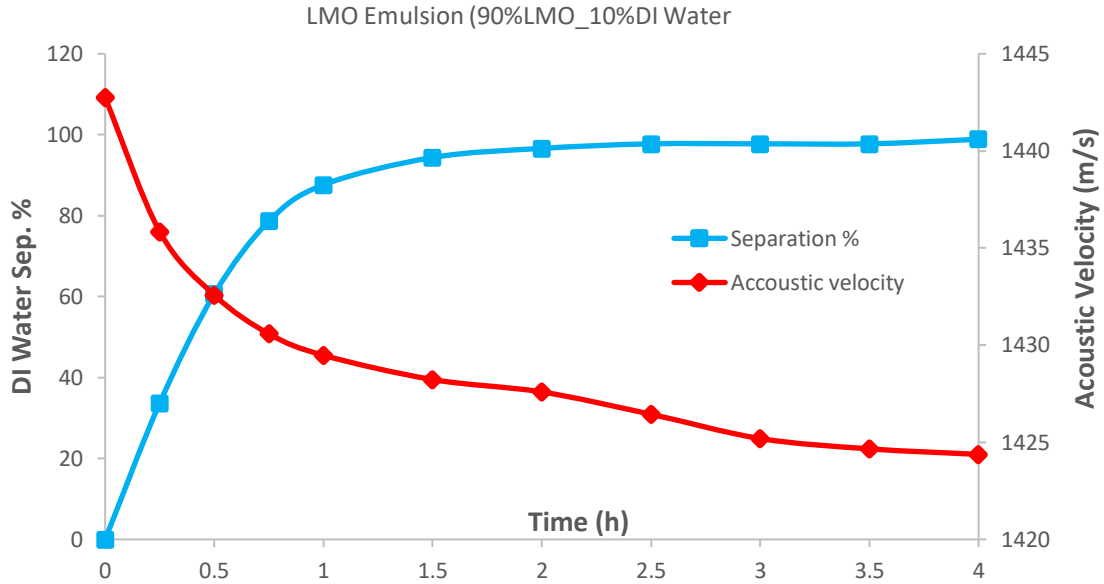


Fig. 3.14. DI Water separation and acoustic velocity in MO emulsions

3.3.3.3 DI Water Separation and Attenuation with Mineral Oil Emulsions

Fig. 3.15 shows the comparison between separation % of DI water and recorded variations of attenuation of propagating waves in the LMO emulsions. The two curves show a revised trend between DI water separation and attenuation. The increase in the separation curve is followed by a decrease in attenuation. This confirms that attenuation has captured changes in the characteristic of LMO emulsions since settling of DI water changes the composition of water in mineral oil emulsions. 80% LMO content and 20% DI water emulsion showed fast separation. Contrary to Fig. 3.13 complete separation for the emulsion of 20% DI water in mineral oil is achieved in about 30 minutes. Thus, fast water separation leads to a corresponding fast drop in attenuation indicating a strong contribution of dispersed water droplets to acoustic attenuation.

On the other hand, 90% MO content and 10% DI water emulsion showed gradual separation. The quick separation of DI water for emulsions of 80% LMO and 20% DI water can be attributed to the formation of large droplets. Since the mixing time and rpm were the same for 10 and 20% DI water emulsions, smaller size droplets would be generated in 10% DI water emulsions. The large dispersed DI water droplets enhance the rate of coalescence and settling, leading to a fast separation of DI water. Changes in the two acoustic parameters of the emulsions were tracked with the probe simultaneously.

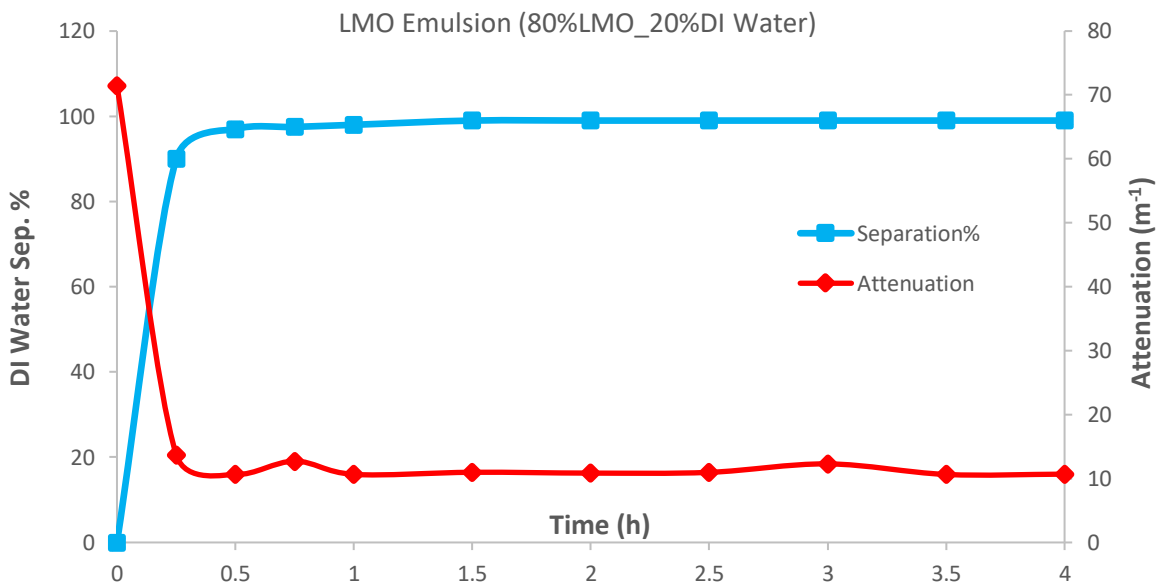


Fig. 3.15. Water separation and attenuation in MO emulsions

As discussed in the later section, several loss mechanisms such as scattering losses, viscous and thermal dissipations can contribute to attenuation of the wave. Their relative contribution needs to be ascertained for the system under investigation.

3.3.3.4 Acoustic Velocity for the Mineral Oil Emulsions

Acoustic velocity calculated from TOF is another important ultrasonic parameter for testing and characterizing emulsions. Fig. 3.16 illustrates a fast decrease in acoustic velocity for the

emulsions of 80% MO content and 20% water content. As noted earlier (Fig. 3.6), acoustic velocity in DI water is higher than in mineral oil. Thus, a decrease in acoustic velocity with time corresponds to a decrease in the water content of the emulsion. This is consistent with the plot of the DI water separation percentage (Fig. 3.16). The highest drop in acoustic velocity is observed at about 30 minutes where there is near complete separation of the water phase. This indicates the ability of the ultrasonic probe to detect changes in the characteristics of MO emulsions using acoustic velocity. On the other hand, the plot for 90% MO content and 10% DI water show a gradual decrease in acoustic velocity. This is like the observation made for the corresponding DI water separation percentage.

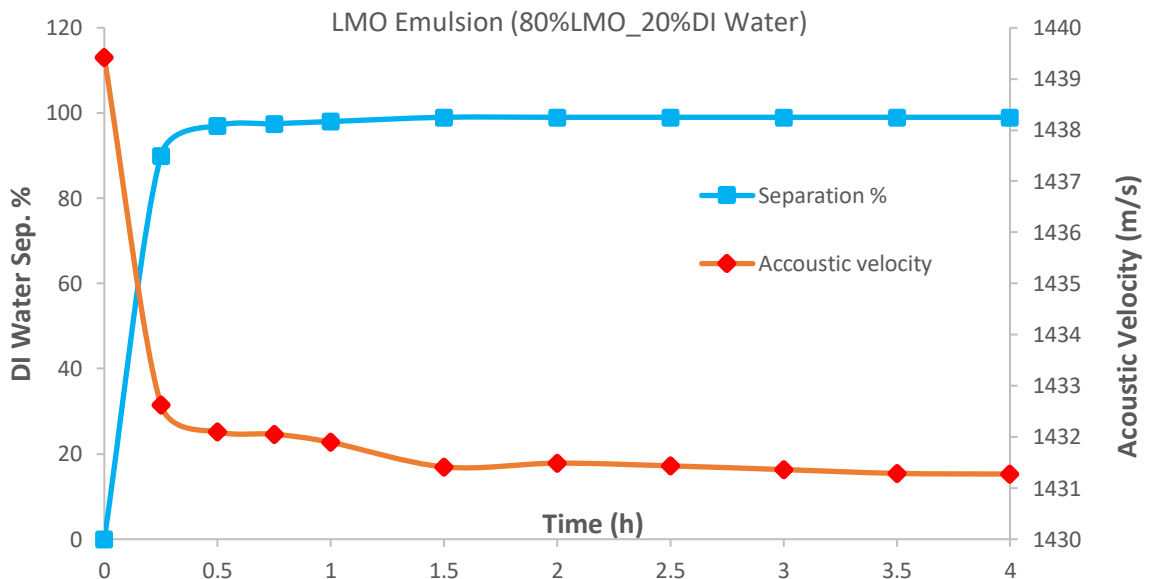


Fig. 3.16. Water separation and acoustic velocity in MO emulsions

3.3.4 Stability Test with Crude oil Emulsions

These tests were carried out with both light and heavy crude oil samples to observe the effects of large asphaltene compounds on the emulsion characteristics of the crude oils. Due to the opaque nature of crude oils, separation of water phase could not be observed clearly in Fig. 3.17

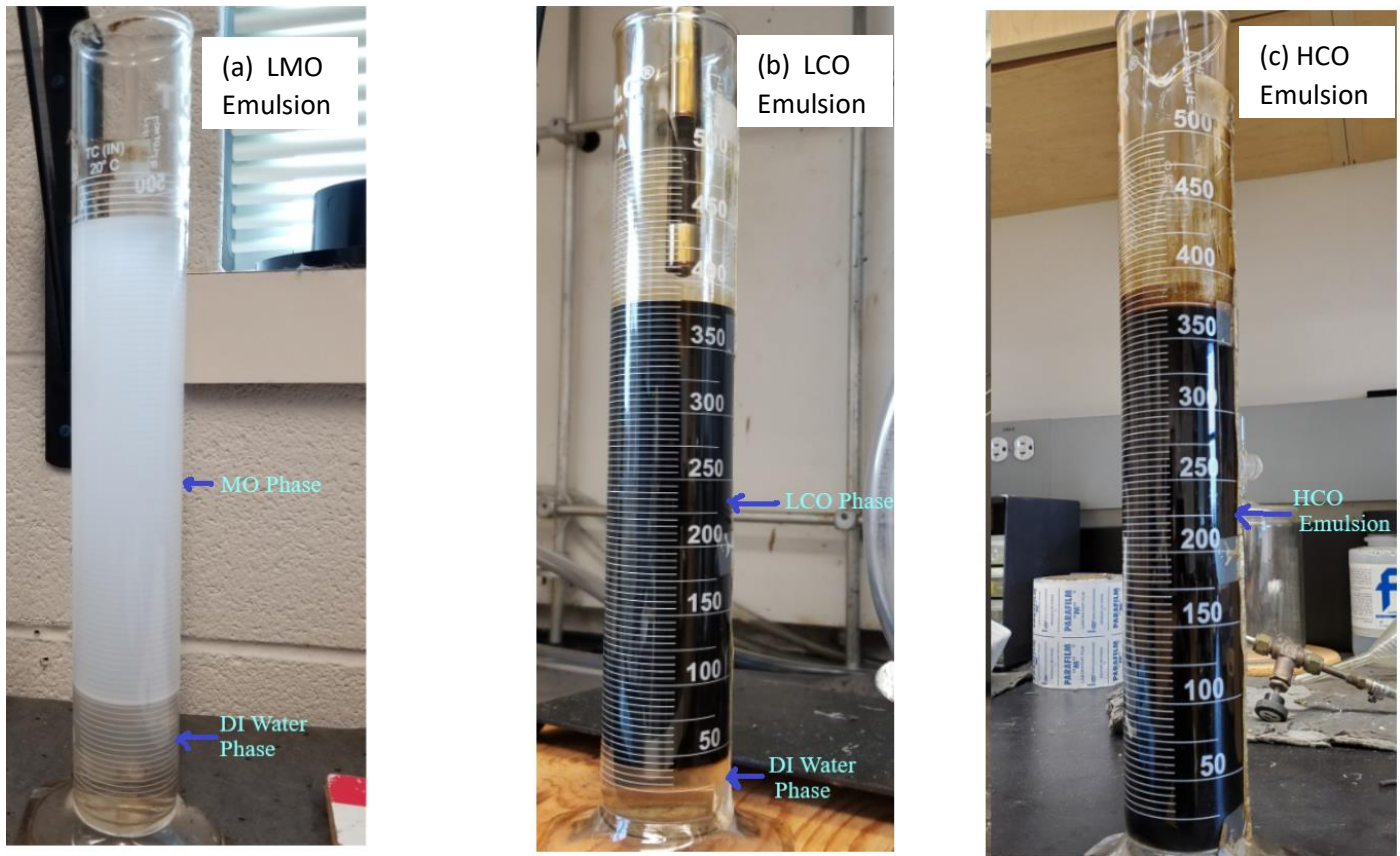


Fig. 3.17. Pictures of light mineral oil and crude oil emulsions

However, variations in acoustic parameters were easily captured with the probe. The trend for the measured amplitude values is plotted in Fig. 3.18 for emulsions with 10 and 20% water content. The rise in amplitude values for the first hour indicates the separation of water droplets as observed with the mineral oil emulsion test. It is also observed that amplitude value is lower in emulsion with 20% water content which can be attributed to a higher concentration of water droplets in the emulsion phase. Some fluctuations observed with the measured amplitude can be attributed to the heterogeneous nature of crude oils. As expected from amplitude plots, higher attenuations are recorded in emulsion with 20% water content and sharper drop can be attributed to a quick separation of larger droplets (Fig. 3.19).

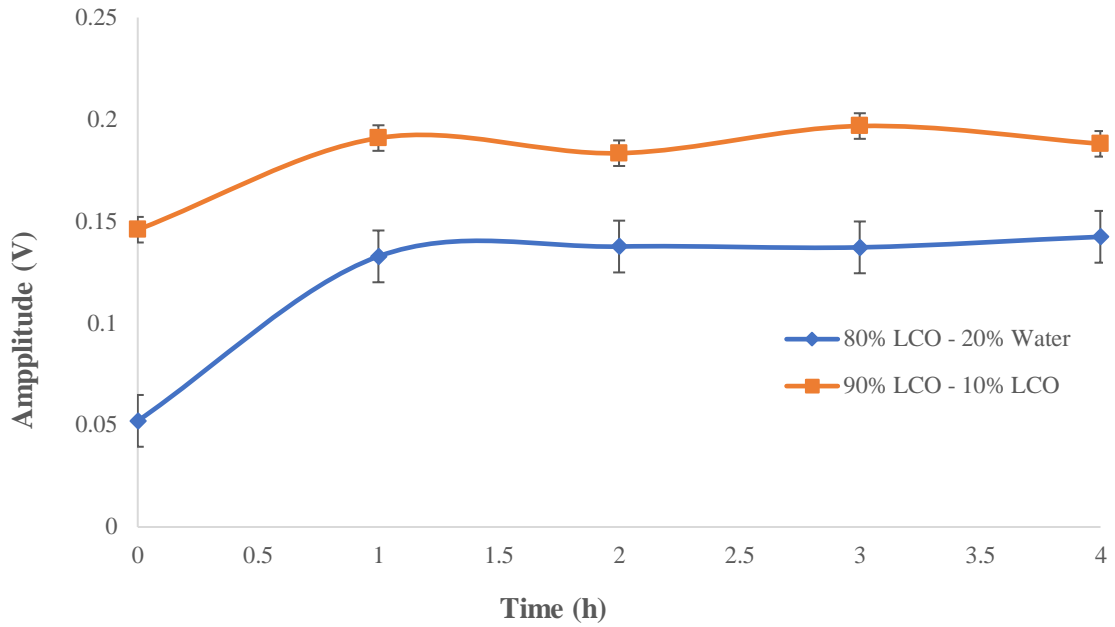


Fig. 3.18. Variations in amplitude values recorded with time with light crude oil emulsions

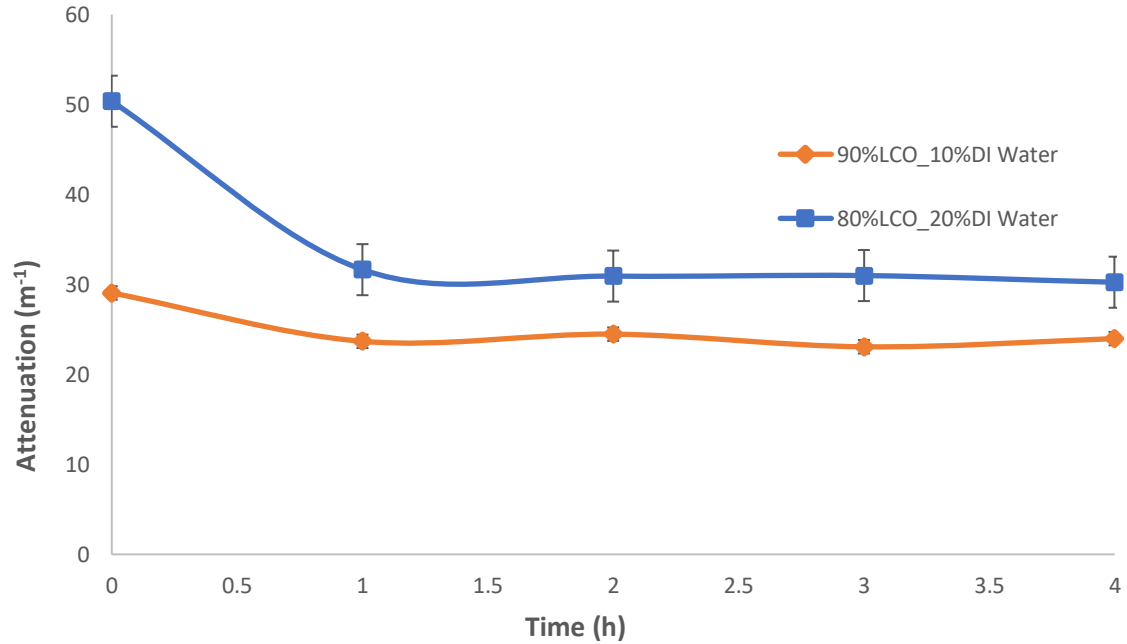


Fig. 3.19 Variations of attenuation obtained with emulsions of LCO

It can be observed from Fig. 3.20 that higher initial velocity is recorded in emulsion with 20% water content compared to 10%. This can be attributed to higher acoustic velocity in the water phase contributing to the observed increase with higher water content. However, as the water droplets settle out, the measured acoustic velocity values drop quickly approaching that of crude oil.

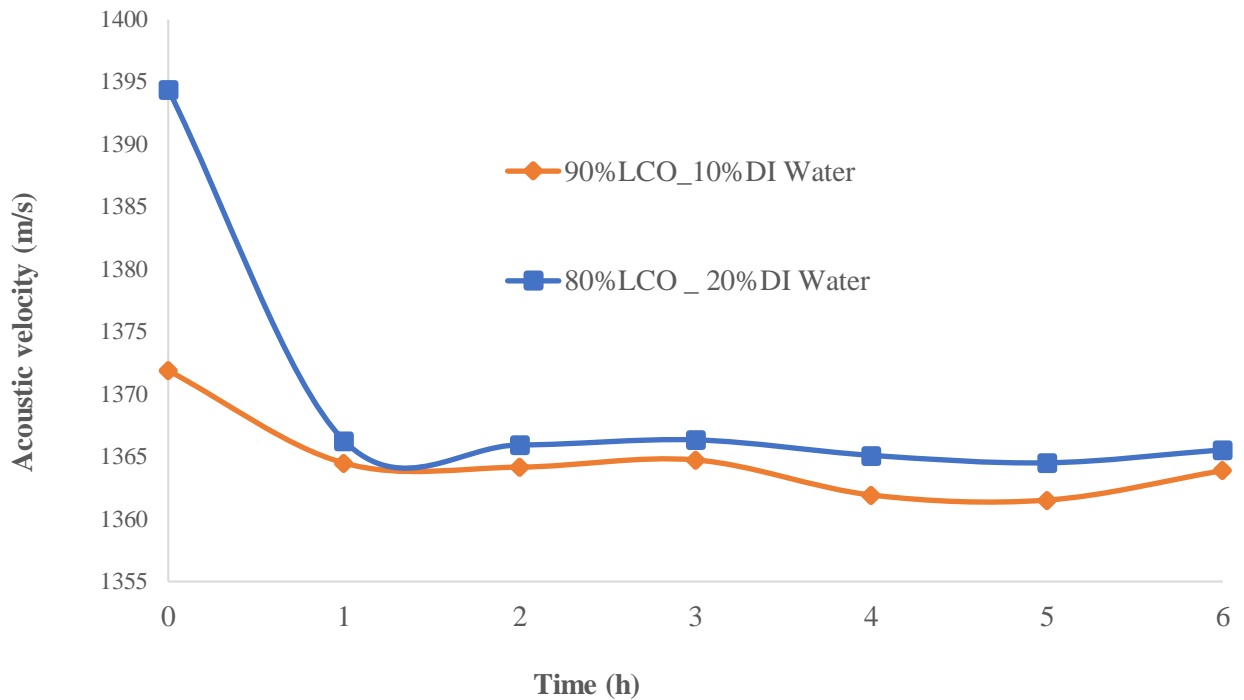


Fig. 3.20. Variations of acoustic velocity with time in LCO emulsions

Equation 3.3 presented earlier, can be used to estimate acoustic velocity in homogenous fluids. However, for application to non-homogenous mediums such as emulsions, this equation needs to be modified by calculating the effective density and elasticity of the suspension (Pinfield and Povey, 1997, Kuster and Toksoz, 1974; Urick, 1947). The modification includes substituting the effective density and effective bulk modulus based on the volumetric fraction of respective phases in Eq. 3.3. the equation for the speed of sound in mixed media

$$v_{emul} = \sqrt{\frac{\sum_{i=1}^n \phi_i \beta_i}{\sum_{i=1}^n \phi_i \rho_i}} \quad (3.8)$$

Where ϕ_i is the volume fraction of component i in the non-homogeneous mixture. For two phase oil-water emulsion we have,

$$\beta_{eff} = (1-\phi)\beta_{oil} + \phi\beta_w \quad (3.8a)$$

$$P_{eff} = (1-\phi)\rho_{oil} + \phi\rho_w \quad (3.8b)$$

Determine Water Fraction from Acoustic Velocity

The above equations can be combined and rearranged to estimate water fraction in the emulsion phase using measured acoustic velocity in the emulsion phase and known density and bulk modulus in each phase. The resulting equation shown below can be used to develop a calibration curve shown in Fig. 3.21.

$$\phi = \frac{[v_{emu}^2 \rho_{oil} - \beta_{oil}]}{[v_{emu}^2 (\rho_{oil} - \rho_w) + (\beta_w - \beta_{oil})]} \quad (3.9)$$

Regarding the separation, even though the clear visible separation was not obtained, drop in attenuation and acoustic velocity confirmed the separation of water from light crude oil.

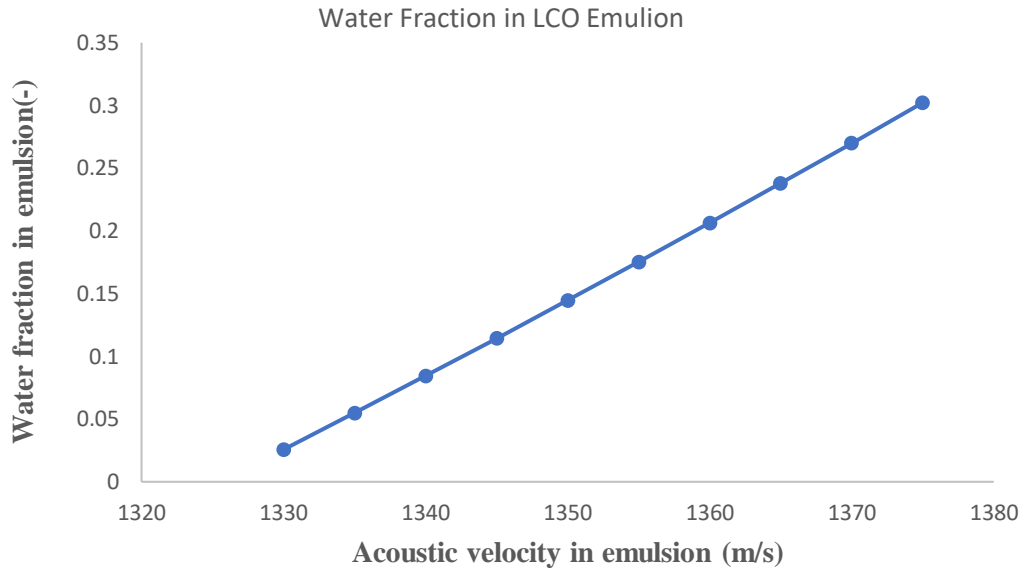


Fig. 3.21. Calibration curve to determine water fraction in emulsions of LCO

Using this calibration procedure, we get a water content of about 3 vol.% in 10% DI water emulsion and 5% in 20% DI water emulsion, after four hours of settling time. This indicates that water droplets are settling out from the bulk of the emulsion phase but seem to be accumulating near the bottom.

Visual observations of water separation from emulsions were even more difficult with emulsions of HCO compared to LCO emulsions. However, both acoustic parameters recorded variations with time. Fig. 3.22 shows that attenuation was nearly constant for about 30 minutes followed by a quick drop for the next 30 minutes and a gradual decrease for the next hour. Fig. 3.23 shows measured acoustic velocity, however, decreased from the beginning reaching a nearly constant value in about an hour. The decrease in acoustic velocity indicates droplet settling taking place even though there is no visible separation.

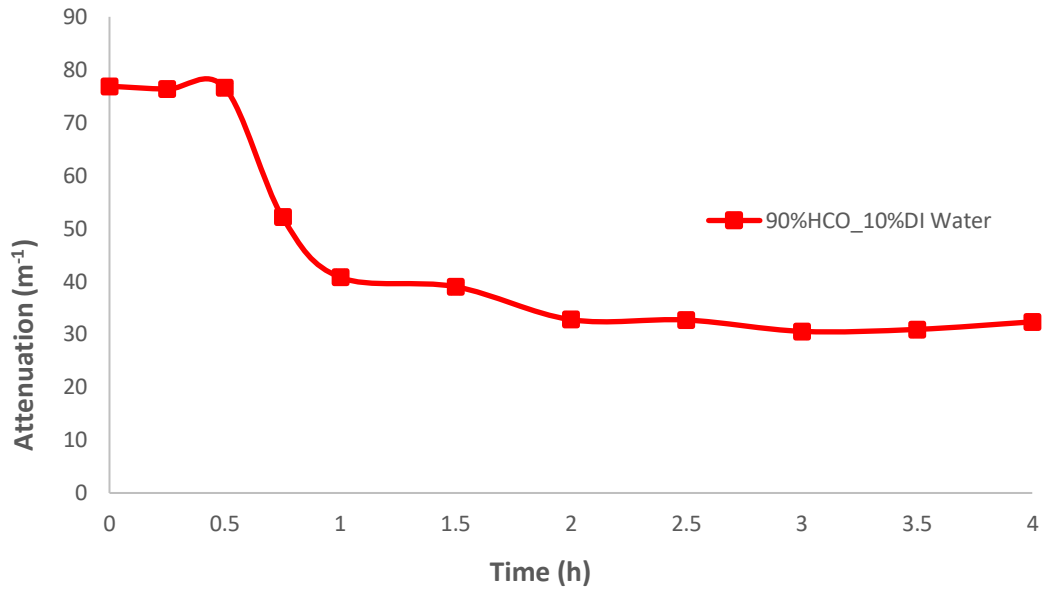


Fig. 3.22. Measured attenuation in HCO emulsions

The presence of asphaltene content makes it difficult to see any possible separation. Most of the change is observed in the first 30 minutes this could be a result of coalescence of larger droplets of the dispersed DI water.

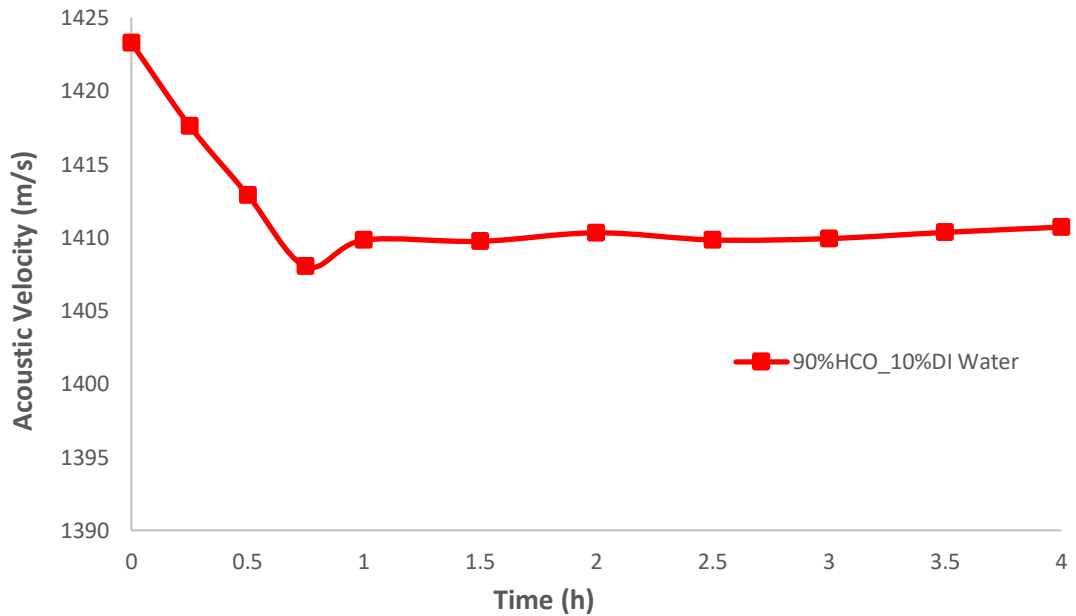


Fig. 3.23. Variation of acoustic velocity in HCO Emulsions

Since there was no clear separation of water, the recorded changes in acoustic parameters could be attributed to the accumulation of settled droplets near the bottom. Higher asphaltene concentration in HCO would prevent the coalescence of droplets by forming an interface layer.

The attenuation measurements in such systems can be complicated by contributing effects of different terms as pointed out in literature studies (Dukhin and Goetz, 2002; Hauptmann et al., 1998).

$$\alpha = \alpha_{int} + \alpha_{sc} + \alpha_{vis} + \alpha_{th} \quad (3.10)$$

Here, α_{ins} represent intrinsic losses of the medium, α_{sc} the scattering losses, α_{vis} describes the viscous losses and α_{th} the thermal losses. Table 3.3 presents equations for each of these dissipation terms, as discussed in various literature studies (Babick et al., 2000; McClements and Coupland, 1996). For a given system, scattering losses (α_{sc}) are proportional to $(k_1r)^3$ leading to the exponential increase in losses with the increase in droplet radius. However, what is observed is lower attenuation in emulsions of larger droplets (Fig. 4 to 6), indicating that the contribution of scattering losses is of little significance here. This could be contributed to relatively small differences incompressibility of liquid-liquid dispersion compared to liquid-solid or gas in liquid dispersions. For comparison, physical and thermal properties of different materials are presented in Table 3.3 from literature sources (Nadolny and Dombek, 2017; Das et al., 2007; Meng et al., 2006; Holman (1990) Perry et al., (1984) Edwards et al. (1983)). In oil-water emulsions, the contribution due to viscous dissipation can be neglected due to the small density difference between the droplets and surrounding liquid (McClements, 1996 and McClements and Coupland, 1996). Thus, high levels of attenuation observed in the emulsion phase can be attributed combination of two thermal losses, due to large differences in thermal properties of the two phases

and intrinsic absorption effects. Similar observations have been made by Hipp et al. (2002), who investigated acoustic attenuations in suspensions and emulsions. It was concluded by these authors that attenuations in emulsions are thermal in nature. Moreover, observed attenuations were higher in emulsions of smaller oil droplets. Additional details on the parameters of acoustic attenuation terms and their approximations are discussed in relevant literature studies (Babick et al., 2000 and McClements and Coupland, 1996).

Table 3.3. Contributing terms and their equation for acoustic attenuation

Contributing loss term	Governing Expression	Remarks
Intrinsic absorption	$\alpha_{\text{int}} = \phi \alpha_1 + (1 - \phi) \alpha_2$	Phase 1 (oil) and phase 2 (particles/droplets)
Scattering losses	$\alpha_{sc} = \phi k_1 (k_1 r)^3 \left(\frac{1}{6} \left(\frac{\kappa_1 - \kappa_2}{\kappa_1} \right)^2 \right)$	Particle/droplet size larger than wavelength
Viscous losses	$\alpha_{vis} = \frac{(1/2) \phi k_1 \left(\frac{\rho_2}{\rho_1} - 1 \right)^2 9/4 \left(\frac{\delta_v}{r} \right) \left(1 + \frac{\delta_v}{r} \right)}{\left[\frac{\rho_2}{\rho_1} + \frac{1}{2} + \frac{9}{4} \left(\frac{\delta_v}{r} \right) \right]^2 + \left[\frac{9}{4} \left(\frac{\delta_v}{r} \right) \left(1 + \frac{\delta_v}{r} \right) \right]^2}$ $\delta_v = \sqrt{2 \nu / \omega}$	Negligible effect when density difference between phases is small
Thermal losses	$\alpha_{th} = \frac{3 \phi k_1 H (\gamma - 1)}{2 b_1} \left(1 - \frac{\beta_2 \rho_1 C_{P1}}{\beta_1 \rho_2 C_{P2}} \right)^2$	Significant when difference between thermal expansion coefficients is large.
H and b_1 parameters defined in McClements and Coupland (1996)		

Table 3.4. Thermophysical properties of materials from literature

Material	Density (kg m ⁻³)	Compressibility (10 ⁻¹⁰ . Nm ⁻²)	Thermal conductivity (W m ⁻¹ K ⁻¹)	Specific heat (J kg ⁻¹ K ⁻¹)	Thermal expansion (10 ⁴ .K ⁻¹)
Water	998	4.16	0.614	4180	2.27
Mineral oil	864	6.25	0.133	1900	7.5
Crude oil	867	5.86	0.134	1907	8
Air	1.22	NA	0.025	1007	37
Silica	2650		1.5	730	0.0075

3.3.5 Measurements with blends of crude oil and mineral oil

These tests were conducted to investigate probe response and trends in the liquid mixtures of the two different oil types.

While mineral oil is mostly paraffinic with an average carbon number of about 25 (C₁₈ to C₃₂), crude oils is a more complex mixture of different hydrocarbon type ranging from C₄ to C₅₀. Fig. 3.24 shows acoustic velocities for the individual oils and their blend. To the left is HCO and thereafter, 30%, 50% and 70% of LMO are added to HCO to form the blend. As expected, acoustic velocity increases to the right with increasing LMO content and ends with the highest acoustic velocity (LMO only).

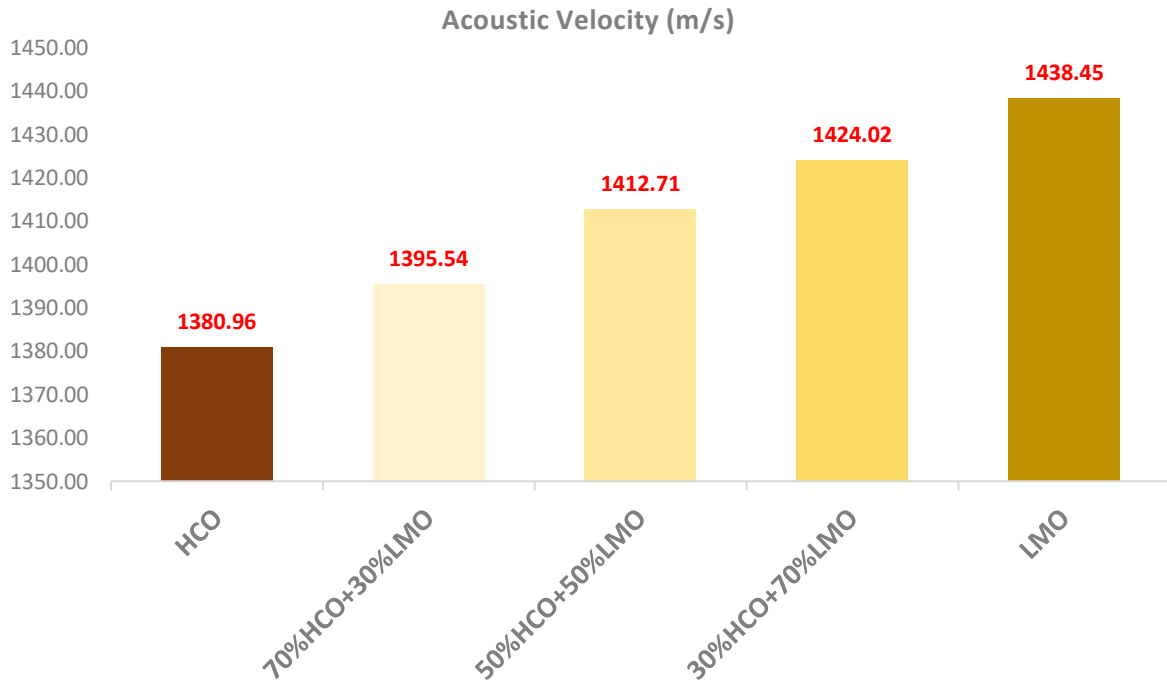


Fig. 3.24. The Acoustic velocity for HCO/LMO and their blend in varying composition

Table 3.5 shows that the acoustic velocity of the blend can be estimated within 1% using weighted average.

$$C_{\text{blend}} = C_{\text{HCO}} (\text{Vol. frac. of HCO}) + C_{\text{LMO}} (\text{Vol. frac. of LMO}) \quad (3.11)$$

Table 3.5. Comparison of measured and calculated values of acoustic velocities in HCO/MO blends

	100%	70% HCO+	50% HCO+	30% HCO+	100%LMO
Blend %	HCO	30% LMO	50% LMO	70% LMO	
Measured Acoustic vel. (m/s)	1380.96	1395.54	1412.71	1424.02	1438.45
Calculated Acoustic Vel. (m/s)	NA	1398.21	1409.71	1421.2	NA
Difference (%)	NA	0.19	0.21	0.5	NA

Fig. 3.25 presents corresponding attenuations obtained in the blends of the two oils. It is observed that the behavior of attenuation is not additive since, with 50% and 70 vol.% LMO/HCO mixtures, attenuation values are higher than expected. This behavior could be partially attributed to settling out of asphaltenes from heavy crude oil by the paraffinic mineral oil. Since the probe was vertically oriented, the settling asphaltenes molecules may have settled on the transducer surface causing additional resistance to wave propagation. Accumulation of a blob of heavy asphaltenic material was noticed at the bottom of the cylinder with an increase in mineral oil fraction in the blend.

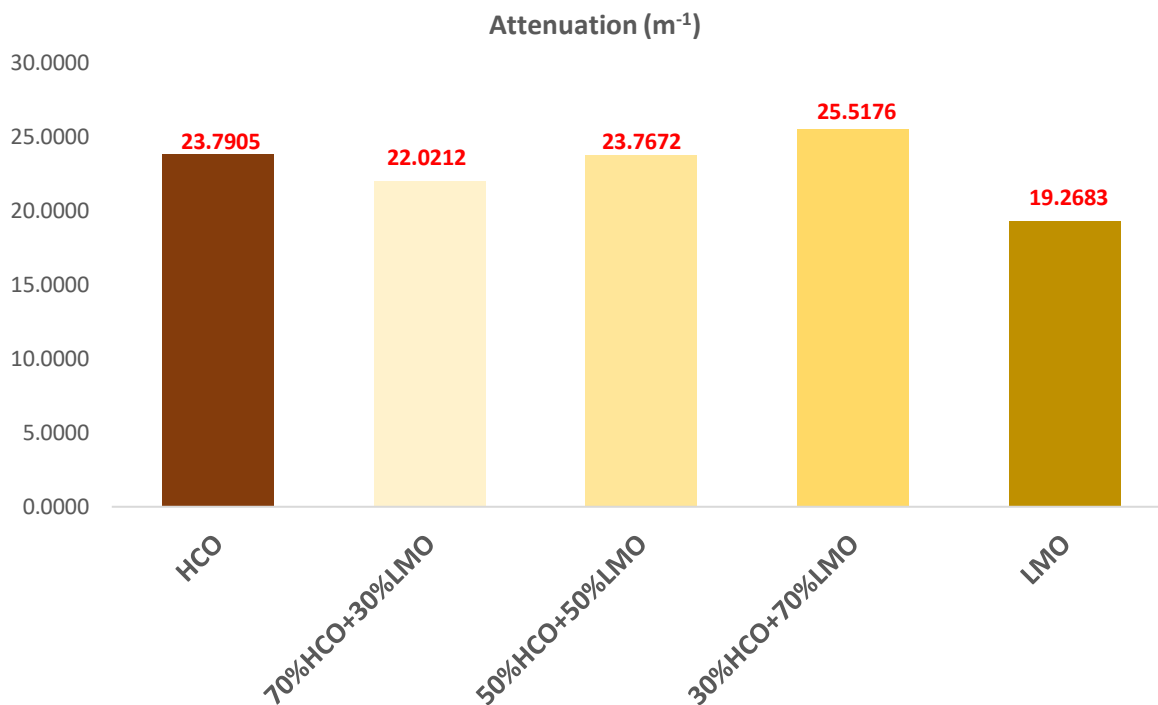


Fig. 3.25. The Attenuations for HCO, LMO and their blend in varying composition

3.3.5.1 Effects of adding LMO to HCO on Emulsions Characteristics

Blends of LMO and HCO in varying proportions were tested for their emulsion characteristics as well as test the potential of the ultrasonic probe to detect changes in the stability of their emulsions. As observed earlier the emulsions of the two oils exhibited extreme stability behavior while water separation was quick with mineral oil emulsions, there was very little separation from heavy crude oil emulsion. Both acoustic velocity and attenuation were calculated to establish the changes and water separations were recorded over 4 hours to test the stability of the emulsions.

3.3.5.2 Water Separation Tests with Emulsions of HCO and LMO Blends

Like HCO, the blend of HCO and LMO emulsions did not show visible water separation in the graduated cylinder. However, this does not imply that there was completely no separation taking place. After transferring emulsions from cylindrical to a conical separation vessel about 2.25%

separation of water was recorded, which is lower than HCO alone. This is contrary to expectation since emulsions of LMO alone show high separation, which implies adding LMO to HCO would increase water separation. The reason for the decreased separation could be a result of observed settling out of asphaltene content. Large dark brown lumps of asphaltenes were observed after 24 hours indicating that LMO contributes to the settling of asphaltenes.

3.3.5.3 Acoustic parameters in Emulsions of the Blend of HCO and LMO

Acoustic velocities measured in emulsions of the blends are compared in Fig. 3.26. The curve with the lowest acoustic velocity is for HCO only where the initial period of decrease is followed by an essentially constant value of acoustic velocity. However, with the LMO blends, after an initial period of decrease, the measured acoustic velocity increases towards that of LMO with its increasing content in the blends. For 70% LMO, at first, the acoustic velocity is low which then increases quickly closer to that of LMO only. In addition to settling out of asphaltenes in crude oil, LMO also separates from HCO over time to form the top layer due to its lower density. It may be noted that measurements are affected by the following simultaneous occurrences.

1. Settling/separation of water droplets from the emulsion.
2. Extraction of asphaltene molecules from the heavy crude oil by paraffinic mineral oil.
3. Separation of mineral oil from the bulk of crude oil.

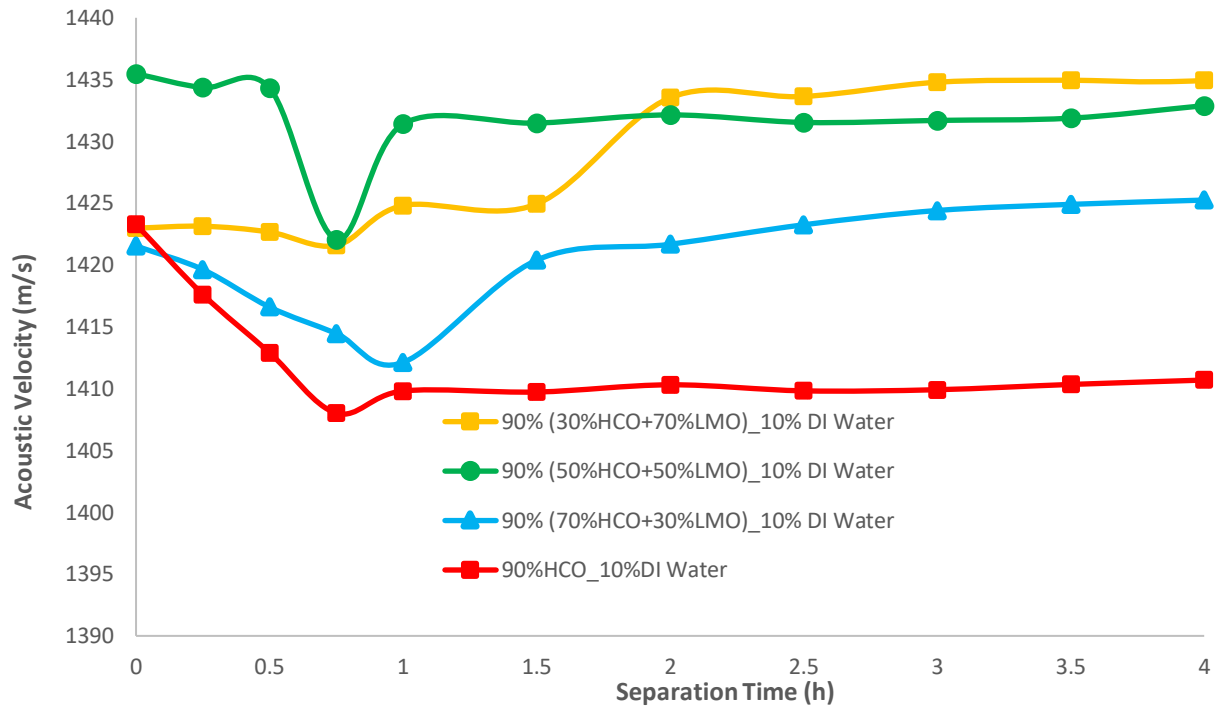


Fig. 3.26. Variations of acoustic velocity with time in emulsions of HCO/LMO blends

Fig. 3.27 Compares the corresponding attenuations recorded simultaneously with acoustic velocities. It is observed that there is little change in attenuation until about 30 minutes. Following which there is a significant drop until about one and a half hours, beyond which there is very little change except for 70:30 LMO/HCO blend. Attenuation changes in this blend were significantly slower and remained higher until about three hours. A trend can be observed between thirty minutes and 1 hour where there is an increase in attenuation with increasing LMO content. This behavior could be attributed to the interferences caused by the simultaneous separation of asphaltenes and water droplets from the suspensions. Also, there is a general decrease in all the curves indicating possible separation of water taking place. Appropriate ultrasonic frequency should be chosen to increase the sensitivity of attenuation and therefore achieve better results.

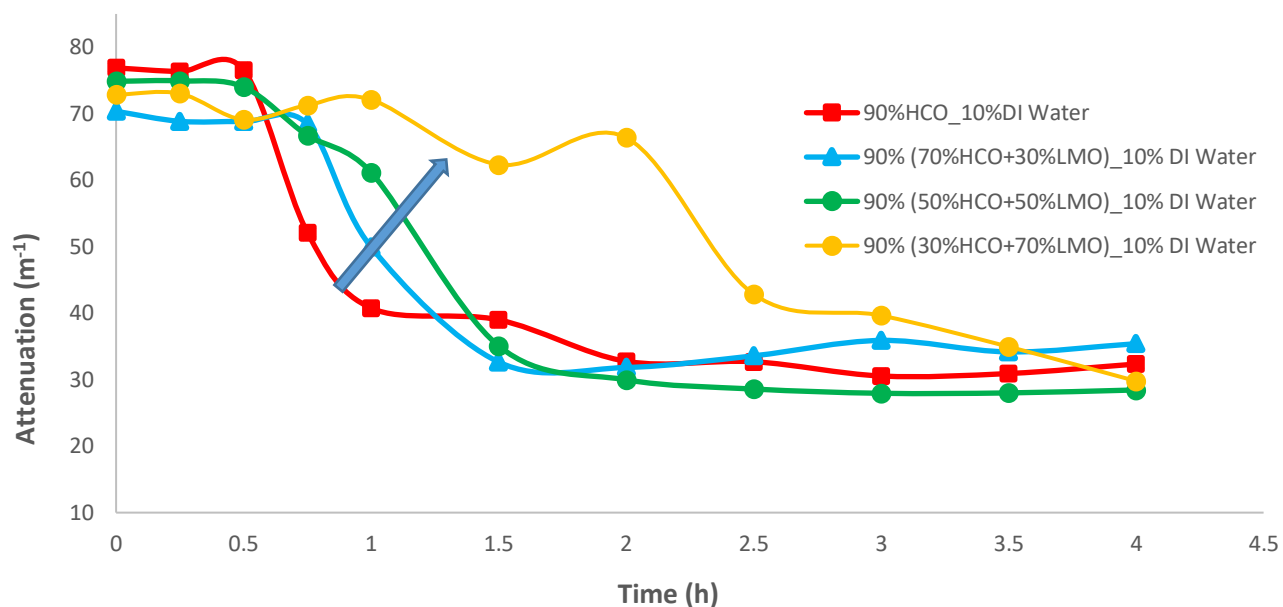


Fig. 3.27. Change of attenuation with time in the emulsions of blends

3.4 Conclusions

The application of ultrasonic based technology to characterize oils and their emulsions has been demonstrated through a series of tests in different systems. The two measured acoustic parameters are the time of flight and amplitude of the received wave from which acoustic velocity and attenuations are estimated. Initial tests with mineral oil and its emulsions allowed visual observations of water separation steps from emulsions and demonstrated the potential of the technique. Mineral oil emulsions with high water content (20% DI water) separated into their phases faster than emulsions with 10% DI water content. This is possible because high water content forms large water droplets which are easy to coalesce. This trend was observed from the acoustic velocity measurements. The technique also captured variations in asphaltene content of crude oil samples which is of practical significance in the petroleum industry. The link between asphaltene content and stability of crude oil emulsion stability is demonstrated. The decrease in acoustic velocity indicates water separation taking place. Therefore, changes in the composition

of HCO emulsions that cannot be seen visually can be analyzed using acoustic velocity. The analyzed results showed that the ultrasonic technique has high potential to be used for monitoring emulsion stability and track changes in emulsions characteristics.

Notations

A	amplitude (V)
A_0	reference amplitude (V)
c	acoustic velocity ($\text{m}\cdot\text{s}^{-1}$)
d	distance between transducer and reflector surface (m)
DI	deionized
f	wave frequency (s^{-1})
h	height of liquid column (mm or m)
I	intensity of acoustic wave ($\text{w}\cdot\text{m}^{-2}$)
k_1	wave number defined by equation 9 (-)
P	pressure (Pa)
r	particle radius (μm)
R	fraction of wave energy reflected from interface (-)
TOF	time of flight (μs)
Z	acoustic impedance of the medium ($\text{kg}\cdot\text{m}^{-2}\cdot\text{s}^{-1}$)

Greek Letters

α	attenuation coefficient (m^{-1})
β	bulk modulus of the medium (Pa)
λ	pulse wavelength (μm)
ρ	density of medium ($\text{kg}\cdot\text{m}^{-3}$)
ω	angular frequency ($\text{rad}\cdot\text{s}^{-1}$)
κ	isentropic compressibility (Pa^{-1})
φ	fraction of dispersed phase (-)

Subscripts

b	bottom
i	interface
o	initial value
r	reflector or reference
w	water

References

- Abdurahman H. Nour, and Rosli Mohd. Yunus. "Stability Investigation of Water-in-Crude Oil Emulsion." *Journal of Applied Sciences*, vol. 6, no. 14, Jan. 2006, pp. 2895–2900., i:10.3923/jas.2006.2895.2900
- Alshaafi, E. (2017). *Ultrasonic Techniques for Characterization of Oil-Water Emulsion and Monitoring of Interface in Separation Vessels*. MESC Thesis, Univ. of Western Ontario.
- Ament, W., (1953). Sound propagation in gross mixtures. *J. of Acous. Soc. of America*. 25(4), 638-641.
- Atkinson, C. M., and Kytömaa. H. K., (1997). Acoustic Wave Speed and Attenuation in Suspensions. *International Journal of multiphase flow* 18, no. 4: 577-592.
- Babick, F., Hinze, F., Ripperger, S. (2000). Dependence of ultrasonic attenuation on the material properties. *Colloids and Surfaces A: Physicochemical and Engineering Aspects*, 172(1-3), 33-46.
- Basaran, T. K., Demetriades, K., and McClements, D. J., (1998). Ultrasonic imaging of gravitational separation in emulsions. *Colloids and Surfaces A: Physicochemical and Engineering Aspects* 136, no. 1-2: 169-181.
- Coupland, J.N. and McClements, D. J., (2001). Droplet Size Determination in Food Emulsions: Comparison of Ultrasonic and Light Scattering Methods, 50, 117–20.
- Das, D.K., Nerella, S., Kulkarni, D., (2007). Thermal Properties of Petroleum and Gas-to-liquid Products. *Petroleum Sci. and Techn.* 25: 415-425.
- Derkach, S. R. (2009). Rheology of emulsions. *Advances in colloid and interface science*, 151(1-2), 1-23.
- Dalgleish, T., Williams, J. M. G., Golden, A.-M. J., Perkins, N., Barrett, L. F., Barnard, P. J. Watkins, E. (2007). *Journal of Experimental Psychology: General*, 136(1), 23–42.
- El-Sayed, Manar. "Factors Affecting the Stability of Crude Oil Emulsions." *Crude Oil Emulsions-Composition Stability and Characterization*, Feb. 2012, doi: 10.5772/35018.
- Dukhin, A. S., & Goetz, P. J. (2002). *Ultrasound for characterizing colloids particle sizing. Zeta Potential Rheology*: Elsevier Science.
- Edwards, D. K., Liley, P. E., Maddox, R. N., Matavosian, R., Pugh, S. F., Schunck, M., Schwier, K., and Shulman, Z. P. (1983). *Heat Exchanger Design Handbook*, Vol. 5.

Ensminger, D. and Bond, L. J. (2012). *Ultrasonics – Fundamentals, Technologies and Applications*, 3rd ed., CRC Press.

Graham, B. F., May, E. F., and Trengove, R. D., (2008). Emulsion inhibiting components in crude oils. *Energy & fuels*, 22(2), 1093-1099.

Hauptmann, P., Lucklum, R., Püttmer, A., & Henning, B. (1998). Ultrasonic sensors for process monitoring and chemical analysis: state-of-the-art and trends. *Sensors and Actuators A: Physical*, 67(1-3), 32-48.

Hipp, A. K., Storti, G., and Morbidelli, M. (2002). Acoustic characterization of concentrated suspensions and emulsions. 1. Experimental validation. *Langmuir*, 18, 405-412.

Holman, J.P. *Heat Transfer*, 7th ed., McGraw-Hill Inc. 1990

Kokal, S. L. (2005). Crude oil emulsions: A state-of-the-art review. *SPE Production & facilities*, 20(01), 5-13.

Kuster, G. T., Toksöz, M. N., (1974). Velocity and attenuation of seismic waves in two-phase media: Part II. Experimental results. *Geophysics*, 39(5), 607-618.

McClements, D. J., Coupland, J. N., (1996). Theory of droplet size distribution measurements in emulsions using ultrasonic spectroscopy. *Colloids and Surfaces A: Physicochemical and Engineering Aspects*, 117(1-2), 161-170.

McClements, D. J., (1996). Principles of Ultrasonic Droplet Size Determination in Emulsions, *Langmuir*, 12.14, 3454–61.

Meng, G., Jaworski, A.J. and White, N.M., (2006). Composition measurements of crude oil and process water emulsions using thick-film ultrasonic transducers. *Chemical Engineering and Processing: Process Intensification*, 45(5), pp.383-391.

Moradi, M., Alvarado, A. and Huzurbazar, S., (2011). Effect of Salinity on Water-in-Crude Oil Emulsion: Evaluation through Drop-Size Distribution Proxy, *Energy & Fuels*, vol. 25, 260-268.

Nadolny, Z. Dombek, G., (2017). Thermal properties of mixtures of mineral oil and natural ester in terms of their application in the transformer. *Int. Conf. Energy, Environment and Material Systems (EEMS)*, 1-6.

Perry, R.H., Green, D.W, Maloney, J.O. (1984). *Perry's Chemical Engineers Handbook*, 6th ed., McGraw-Hill Inc.

Pinfield, V.J., (2014). Advances in ultrasonic monitoring of oil-in-water emulsions. *Food Hydrocolloids*, 42, 48-55.

Pinfield, V. J., Povey, M. J., (1997). Thermal scattering must be accounted for in the determination of adiabatic compressibility. *The Journal of Physical Chemistry B*, 101(7), 1110-1112.

Su, M., Xue, M., Cai, X., Shang, Z., and Xu, F., (2008). Particle Size Characterization by Ultrasonic Attenuation Spectra”, *Particuology*, 6(4), 276-281.

Urick, R., 1947. A sound velocity method for determining the compressibility of finely devided substances. *Journal of Applied Physics*, 18(11), 983-987.

Wang, X., and Alvarado, V. (2009). Direct current electrorheological stability determination of water-in-crude oil emulsions. *The Journal of Physical Chemistry B*, 113(42), 13811-13816.

Yan, N., Gray, M. R., and Masliyah, J. H. (2001). On water-in-oil emulsions stabilized by fine solids. *Colloids and Surfaces A: Physicochemical and Engineering Aspects*, 193(1-3), 97-107.

Appendix A

Reproducibility of experimental results

To ensure that experiments are reproducible, repeat runs were conducted. Fig. A3.28 shows the repeat run completely the same as the first run. Therefore, using this procedure the same results can be reproduced. On the other hand, Fig. A3.29 & A3.30 showed similar trends between the two runs and detected the slight difference in the two emulsions. This indicates that both ultrasonic parameters (acoustic velocity and attenuation) can capture the small difference in the emulsions that can be due to experimental errors when preparing emulsions. Therefore, this technique very reliable and has high accuracy.

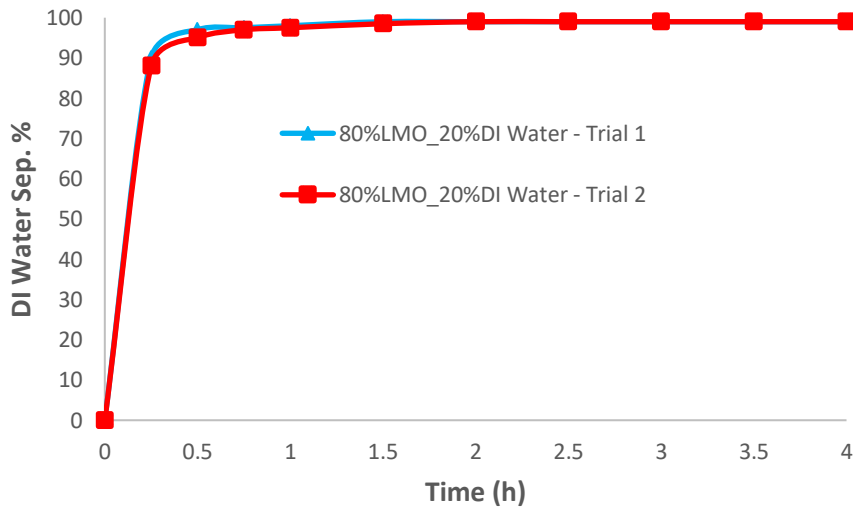


Fig. A3.28 Water separation % for LMO emulsions

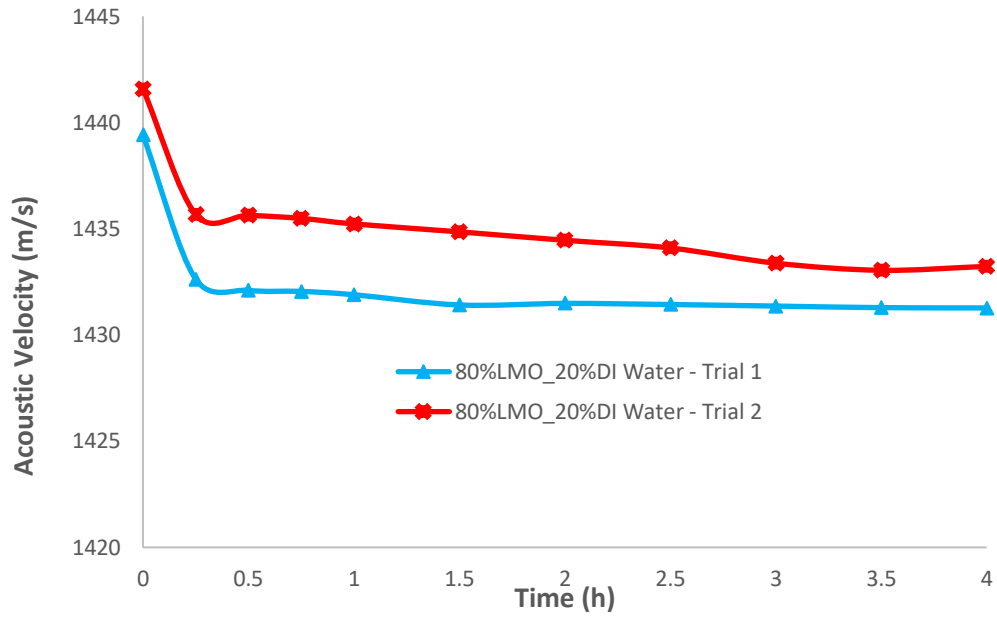


Fig. A3.29. Acoustic Velocity for LMO emulsions

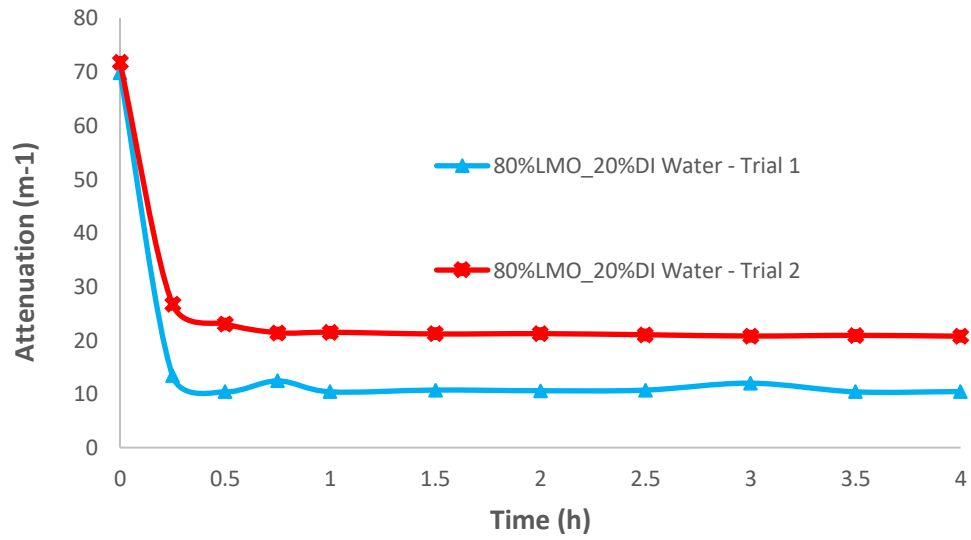


Fig. A3.30. Attenuation for LMO emulsions

Fig. A3.31 shows that the ultrasonic technique can capture the change in the characteristic of HCO when LMO is added. Acoustic velocity increases with an increase in LMO content. This is expected since LMO alone has higher acoustic velocity than HCO alone.

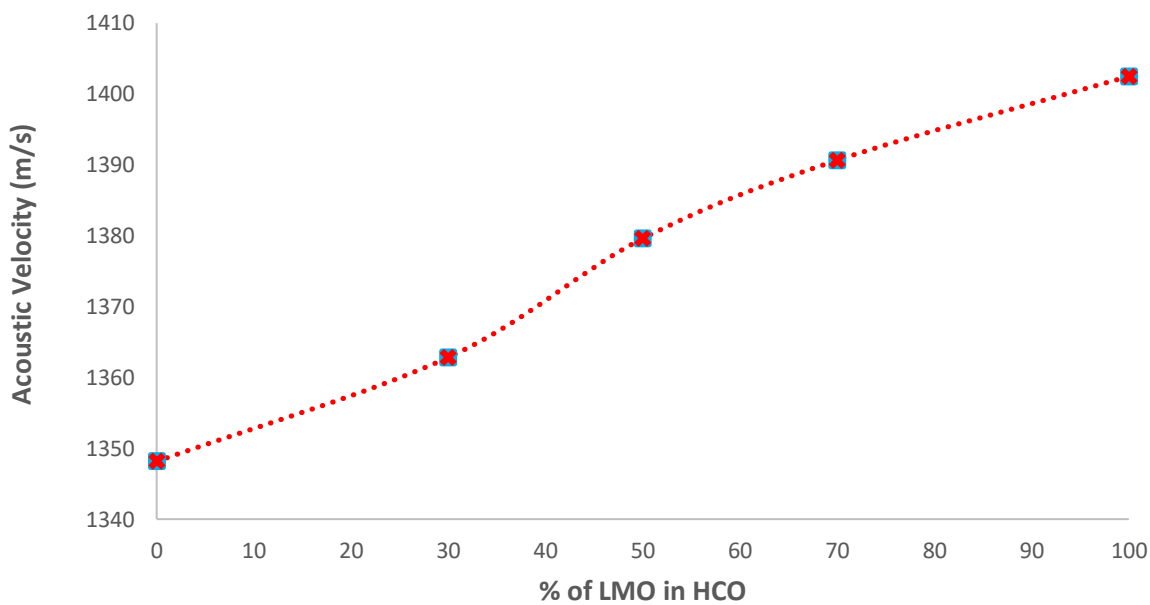


Fig. A3.31. Effect of adding LMO in HCO on its acoustic velocity

HCO only and LMO only are added for more understanding. As explained in Fig. 3.25, Fig. A3.32 shows the acoustic velocity of the blends of HCO and LMO is between the acoustic velocity of the individual oils.

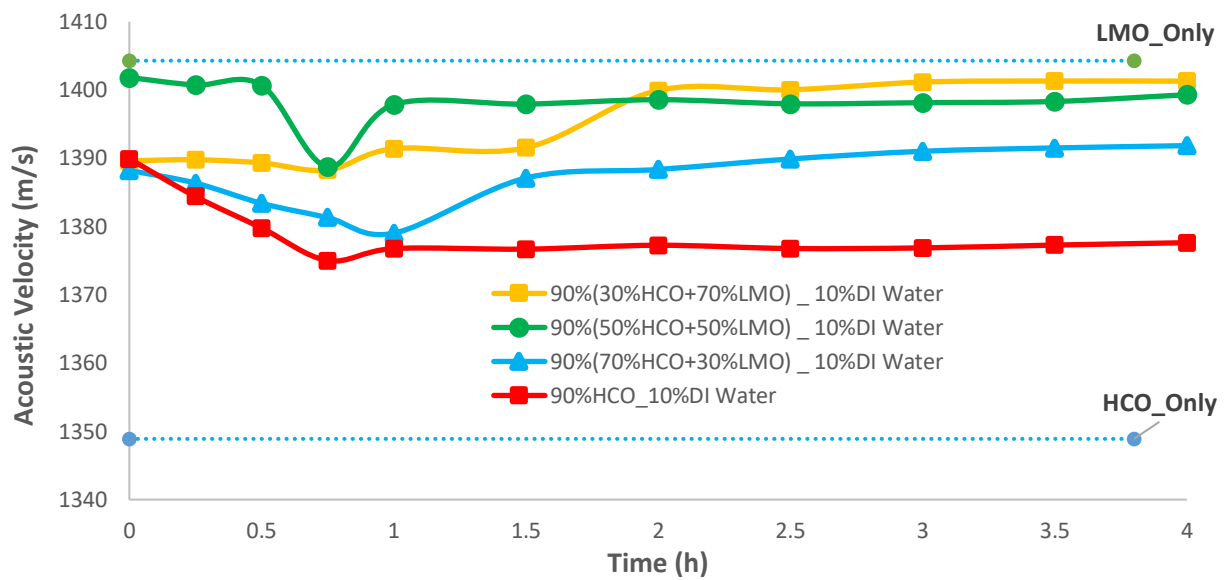


Fig. A3.32. Variations of acoustic velocity with time in emulsions of HCO/LMO blends

Chapter 4. Ultrasonic based techniques to monitor oil layer depth of spills

Abstract

There is a growing concern about the harmful environmental impact caused by spills of petroleum and its products during their storage and transportation. Currently, there is a lack of suitable measurement techniques to monitor these leaks. The applicability and potential of ultrasonic based methods to detect and monitor oil layer thickness of petroleum product spills have been demonstrated by conducting a series of tests. Initial tests were conducted with mineral oil samples to establish procedures and determine potential sources of errors. It is shown that simultaneous measurements of acoustic velocity and attenuation provide a strong combination to detect the presence of oil and emulsion layers. For the oil layer on the surface of the water, a simple method to determine oil layer thickness is proposed. Moreover, a more general and robust procedure has been proposed based on the observations and tests of the study.

4.1 Introduction

The high dependency of the economic base and industrial activities on crude oil and petroleum products has immensely increased their quantity being transported across the seas and other waterways. In addition, their storage underground poses a lot of environmental concerns. This is due to the occurrence of oil spills that cause both local and global environmental concerns (Onwurah et al., 2007). The toxic effect of the oil spill can last over a decade since the bulk of oil remains in the less-weathered subsurface. In their random sampling of underground fuel storage tanks, U.S. Environmental Protection Agency (USEPA) found 35% leaks in the sampled tanks (United Press International, 1986). One of the biggest challenges facing researchers in the study of oil spills is the ability to measure oil layer thickness. More specifically, there are no laboratory methods or reliable field techniques to measure oil on water thickness. The desire to measure oil thickness is driven by the need for significant advances in the primary understanding of how oil

thickness spread and the effective response like spill cleanup. Another motivation for determining the oil thickness is to determine the amount of oil spilled. The existing method of using airborne surveillance of oil thickness with the sensors usually overestimates oil quantity (Brown et al., 1998).

A common and economical remote sensor is the one based on ultraviolet/infrared (UV/IR) scanners and cameras (Brown et al., 1995). While the UV portion of the sensor can detect the entire area of the slick including the thin sheen area, the thermal IR portion provides information on the thicker portions of the slick. These optically thick layers will absorb solar radiation, a portion of which is re-emitted in the thermal IR region. However, a thin sheen of the oil slick is undetectable in the thermal IR region of the spectrum. The data collected from the UV and IR portions can be integrated to provide an indication of the thick and thin portions of the slick. The UV/IR scanners, however, do not provide values for actual oil layer thickness and there is a need for calibration with a sensor capable of absolute slick thickness measurement (Brown et al., 1995; Belore, 1982). A sensor based on ultraviolet laser pulse has shown limited success in its ability to measure the slick thickness (Hoge and Swift, 1980; Kung and Itzkan, 1976). The ultraviolet laser pulse is used to excite the OH stretching vibration in water which leads to a phenomenon known as Raman scattering. When the oil is present on the water surface, the Raman signal is depressed in a manner proportional to the thickness of the oil. However, oil thickness cannot exceed its optical thickness – up to about 20 microns depending on the absorption properties of the oil. The Laser Ultrasonic Sensing of Oil thickness (LURSOT), is the most promising remote sensing technique that uses the concept of speed of sound being relatively constant in the liquid oils (Fingas, 2018). The sensor employs a short laser pulse to produce ultrasonic waves in an oil layer in conjunction with a second laser coupled to an optical interferometer for the remote detection

of ultrasonic surface movements (Brown et al., 1995). First, a thermal pulse is created in the oil layer by absorption of a powerful CO₂ laser pulse which initiates a rapid thermal expansion of the oil near the surface where the laser beam was absorbed. As a result, there is a step-like rise of the sample surface together with an acoustic pulse of high frequency and large bandwidth. The generated acoustic pulse travels down the oil layer until it meets the oil-water interface, where it is partially transmitted and partially reflected toward the oil-air interface where a slight displacement of the oil surface occurs. The total time lapsed for the acoustic pulse to travel through the oil and back to the surface again is a function of the thickness and the acoustic velocity of the oil. A second laser probe aimed at the surface measures the displacement of the surface. This complex technique has met with only limited success due to several sources of errors and current instrument limitations, as listed below.

- The weak acoustic impedance mismatch between oil and water results in a weak acoustic reflection coefficient leading to weak reflected signals.
- Under certain conditions, the oil spills can also lead to the formation of water-in-oil emulsions which have acoustic properties even closer to those of water, reducing the reflection coefficient even further. This leads to an even weaker signal of echoed acoustic pulse, requiring more sensitive and expensive equipment. Impurities such as asphaltene and fine solid particles, found in crude oil, stabilize emulsions, making them persist for long (El-Sayed, 2012).
- The accuracy of the laser-ultrasonic measurement of oil thickness also depends on the accuracy of the measurement of the acoustic velocity of the oil which can vary from 10 to 25% depending on composition and weathering effects (Brown et al., 1995; Wang and Nur, 1991).

The focus of the current work is the development of low-cost ultrasonic-based techniques to detect the presence of oil spills as well as to measure the thickness of oil and emulsion layers. The approach is based on simultaneous measurements of two main acoustic parameters, namely acoustic velocity (or time of flight) and attenuation (or amplitude). These parameters depend on the physical and thermodynamic properties of the propagating medium. It is envisaged that a low-cost device with acceptable accuracy can be developed based on ingenious ideas while taking advantage of the new developments in the field.

4.2 Experimental Details

4.2.1 Materials and Methods

The two types of oil used are Light mineral oil (LMO), and crude oil (CO). The LMO was purchased from VWR international while CO was provided by Imperial Oil Ltd. The commercial non-ionic hydrophilic surfactant Tween 20 (Polyoxyethylene-20-sorbitan Monolaurate) with chemical formula $C_{58}H_{114}O_{26}$, was used as emulsifier during the preparation of mineral oil emulsions. Brookfield digital Rheometer was employed to determine the viscosity of the oils. Density measurements were conducted using SG-Ultra Max Ex Petrol Density Meter, by Eagle Eye Power Solutions. IKA mechanical mixer (model RW 20D), with a four-blade stainless steel propeller-type stirrer, was used to prepare the emulsion mixtures. The measured physical properties are summarized in Table 4.1.

Table 4.1. Physical properties of different oils used to prepare emulsions.

Fluid	Density (kg/m ³)	Viscosity (cP)	Specific gravity	°API	Asphaltene content (wt. %)
DI Water	997.7	1.02	1	-	-
LMO	858.7	91.20	0.861	-	-
HCO	907.4	107	0.909	24.23	13.17

4.2.2 Experimental Setup and Procedures

A schematic of the experimental setup used is shown in Fig. 4.1. It consists of a jacketed vessel for preparing emulsions and taking readings of the thickness of oil and their emulsions layers. The ultrasonic measurements were taken with the help of a probe shown in Fig. 4.2. Its total length was 330 mm and the distance between the transmitting and receiving surface was 51.2 mm. It was inserted vertically into the vessel containing the liquid layers while ensuring that its transmitting and receiving surfaces were fully immersed in the liquid phase. The transducer was connected to the pulse-receiver (UTEX Inc.), capable of exciting ultrasonic transducers with center frequencies from 1 MHz to 150 MHz. However, the probe used in this study had a frequency of 3.5MHz. For every reading of the time of flight (TOF) and amplitude, 1200 data points are taken over 60 seconds. The averages of these data points were then used to calculate the acoustic velocity and attenuation, respectively. It was controlled by a software interface which allowed remote control and configuration of the instrument. Transducer excitation was achieved with an ultra-fast square wave pulse featuring adjustable pulse width and adjustable pulse voltage. The amplifiers in the instrument were directly gain controllable eliminating the need for attenuators that contribute to receiver noise.

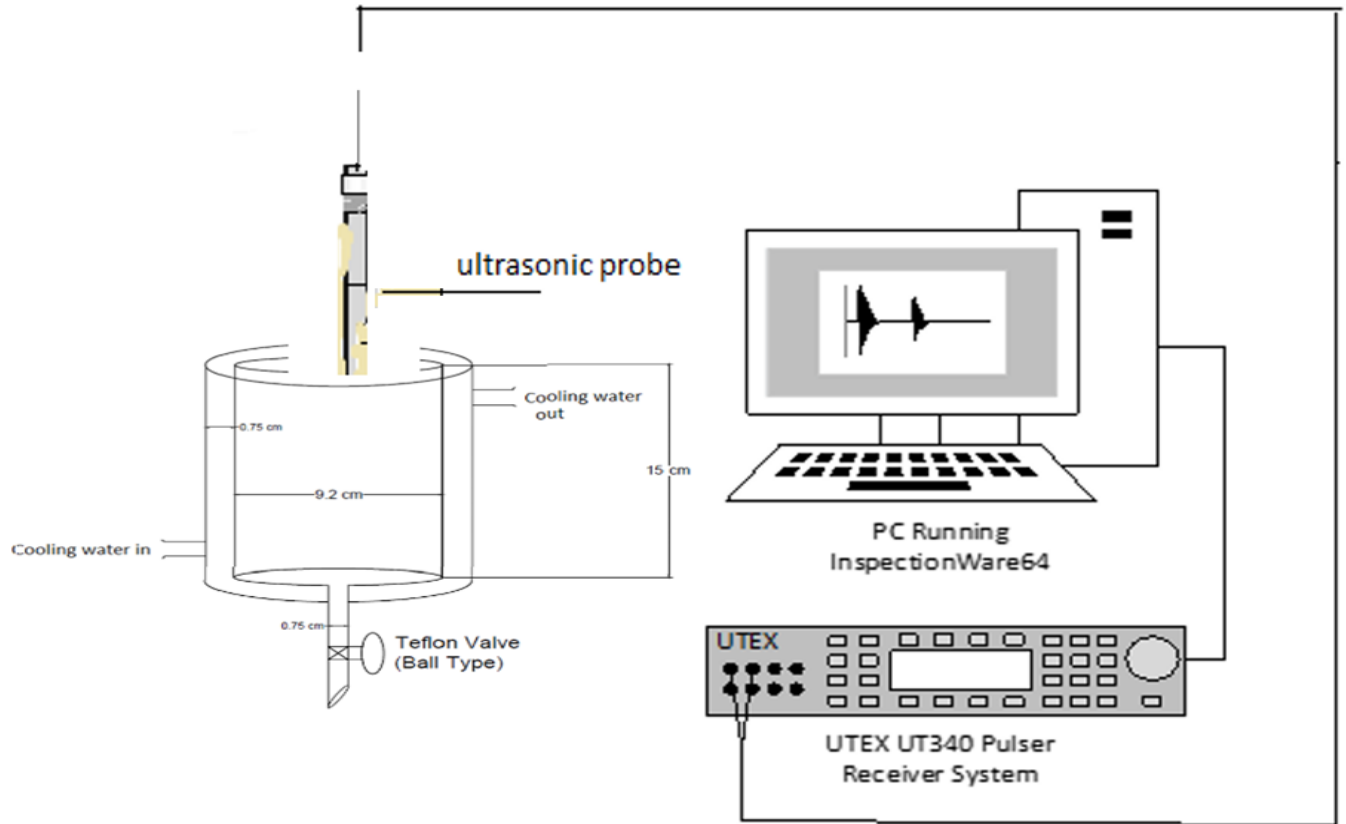


Fig. 4.1. Schematic diagram of the experimental setup

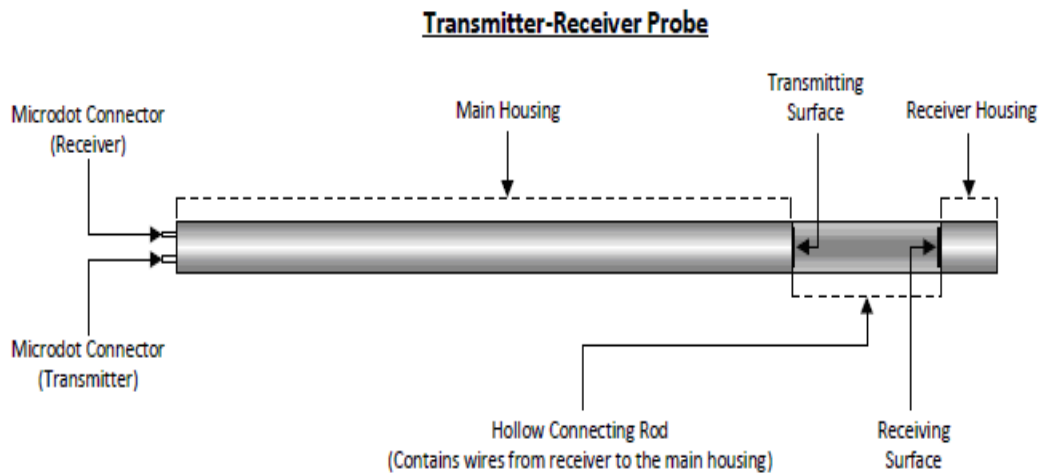


Fig. 4.2. Details of the ultrasonic probe

At first, the experiment was conducted by taking readings of layers of DI water and oil samples without emulsions. For the second set of experiments, the emulsion was prepared with samples of oil content (90 %) and 10% DI water at an agitation speed of 1200 rpm. For LMO, 4% Tween 20 emulsifier was added to create a tight emulsion, then agitated for 5 minutes for a homogenous solution. On the other hand, crude oil does not require emulsifiers because it already has asphaltenes which act as natural surfactants. The final mixture is let to agitate for 30 minutes. A 3 mm thick layer of this emulsion was placed at the DI water surface before taking the reading. A maximum of 10 mm of oil sample was added to the DI or emulsions layer. First, DI water is placed in the vessel then the oil layer or emulsion layer of different thickness is added to track changes in layer thickness. For three-layer DI water, emulsion and oil systems, the emulsion layer was added to the surface of DI water first followed by the oil sample layer.

For initial tests, the probe was inserted into the container, every time a new layer of oil sample was added and was removed after taking the readings. This method was later changed especially with crude oil since oil was found sticking to the surface of the probe thus influencing the readings. In the revised method, the probe was inserted into the vessel containing DI water before adding the oil sample to avoid oil sticking on the active surface of the probe that will be in the DI water layer. The following steps were followed when taking the readings:

1. First, DI water is added into the jacketed vessel, then the probe is inserted until its distance d is in the DI water layer.
2. The emulsion is then added gradually. If emulsion is not used, oil sample is added instead
3. DI water is drained out for emulsion or oil sample to reach the section of d .
Measurements for ToF and amplitude are taken.
4. The oil sample is added in the increments of 1 mm

5. DI water is now drained out to bring the oil layer within the active area of the probe.
6. The maximum thickness of the oil sample is 10 mm or (3 mm emulsion+ 7 mm) of oil

4.2.3. Calculation of Acoustic Parameters

Acoustic velocity and attenuation of the propagating wave are the two ultrasonic parameters used to track the layers of oil and emulsions prepared in the experimental part of this work. The ultrasonic probe which operates in transmission mode is used to measure amplitude and TOF. Fig. 4.3 is captured waveform when the probe moves from DI water to a layer consisting of 3 mm thickness of LMO emulsion and 1 mm thickness of LMO and remaining water phase.

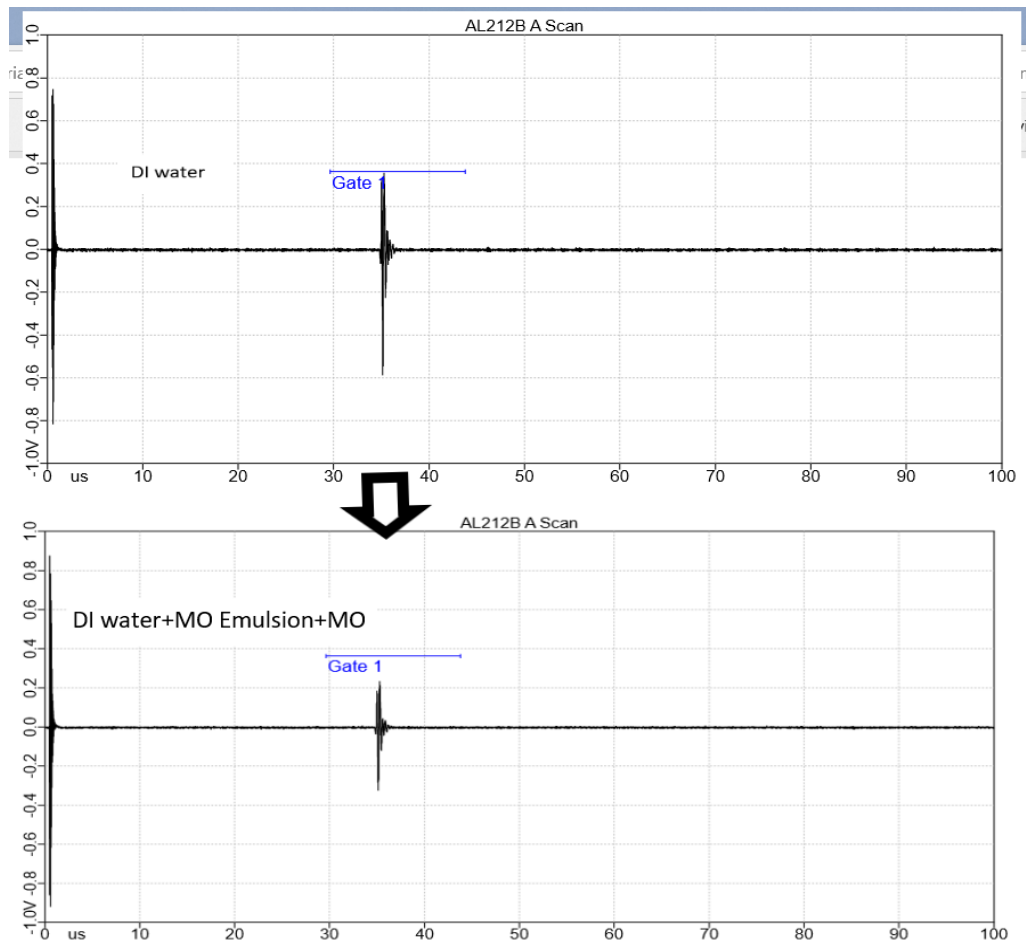


Fig. 4.3. Comparison of ultrasonic signal in DI water vs. layer of MO and its emulsion in DI water

The amplitude (voltage) is on the y-axis while TOF on the x-axis. As observed, the probe captured a bigger signal for the DI water compared to the thickness of (LMO + LMO emulsion) where the signal is reduced. TOF is the time it takes the wave to travel from the transmitter to the receiver. The speed of sound is then calculated in each medium using equation

$$v = \frac{d}{TOF} \quad (4.1)$$

Acoustic velocity is governed by thermodynamic properties of the medium through which it is traversing. This is based on the sound propagation as a harmonic longitudinal compression wave, The Newton-Laplace equation presents acoustic velocity through a given medium as a function of this bulk modulus (β) and density (ρ) (Povey, 1997; Ament, 1953; Urick, 1947).

$$v = \sqrt{\frac{\beta}{\rho} = \frac{1}{\sqrt{\rho K_s}}} \quad (4.2)$$

Equation 4.2 can be used to predict values of acoustic velocity for different media if data for bulk modulus and density are provided. The drawback of this equation is that it is only applicable for homogenous fluids. For emulsions, which is the non-homogenous system, effective density and elasticity of the suspension are calculated to modify this equation. This is based on the volumetric fractions of the suspension.

An acoustic wave traveling through a medium experiences energy loss which depends on the composition of the medium as well the frequency of the wave. This is measured by the decline in the amplitude of the wave traveling a known distance through the medium and expressed as the attenuation coefficient (α) as presented in equation 4.3.

$$\alpha = -\frac{1}{d} \ln\left(\frac{A}{A_0}\right) \quad (4.3)$$

Where A_0 , is the reference amplitude and A is the final amplitude of the transmitted signal. The reference amplitude in this work is the amplitude of the transmitted signal in the DI water sample. Whereas A is the amplitude of other samples or emulsions.

Data Analysis

Prior to plotting, the data set collected was analyzed for possible outliers, random errors, etc. Two methods used to analyze the data set were frequency distribution and scatter plots to eliminate possible errors before using it to calculate acoustic velocity and attenuation. Fig 4.4 and 4.5 are the representation of frequency distribution and scatter plots for readings of 1 mm thickness of MO on DI water. The readings are very consistent as can be seen in Fig. 4.5. The purpose of the scatter plot is to identify the outliers and use a frequency distribution to eliminate them. In this case, there are no outliers. However, frequency distribution was still plotted to show how close data points are. Theory suggests that the data point of emulsions fall within the range of DI water and oil sample which is consistent with the observation. Therefore, it was not necessary to apply data filtering in these experiments.

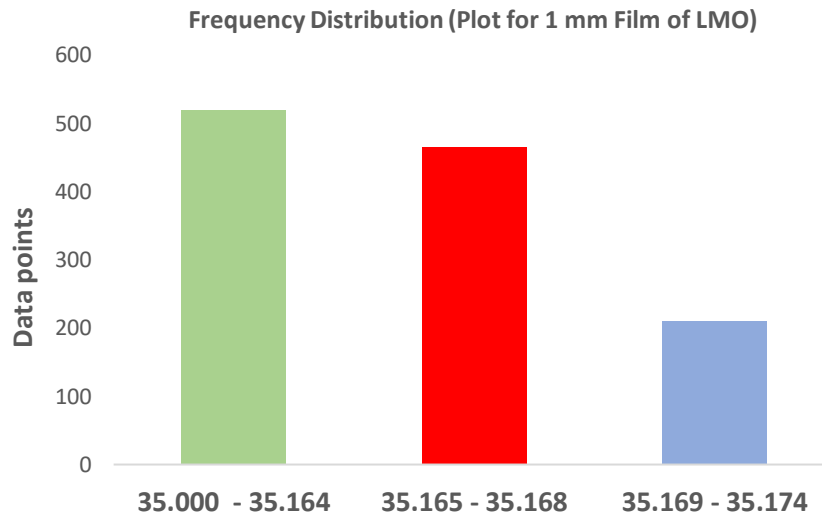


Fig 4.4. Frequency distribution plot for 1 mm film of LMO

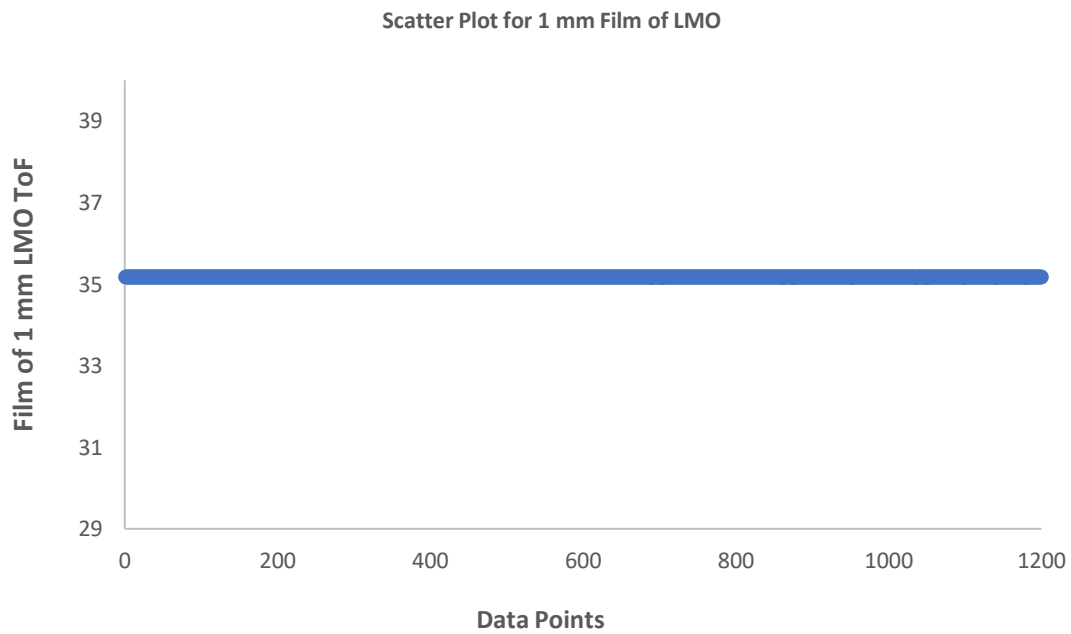


Fig 4.5. Scatter plot for data collected with 1 mm oil film of LMO

4.3 Results and Discussions

Acoustic parameters were first measured in the oil samples and compared with DI water values, wherever applicable. Figure 4.6 presents the calculated acoustic velocity for samples of liquids used in this work. Water has the highest acoustic velocity as expected followed by LMO and crude oil. The low acoustic velocity in crude oil samples can be attributed to its complex composition. Table 4.2 compares the experimentally obtained acoustic velocities with predicted values using Urick's equation 4.2. Part of the error can be attributed to fluid from literature having a density different than the density measured in the lab. Furthermore, it can be seen from Urick's equation, the acoustic velocity is inversely proportional to the density of the fluid. However, considering the Urick's equation, the bulk modulus contributes to the higher acoustic velocity. Therefore, the higher acoustic velocity for water and mineral oil is justifiable despite the higher value of density.

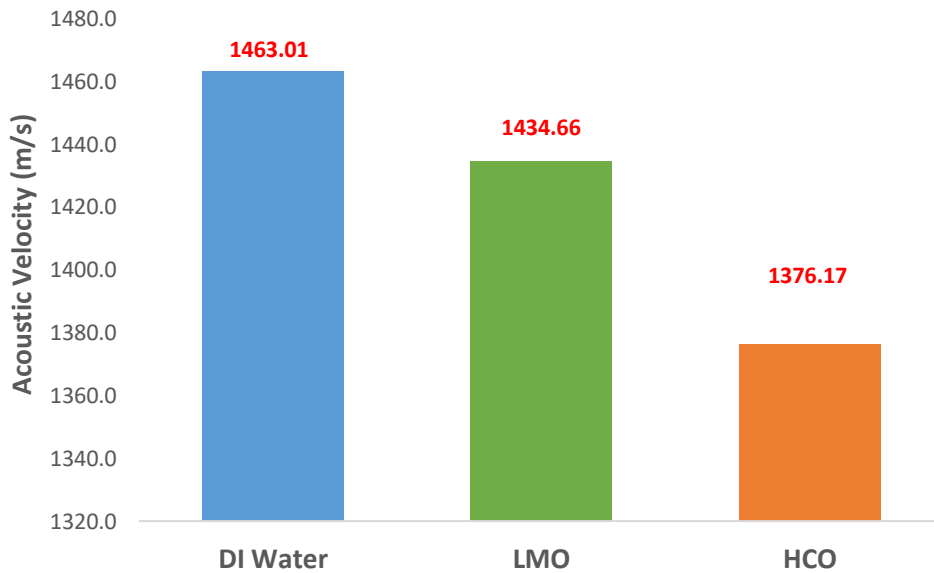


Fig. 4.6. The acoustic velocities for fluids used in this work

Table 4.2. Comparison of acoustic velocity using experimental and literature data

Sr. No.	Fluid	Density (Kg/m ³)	Bulk Modulus (pa) [18]	Acoustic velocity (m/s) [Experimental]	Acoustic velocity (m/s) [Literature]	% Error
1	Water	997.7	2.15E+09	1463.01	1467.976975	0.338355
2	LMO	858.7	1.66E+09	1434.66	1391.384334	3.110260
3	HCO	909.4	1.50E+09	1376.17	1320.215899	4.2382538

Fig. 4.7 illustrates attenuations for the fluids used in this work. Low attenuation implies low energy loss. Attenuation plot does not have DI water since it is used as the reference point amplitude (A₀) in the calculation of attenuation for oil samples.

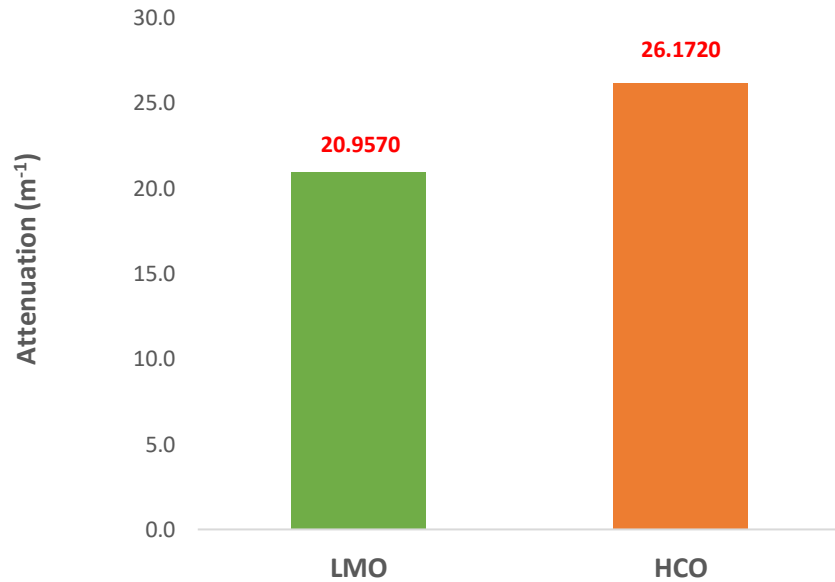


Fig. 4.7. Amplitude and the Calculated Attenuation values for fluids

4.3.1 Measurements with layers of MO on Surface of DI water

The potential of the ultrasonic technique to detect the presence of oil and its emulsion layers was first tested with mineral oil and its emulsions. Mineral oil consists of a mixture of mostly paraffinic

hydrocarbons in the carbon number range of 18 to 28 making. LMO is difficult to evaporate during an experiment. Moreover, it is a clear liquid, allowing visual observations to be recorded more easily thus serving as a good reference for trends of measured parameters. Measurements of acoustic velocity with increasing thickness of the LMO layer on DI water are presented in Fig. 4.8. The first reading is for the acoustic velocity of DI water without the addition of the LMO layer on the surface. It is observed that the acoustic velocity decreased with increasing thickness of the oil layer. The initial drop in the velocity is steep up to 1 mm oil layer thickness followed by a gradual decrease. Each additional increase in the thickness of the LMO resulted in a decrease in acoustic velocity towards the velocity of LMO only. At a low thickness of less than 1 mm, the transducer surface would be very close to the oil-water interface, where interference may occur with wave propagation from the transducer surface.

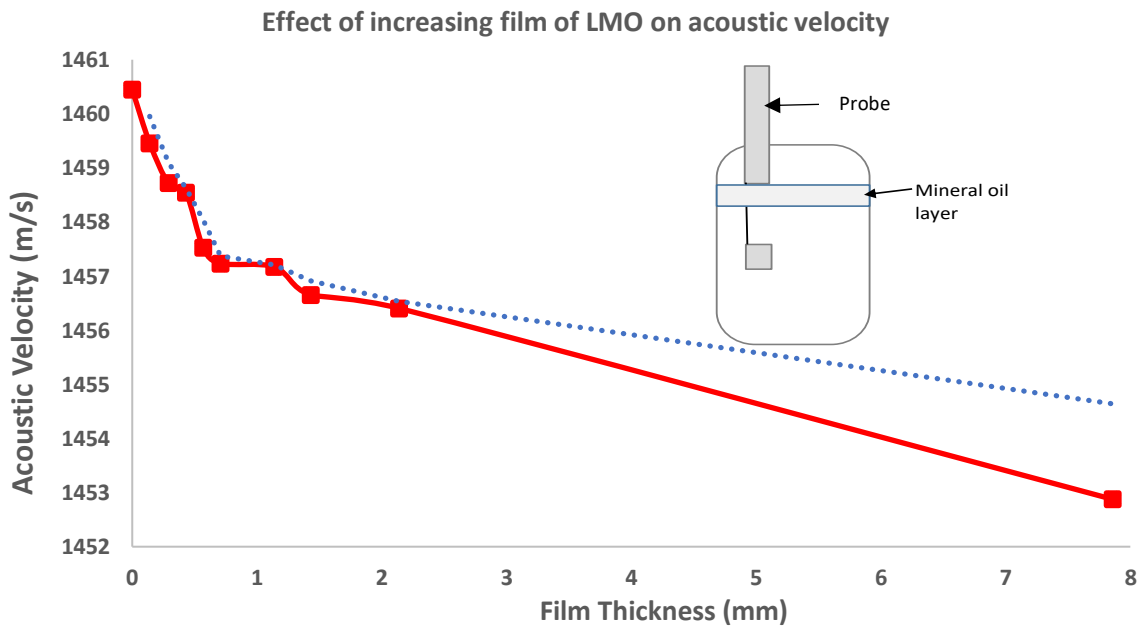


Fig.4.8. Variation of acoustic velocity with increasing thickness of MO layer

Fig. 4.9 shows the attenuations obtained from amplitude measurements of the corresponding acoustic velocity measurements. It can be observed that initially, attenuation increases quickly with the addition of the MO layer on the water surface, followed by a more gradual increase.

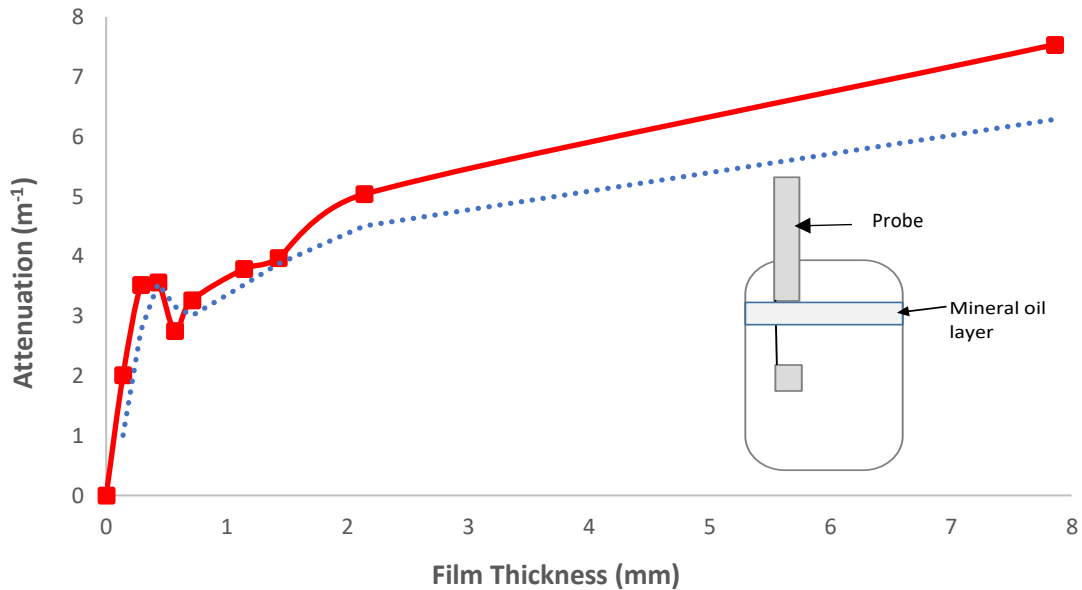


Fig. 4.9. Changes in attenuation recorded with increasing thickness of MO layer

This behavior is like the one observed with acoustic velocity measurements. This may again be attributed to the somewhat dominant effect of the proximity of the oil-water interface on the measurements. It may be pointed out that, for these initial experiments, the probe was inserted into the liquid phase for the measurements every time more LMO was added. It was observed that small amounts of LMO were remaining adhered to the probe surface every time it was removed from the vessel (see Fig. 4.10). These observations helped improve the procedure used later with crude oil experiments.

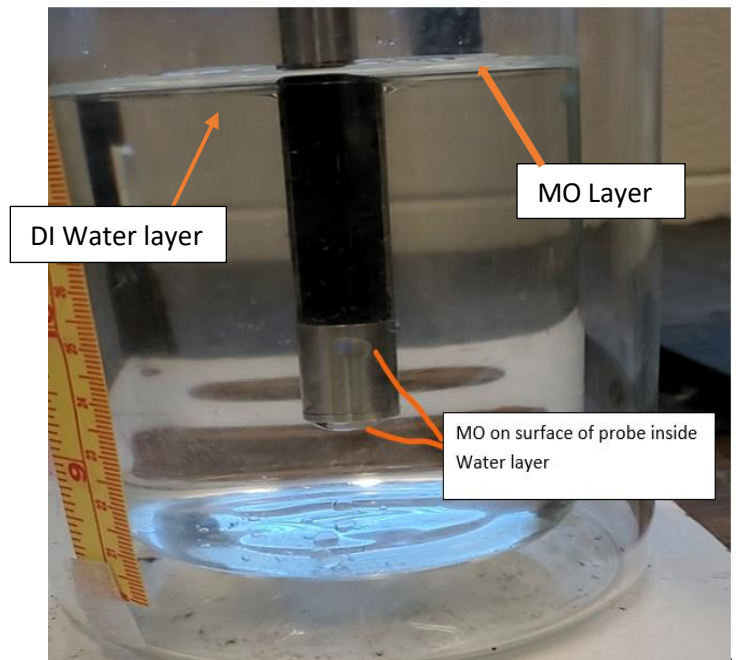
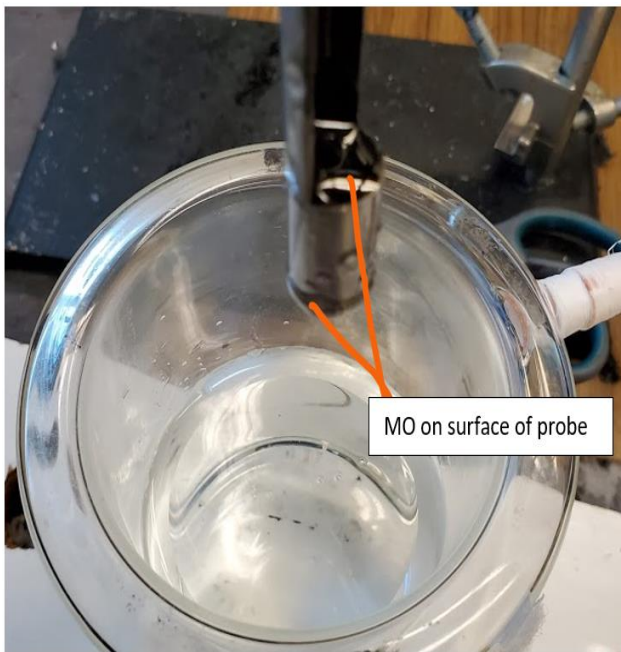


Fig. 4.10. Pictograph showing mineral Oil sticking on the surface of the Probe

4.3.2 Measurements with Layers of LMO and its Emulsion on DI Water Surface

When oil spills occur on a large water body, water current or waves generated by wind, etc. can cause the formation of emulsions due to mixing effects. This emulsion layer can be difficult to detect as well vary in thickness. To determine the effects of the emulsion layer on the measured parameters, experiments were conducted by adding a layer of LMO emulsion on the surface of the DI water, followed by the LMO layer. Measurements were conducted first by adding the emulsion layer on the water surface followed by the addition of the oil layer for the combined effects. It is observed from Fig. 4.11 that the addition of 3 mm of the emulsion layer led to a slight decrease in

acoustic velocity followed by a larger drop when only 1 mm of oil layer was added. However, essentially no change was observed when the next 2 mm of oil layer was added. It was also noted that due to its inherent instability, the emulsion layer thickness was decreasing slowly thus affecting the measurements. Moreover, there was a tendency for the emulsion to stick to the surface of the probe which further exacerbated the effects. As discussed later, the measurement procedure was altered for crude oil to minimize these observed effects.

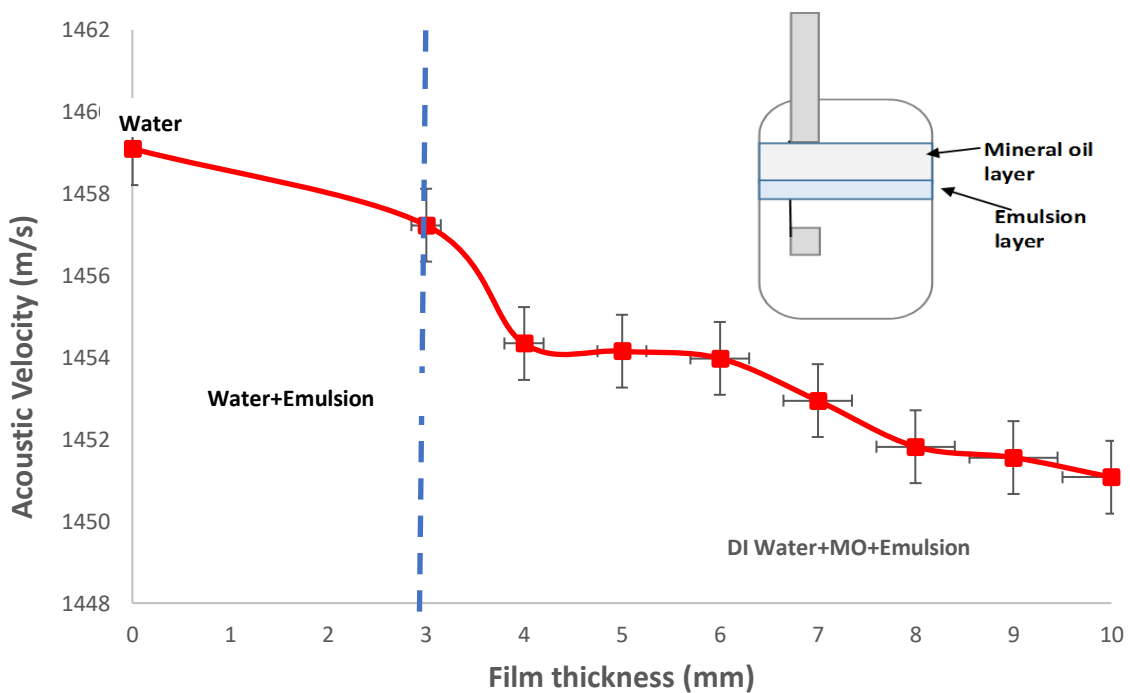


Fig. 4.11. Ultrasonic velocity for the Film of MO + Emulsion

Fig. 4.12 presents the corresponding attenuation data obtained with acoustic velocity measurements. There is an increase in attenuation due to the addition of the emulsion layer which can be attributed to the presence of water droplets and their interactions with the propagating wave. The addition of the first oil layer on the surface of the emulsion layer led to a quick increase in attenuation followed by a slower increase up to about 6 mm and a further increase thereafter. As

observed with acoustic velocity, this behavior can be mainly attributed to changes in the emulsion layer due to its instability and water droplet separation effects. This illustrates that acoustic velocity and attenuation data can be used together to detect the presence of different layers on the water surface. This would, however, require the development of calibration plots appropriate for the desired application.

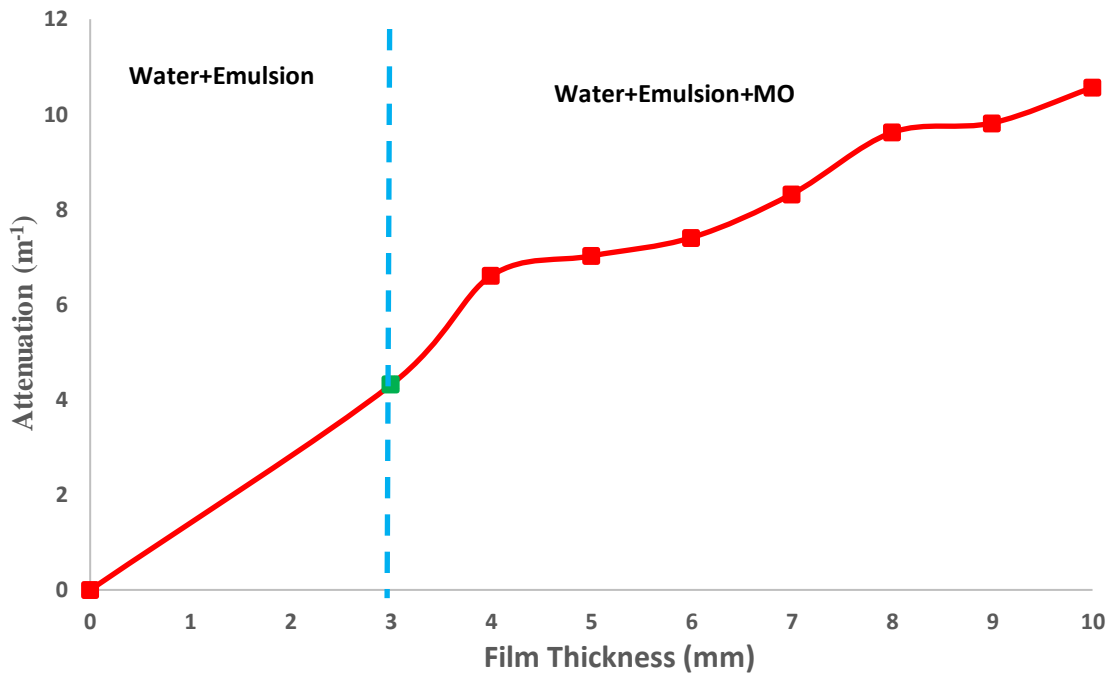


Fig. 4.12. Attenuation of the Film of LMO + Emulsion

The time-dependent behavior of the emulsion phase was further investigated by recording changes in attenuation with time (Fig. 4.13). It is observed that there is an initial drop in attenuation followed by a nearly stable phase with little change in attenuation. The drop indicates the separation of larger droplets of the dispersed water phase in the emulsion while the stable region is indicative of the emulsion of slow-moving smaller droplets. Fig. 4.13 also compares the characteristics of the emulsion of mineral and crude oils which have similar trends but different

attenuation levels. Thus, the technique can detect differences in the characteristics of LMO and LCO emulsions.

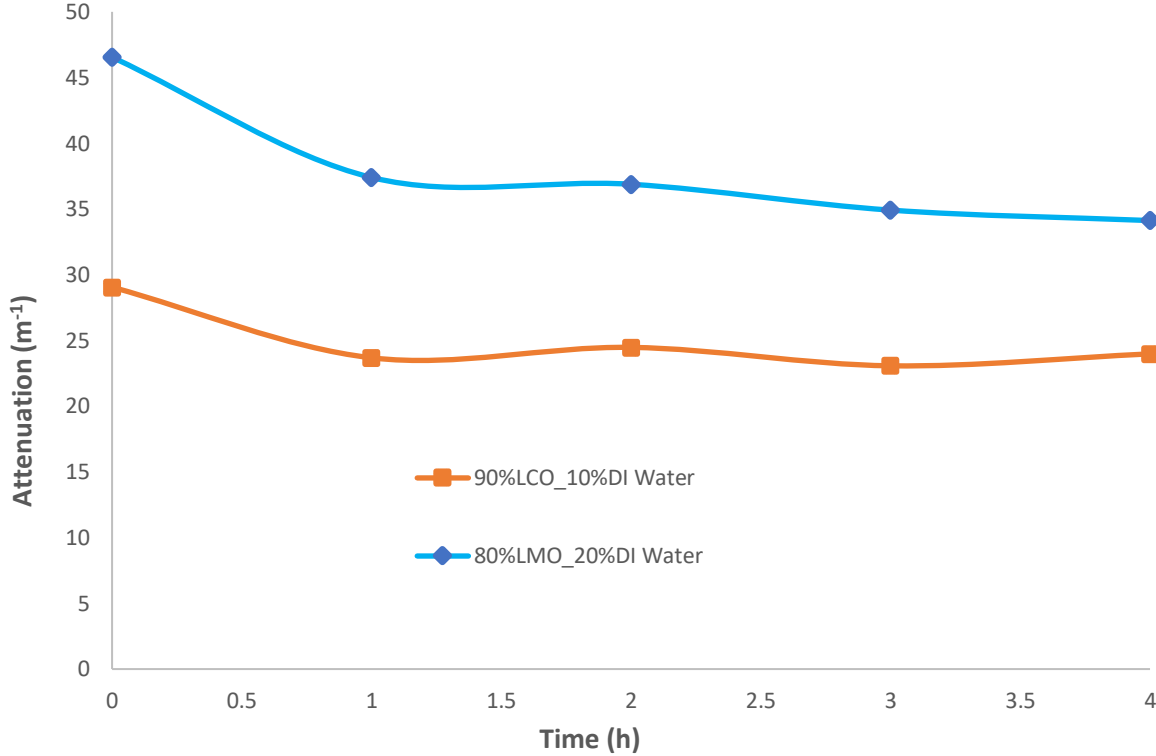


Fig. 4.13. Comparison of stability of LMO and LCO emulsions

4.3.3 Measurements of Acoustic Parameters with Layer of HCO and Its Emulsion on Water Surface

Crude oil spills are encountered during their storage and transportation operations in the petroleum industry. As discussed earlier, there is a need for a suitable device to monitor and assess the buildup of crude oil slick thickness resulting from a spill. Fig. 4.14 shows layers of crude oil and their emulsions placed on the water column in the vessel used for the measurements. While changes to crude oil layer thickness were easy to measure, the opaque characteristics of crude oil and its emulsions made it difficult to visually differentiate the two layers when placed one above the other. Water current and wave cause the spilled oil to form emulsions that are difficult to detect using the existing technologies. In this section, the main purpose is to test the ability of the ultrasonic

technique to detect the presence of crude oil and its emulsion layers as well as to measure their thickness.

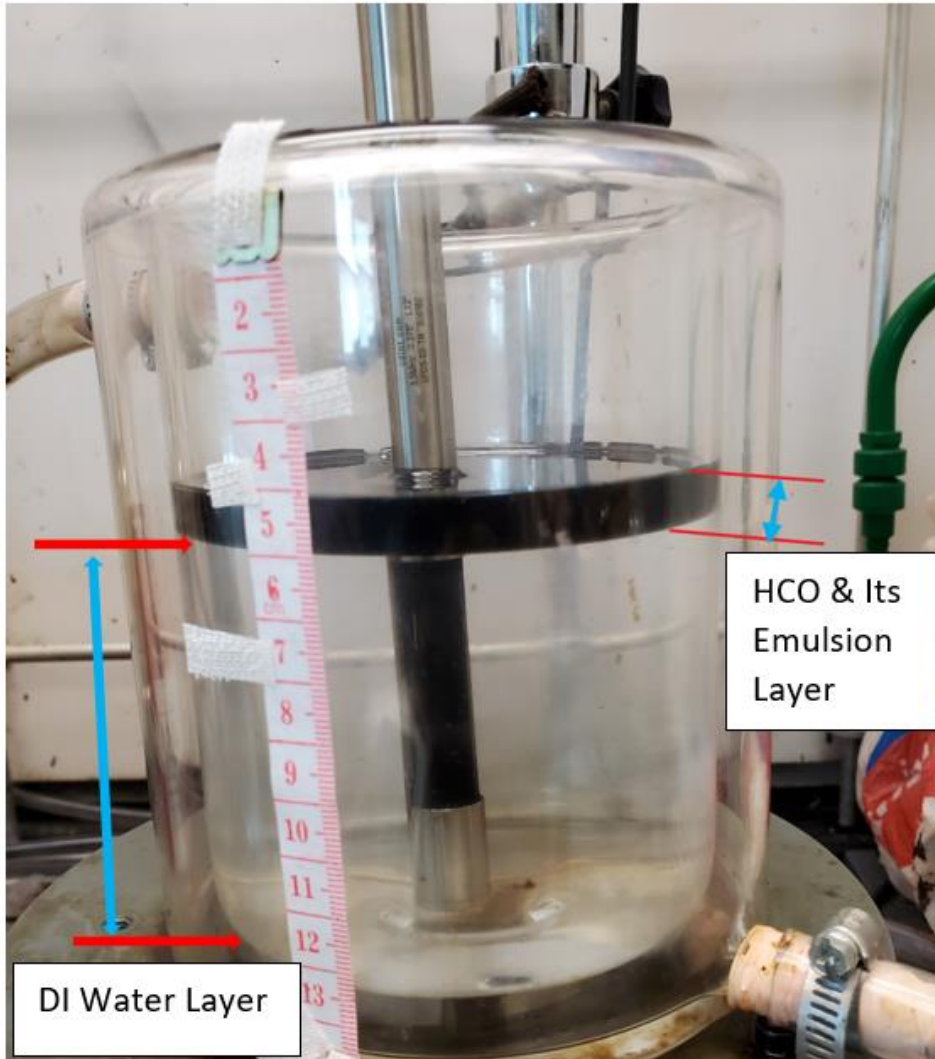


Fig. 4.14. Photographs showing layers of crude oil on water surface in the test vessel

Fig. 4.16 demonstrates variations of acoustic velocity with increasing thickness of the crude oil layer on the surface of the DI water and crude oil emulsion layer. A good trend can be seen from both curves. Following interesting observations can be made from these plots.

- For the crude oil on the DI water surface plot, the addition of 1 mm of crude oil layer leads to a steep drop in acoustic velocity, followed by a more gradual decrease with a further build-up of the crude oil layer.

- As can be seen in Fig. 4.15 adding 5 mm layer of HCO decreased the ultrasonic signal

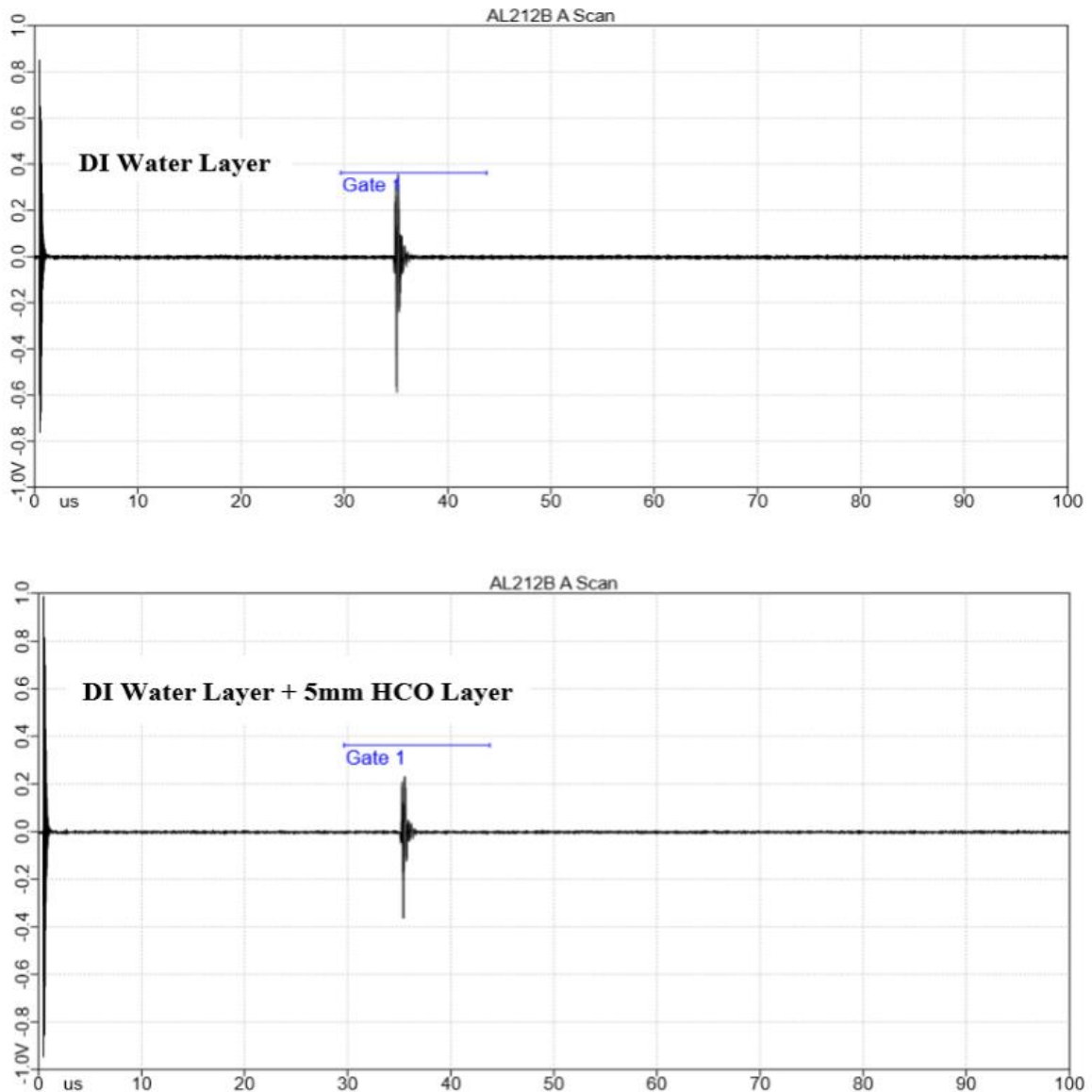


Fig. 4.15. Changes in ultrasonic signal for DI Water Layer + 5 mm HCO Layer

- Similar behavior was also observed with mineral oil (Fig. 4.8) which indicates an underlying effect due to the creation of an oil-water interface. This initial effect remains essentially constant for subsequent values.

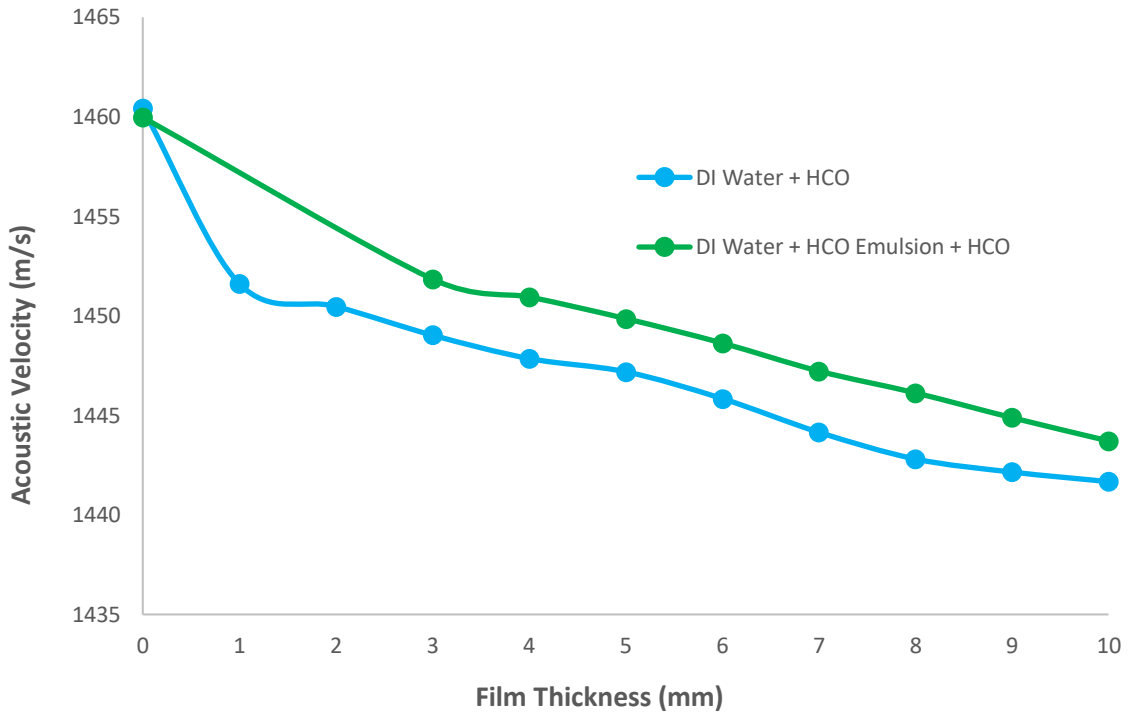


Fig. 4.16. Acoustic Velocity of DI water + HCO layers and DI water + HCO Emulsions + HCO using the new procedure.

- When 3 mm of the water-crude oil emulsion is added on the water surface, there is a decrease in acoustic velocity that is lower than when 3 mm of crude oil added. This can be attributed to the contribution of the water phase (in the emulsion) which has higher acoustic velocity. This is an important observation since it shows that the presence of water has been detected in the crude oil layer. It may be pointed out that it is not possible to visually differentiate between crude oil and its emulsion due to its dark brown opaque color. It may also be noted that similar behavior was observed with mineral oil emulsion (Fig. 4.17) where the emulsion layer could be differentiated from the oil layer, given its near-transparent optical characteristics.

Fig. 4.17 shows corresponding attenuation data obtained from measured amplitudes. Like acoustic velocity, attenuation showed a good trend in both curves from which the following important observations can be made.

- There is a significant increase in attenuation at the crude oil emulsion layer of 3 mm on the water surface. However, the subsequent increase in oil layer thickness results in a slower increase.
- When 3 mm of crude oil emulsion is added above the surface of the water, there is a high increase in attenuation that is about four times higher than 3 mm of crude oil added on the surface of the water. This can again be attributed to heterogeneous nature of the emulsion phase.
- After adding crude oil on the layer of emulsion, attenuation continued to increase significantly with a smooth trend. Overall, adding crude oil with emulsions increased attenuation more than when crude oil is added without emulsion.
- Observations from Figure 4.16 and 4.17 show that when an emulsion layer is present, both attenuation and acoustic velocity will be on the higher side.

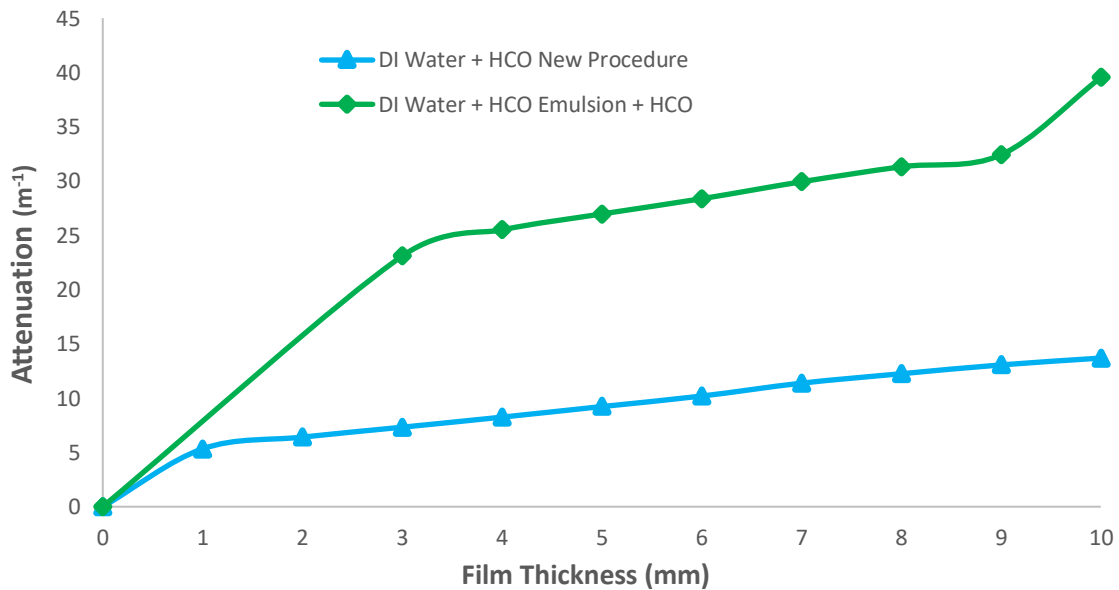


Fig. 4.17. Attenuation of DI water + HCO layers and DI water + HCO Emulsions + HCO using the new procedure

4.4 Estimation of Oil Layer Thickness Based on Measurement of Acoustic Parameters

The measured acoustic velocity could be used to estimate oil layer thickness using the following procedure. Since the distance between the transmitter and receiver' is fixed, it can be written as the sum of the oil layer thickness (d_o) and the remaining water layer (d_w).

$$d = d_o + d_w \quad (4.4)$$

The time of flight recorded with layers of oil and water can be assumed to be additive.

$$ToF_{ow} = ToF_o + ToF_w \quad (4.5)$$

Each of the distances in equation 4.4 can be divided by the corresponding acoustic velocity, making it equivalent to equation 4.5. Thus,

$$\frac{d}{V_{o-w}} = \frac{d_o}{V_o} + \frac{d_w}{V_w} \quad (4.6)$$

Substituting for d_w from equation 4.4 into equation 4.6.

$$\frac{d}{V_{o-w}} = \frac{d_o}{V_o} + \frac{d}{V_w} - \frac{d_o}{V_w} \quad (4.7)$$

Rearranging and solving for oil layer depth (d_o) gives,

$$d_o = \frac{d \left[\frac{1}{V_{o-w}} - \frac{1}{V_w} \right]}{\left[\frac{1}{V_o} - \frac{1}{V_w} \right]} \quad (4.8)$$

Equation 4.8 Was used to calculate oil layer thickness from measured acoustic velocity data. It is observed from Table 4.3 That the calculated values were higher by a nearly constant value of about 5.1 mm. As noted earlier, this can be attributed to the presence of an oil-water interface which imparts additional resistance to the propagating wave due to acoustic impedance effects. When this constant value is subtracted from the calculated values, the difference between calculated and actual values become much smaller with an average absolute error of less than 10%. The highest

error is obtained with the lowest thickness and the error reduces with increasing oil layer thickness. It may be pointed out that there are expected to be higher measurement errors while measuring the oil layer thickness of less than 3 mm in an apparatus used in the study. So, this could be a significant error source for smaller oil layer thickness in this study.

Table 4.3. Comparison of measured and estimated oil layer thickness

Crude oil thickness (mm)	Acoustic velocity (m/s)	Calculated oil layer thickness (mm)	Difference between calc. and measured values (mm)	Corrected oil layer thickness (mm)	Absolute relative error (%)
1.0	1450.7	6.5	5.5	1.4	40.0
3.0	1448.7	8.4	5.4	3.3	10.0
6.0	1445.7	10.6	4.6	5.5	8.3
8.0	1442.44	13.0	5.0	7.9	1.25
Avg.: 5.1					

When all three layers are present, the distance between the transmitter and receiver ‘d’ can be written as the sum of the oil layer thickness (d_o), emulsion layer (d_{em}) and the remaining water layer (d_w).

$$d = d_o + d_{em} + d_w \quad (4.4)$$

The time of flight recorded with layers of oil and water can be assumed to be additive.

$$ToF_{owe} = ToF_o + ToF_{em} + ToF_w \quad (4.5)$$

Each of the distances in equation 4.4 can be divided by the corresponding acoustic velocity, making it equivalent to equation 4.5. Thus,

$$\frac{d}{v_{owe}} = \frac{d_o}{v_o} + \frac{d_{em}}{v_{em}} + \frac{d_w}{v_w} \quad (4.6)$$

Substituting for d_w from equation 4.4 into equation 4.6.

$$\frac{d}{V_{owe}} = \frac{d_o}{V_o} + \frac{d_{em}}{V_{em}} + \frac{d}{V_w} - \frac{d_o}{V_w} - \frac{d_{em}}{V_w} \quad (4.7)$$

The above set of equations can be used to estimate oil layer thickness in different ways.

1. For some applications, emulsion layer thickness and acoustic velocity may be known or easily determined because the emulsion layer can stabilize under certain conditions of use.
2. By using proper vertical movements of the probe (using suitable fixtures), it is possible to determine when it is only in the water phase. This procedure can provide combined thickness of oil and emulsion layers.
3. Suitable calibration procedures/plots can be developed to cover the range of applications.

Figure 4.18 shows a proposed procedure.

- a. The probe is initially located so that the transmitter is in contact with the oil layer.

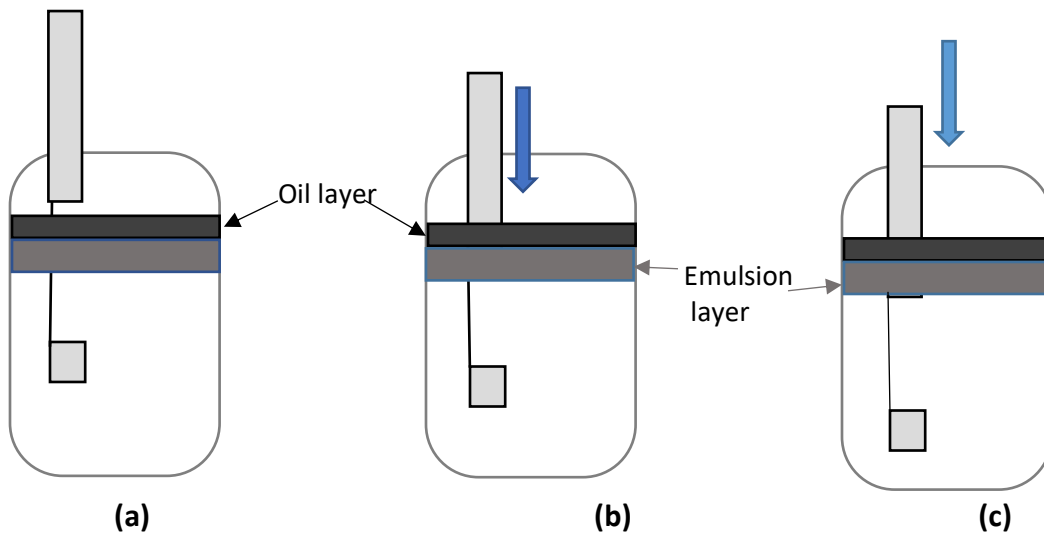


Fig. 4.18. Proposed procedure to detect oil and emulsion layers a) probe at the surface of oil layer; b) probe at the surface of emulsion layer; c) probe at the surface of water column

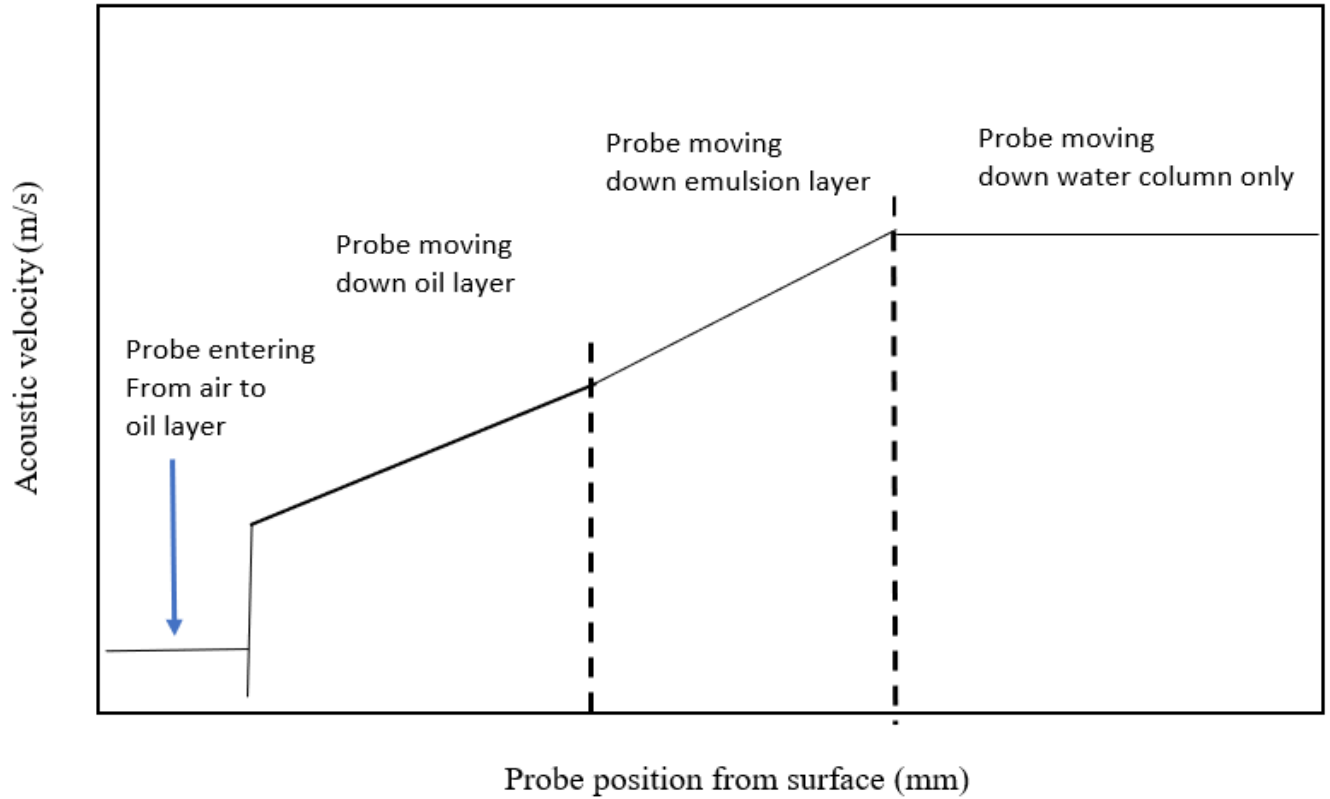


Fig. 4.19. Expected trajectory of the measured acoustic velocity as the probe moves from oil layer to water phase

- a. It is then moved down and changes in acoustic velocity are recorded
- b. As it enters the emulsion phase, leaving the oil layer, there would be a change in the slope of recorded velocity, reflecting the high velocity of the emulsion phase.
- c. As the probe moves into the water phase only, the velocity will reach a constant value of the water phase.

4.5 Conclusions

The potential of the proposed ultrasonic based technique to monitor oil spills has been demonstrated through a series of tests and oil layer thickness estimations. It is shown that simultaneous measurements of acoustic velocity and attenuation provide a strong combination to detect presence of oil and emulsion layers. For the oil layer on the surface of the water, a simple method to determine oil layer thickness is proposed based on acoustic velocity measurements. This can be extended to the oil-emulsion-water layer system for some cases. In the end, a more general and more robust procedure has been proposed based on the observations and tests of the study. As per the proposed method, the probe will be mounted on a retractable fixture to move the probe vertically up and down the layers while recording the signals. A plot of recorded acoustic parameters with respect to probe position can easily provide the thickness of each layer due to changes in the slope of the recorded parameter moving from one phase to next. The probe response could be further improved by suitable alterations to probe design and selection of more appropriate frequency based on more extensive testing.

Notations

CO	Crude oil
MO	Mineral Oil
LMO	Light Mineral Oil
LCO	Light Crude Oil
HCO	Heavy Crude Oil
LURSOT	The Laser Ultrasonic Sensing of Oil thickness
c	acoustic velocity (m.s^{-1})
d	distance between transducer and receiver (m)
UV/IR	ultraviolet/infrared
USEPA	U.S. Environmental Protection Agency
d_w	Water layer (mm)
d_{em}	Emulsion layer (mm)
d_o	Oil layer thickness (mm)
ToF_{owe}	Time of flight recorded with layers of oil, emulsion and water (μs)
ToF_o	Time of flight of oil (μs)
ToF_w	Time of flight of water (μs)
ToF_{em}	Time of flight of emulsion (μs)
V_o	Acoustic velocity of oil (m.s^{-1})
V_w	Acoustic velocity of water (m.s^{-1})
V_{em}	Acoustic velocity of emulsion (m.s^{-1})
V_{owe}	Acoustic velocity of oil, water and emulsion (m.s^{-1})
TOF	Time of flight (μs)
A_0	Reference amplitude (V)
A	Reference amplitude (V)
DI	Deionized

Greek Letters

α attenuation coefficient (m^{-1})

β bulk modulus of the medium (Pa)

ρ density of medium (kg.m^{-3})

Subscripts

em emulsion

w water

o oil

r reflector or reference

References

- Akkartal, A., & Sunar, F. (2008). The usage of radar images in oil spill detection. *International Archives of the Photogrammetry, Remote Sensing and Spatial Information Sciences - ISPRS Archives*, 37, 271–276.
- Ament, W. S. (1953). Sound propagation in gross mixtures. *Journal of Acoustical Society of America*, 25, pp. 638-641.
- Atkinson, C. M., and H. K. Kytömaa. "Acoustic Wave Speed and Attenuation in Suspensions." *International Journal of multiphase flow* 18, no. 4 (1992): 577-592.
- Belore, R.C., (1982). A device for measuring oil slick thickness, *Spill Technology Newsletter*, Vol. 7, No. 2, pp. 44-47.
- Brown, et al (1998). Oil-spill remote sensors: New tools that provide solutions to old problems. *Environment Canada Arctic and Marine Oil Spill Program Technical Seminar (AMOP) Proceedings*, 21(2), 783–794.
- Derkach, Svetlana R. (2009). Rheology of emulsions. *Advances in Colloid and Interface Science* 151, no. 1 (2009): 1-23.
- Ensminger, D. and L. J. Bond, (2012). *Ultrasonics – Fundamentals, Technologies and Applications*, 3rd ed., CRC Press.
- Dagleish, T., et al (2007). *Journal of Experimental Psychology: General*, 136(1)
- Fingas, M. (2018). *Slick Thickness*.
- Hoge, F.E. and Swift, R.N. (1980). Oil film thickness measurement using airborne laser-induced water Raman Backscatter, *Applied Optics* Vol. 19, No. 19, pp. 3269-3281.
- Kilpatrick, P. K. (2012). Water-in-crude oil emulsion stabilization: Review and unanswered questions. *Energy and Fuels*, 26(7), 4017–4026.
- Kung, R.T.V. and Itzkan, I., (1976). Absolute oil fluorescence conversion efficiency, *Applied Optics*, Vol. 15, pp. 409-415.
- Onwurah, et al (2007). Crude oils spills in the environment, effects and some innovative clean-up biotechnologies. *International Journal of Environmental Research*, 1(4), 307–320.
- Povey, M. J. W., (1997). *Ultrasonic techniques for fluids characterization.*, Academic Press, San Diego.
- Silset, A. (2008). *Anne Silset Emulsions (w/o and o/w) of Heavy Crude Oils. Destabilization and Produced Water Quality (Issue November 2008).*

Shukla, A., A. Prakash and S. Rohani, (2010). Online Measurement of Particle Size Distribution during Crystallization Using Ultrasonic Spectroscopy, *Chemical Engineering Science*, 65.10 3072–79.

Urlick, R. J. (1947). A sound velocity method for determining the compressibility of finely divided substance. *Journal of Applied Physics*, 18, pp. 983-987.

Wang, Z. and Nur, A. (1991). Ultrasonic velocity in pure hydrocarbons and mixtures, *J. Acoustical Society of America*, Vol. 89, pp. 2725-2730.

Appendix B

Comparison between results obtained with mineral and crude oils

Mineral oil which is a fraction of crude oil consists of a mixture of hydrocarbons in the carbon number range of 18 to 28. It has some characteristics of petroleum such as high density and viscosity, but it is also different in several ways. In crude oil hydrocarbon molecules with carbon numbers as high as 60 can be found, these are usually asphaltene molecules which also impart a dark brown color to crude oil. Mineral oil, on the other hand, is nearly transparent allowing visual observations during experiments. Due to their similar physical characteristics such as density and viscosity, results obtained with mineral oils and their emulsions usually provide similar trends and provide reliable reference for crude oils measurements. Fig. B4.20 compares the results obtained with the two oils when both emulsion and oil layers were present on the surface of DI water. However, the crude oil (CO) curve is lower than LMO since the acoustic velocity for MO is higher than CO. For an additional increase in the thickness of CO, there is a higher decrease in acoustic velocity compared to LMO.

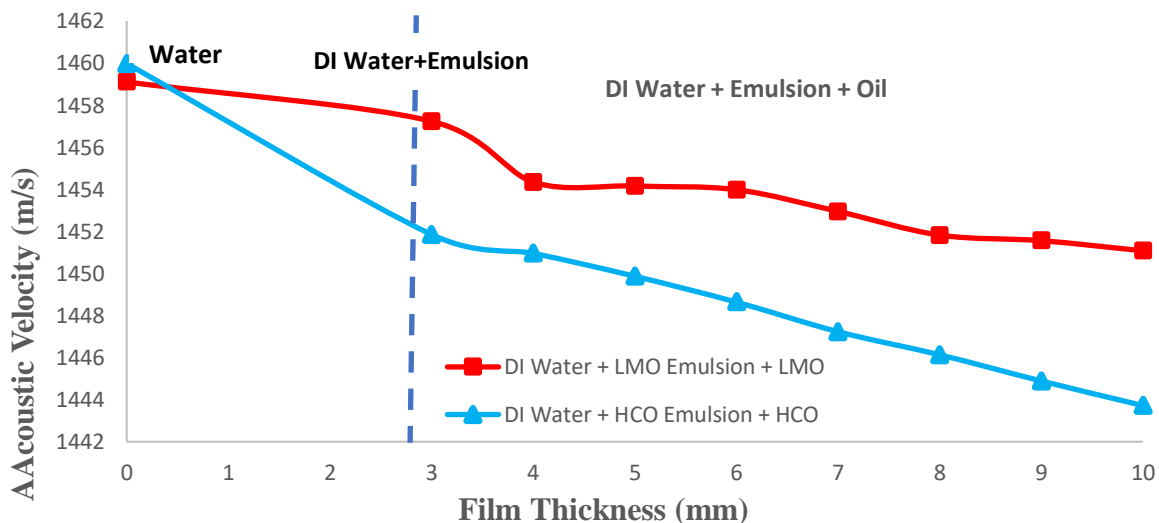


Fig. B4.20. Comparison of acoustic velocity for film of LMO and CO and their emulsions layers

Fig. B4.21 shows the corresponding attenuation for acoustic velocity in Fig. B4.20 HCO curve is higher than LMO since the attenuation for HCO alone is higher than MO. For an additional increase in the thickness of HCO, there is a higher increase in attenuation compared to LMO.

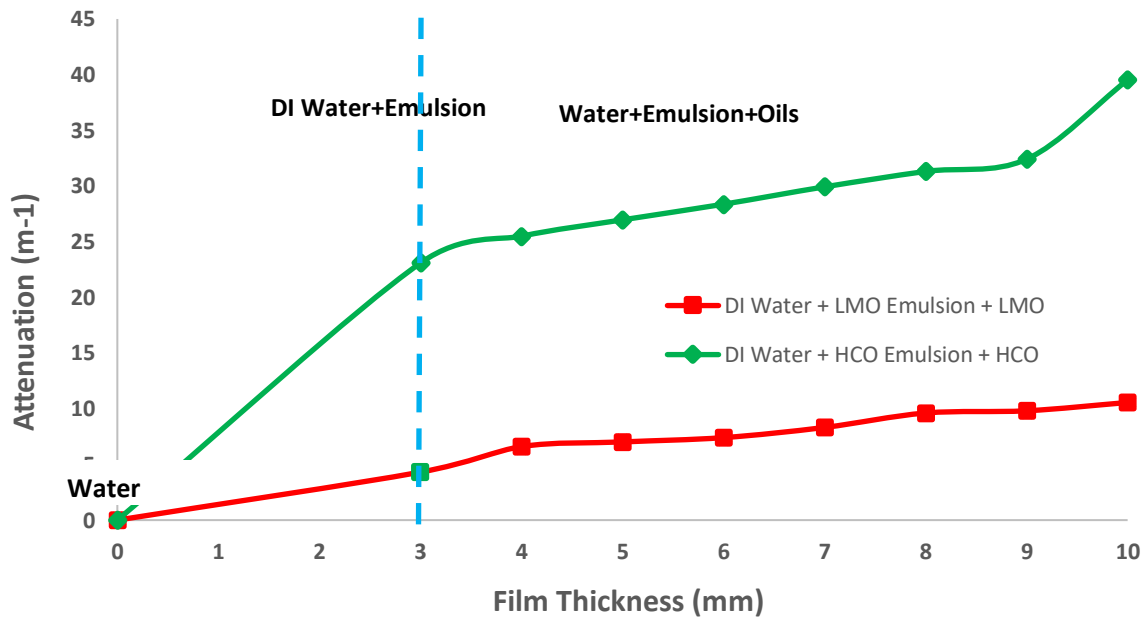


Fig. B4.21. Attenuation of mineral oil – Water content (10 & 20%)

Chapter 5. Conclusion

In this work, ultrasonic based technology was developed to characterize oils and their emulsions, as well as to detect oil spill and estimate their thickness. Characteristics of oils such as acoustic velocity and attenuation that are calculated from the time of flight and amplitude respectively, of oils and their emulsions were studied. The initial tests were performed with mineral oil and its emulsions to allow for visual observations of water separation percentages from emulsions and demonstrated the potential of this technique to monitor emulsions stability. Mineral oil emulsion with 20% DI water content separated into their phases faster than emulsion with 10% DI water content. This is possible because high water content led to the formation of large water droplets which are easy to coalesce. The corresponding acoustic velocity and attenuations captured similar trends. The decrease in acoustic velocity corresponds to a decrease in DI water content in the emulsions. Therefore, indicating water separation taking place. Changes in the composition of heavy crude oil emulsions that cannot be seen visually observed can be analyzed using acoustic velocity since there was no water separation observed for heavy crude oil emulsion. Although, acoustic velocity showed separation taking of water taking place. The analyzed results showed that the ultrasonic technique has high potential to be used for monitoring emulsion stability and track changes in emulsions characteristics such as acoustic velocity and attenuation.

The ultrasonic technique captured variations in asphaltenes content of crude oil samples which is of practical significance in the petroleum industry. It is, therefore, a time-saving method to measure asphaltene concentration compared to the time-consuming offline solvent-based treatment and filtration method. The link between asphaltene concentration and stability of crude oil emulsions was very clear as high asphaltene content increased the stability of the emulsion.

While for oil spill monitoring, it is shown that simultaneous measurements of acoustic velocity and attenuation provided a strong combination to detect the presence of oil and emulsion layers. For the oil layer on the surface of DI water, a simple method to determine oil layer thickness is proposed based on acoustic velocity measurements. This can be extended to the oil-emulsion-water layer system for some cases. Through a series of simulated experiments, the result showed that the ultrasonic technique easily detected oils and their emulsions layers on the water surface. The acoustic velocity decreases immediately when oils and their emulsions were added on the surface of DI water. The decrease in acoustic velocity is due to the lower velocity of oils than DI water. Therefore, the technique detected the presence of oil and emulsions layers. It provided reasonable estimates of the thickness of the oil layer by tracking changes in acoustic velocity when an additional sample of oil is added. High acoustic velocity was observed in the first 1 mm oil layer. Each additional layer of the oil resulted in a gradual decrease in acoustic velocity. The corresponding attenuations showed a reversed trend. These results provided the expected trends. Therefore, paving the way for further studies to fully develop the ultrasonic technique for field testing.

5.1 Recommendations

Based on the analyzed results, the following are the recommendations:

- Further development of probe design based on the probe response with different emulsions. The probe did not provide a good trend in some cases, more specifically the attenuation of the blend of HCO and LMO emulsions. To increase the sensitivity of the probe to get a good attenuation trend, a probe with higher frequency than the currently available one (3.5 MHz) can solve this issue and provide accurate results.

- Blend heavy and light crude oil to form intermediate to study characteristics of its emulsions. These characteristics include acoustic velocity and attenuation, density, and emulsions stability. The purpose of this is to test the ability of this technique to detect the difference between emulsions of LCO and HCO and their blend. This will eventually show how reliable this technique in monitoring emulsions during refinery.
- Investigate the distribution of droplets in emulsions. It is important to understand how droplet concentration and size distribution affects the stability of emulsions. This can be done by testing a wide range of water content in emulsions. The higher the water content in the emulsion the larger the size of the droplets.
- For the ultrasonic based technique to monitor the oil spill, a new method for field testing is proposed where the probe will be mounted on a retractable fixture to move the probe vertically up and down the layers with ease while recording the signals. This can be installed on a drone and be remotely controlled. A plot of the recorded acoustic parameters with respect to probe position can easily provide the thickness of each layer due to changes in the slope of the recorded parameter moving from one phase (i.e. oil, emulsion, and water layers) to the next.
- The probe response could be further improved by suitable alterations to probe design and selection of more appropriate frequency based on more extensive testing. For field testing, the proposed new method will require changing the design of the probe. First, the size of the probe will have to be increased, thereby increasing d - the active part of the probe which is the distance between transmitting and receiving surface. The frequency should be increased from the current 3.5 MHz to 5 MHz to increase the sensitivity of the probe since seawater has a high content of impurities.

CURRICULUM VITAE OF KANU RAIGAN

EDUCATION

Master of Engineering Science, Chemical Engineering January 2018 – April 2020
WESTERN UNIVERSITY, Faculty of Engineering, London, ON

Bachelor of Engineering Science: Chemical Engineering September 2012 - June 2016
WESTERN UNIVERSITY, London, ON

AWARDS/HONOURS

Achieved Western Scholarship of Distinction September 2012 – April 2016
WESTERN UNIVERSITY, Faculty of Engineering, London, ON

RELATED WORK EXPERIENCE

Graduate Teaching Assistant September 2018 – April 2020
WESTERN UNIVERSITY, DEPARTMENT OF ENGINEERING | London, ON

Graduate Research Assistant December 2018 – April 2020
WESTERN UNIVERSITY, DEPARTMENT OF ENGINEERING | London, ON

Production Team Member October 2016 – January 2018
TOYOTA MOTOR MANUFACTURING CANADA | Woodstock, ON

Group Project-Wastewater Treatment in SAGD Process Project September 2015 – April 2016
WESTERN UNIVERSITY, DEPARTMENT OF ENGINEERING | London, ON